

THE PROCEEDINGS OF THE PHYSICAL SOCIETY

Section B

VOL. 63, PART 10

1 October 1950

No. 370 B

CONTENTS

	PAGE
Dr. H. H. HOPKINS and Mr. P. M. BARHAM. The Influence of the Condenser on Microscopic Resolution	737
Dr. H. KUHN and Mr. B. A. WILSON. Reflectivity of Thin Silver Films and their Use in Interferometry	745
Dr. A. F. GIBSON. The Absorption Spectra of Solid Lead Sulphide, Selenide and Telluride	756
Dr. M. S. B. CHAGHTAI. Note on the Electron Velocity Distribution in Low Voltage Arcs	768
Mr. M. R. HOPKINS and Mr. T. C. TOYE. The Determination of the Viscosity of Molten Metals	773
Dr. R. MILLERSHIP and Mr. F. V. WEBSTER. High Frequency Permeability of Ferromagnetic Materials	783
Mr. K. S. W. CHAMPION. The Production of Pulsed Magnetic Fields using Condenser Energy Storage	795
Dr. G. G. MACFARLANE. A Theory of Contact Noise in Semiconductors	807
Dr. C. DODD and Mr. G. N. ROBERTS. Dielectric Loss and Dielectric Constant Measurements in Supercooled Liquids	814
Letters to the Editor :	
Mr. P. D. LOMER. The Dielectric Strength of Aluminium Oxide Films	818
Mr. G. D. ADAM and Dr. K. J. STANDLEY. Ferromagnetic Resonance in Manganese Arsenide	820
Mr. J. T. KENDALL. Electrical Conductivity of Gray Tin	821
Mr. G. FRANCIS and Dr. A. VON ENGEL. Development of the Low Pressure Electrodeless Discharge in a High-Frequency Electric Field	823
Reviews of Books	824
Contents for Section A	830
Abstracts for Section A	831

Price to non-members 10s. net, by post 6d. extra. Annual subscription: £5 5s.

Composite subscription for both Sections A and B: £9 9s.

Published by

THE PHYSICAL SOCIETY

1 Lowther Gardens, Prince Consort Road, London S.W.7

PROCEEDINGS OF THE PHYSICAL SOCIETY

The *Proceedings* is now published monthly in two Sections.

ADVISORY BOARD

Chairman : The President of the Physical Society (L. F. BATES, D.Sc., Ph.D., F.R.S.).

E. N. da C. ANDRADE, Ph.D., D.Sc., F.R.S.
 Sir EDWARD APPLETON, G.B.E., K.C.B.,
 D.Sc., F.R.S.
 P. M. S. BLACKETT, M.A., F.R.S.
 Sir LAWRENCE BRAGG, O.B.E., M.A., Sc.D.,
 D.Sc., F.R.S.
 Sir JAMES CHADWICK, D.Sc., Ph.D., F.R.S.
 Lord CHERWELL OF OXFORD, M.A., Ph.D.,
 F.R.S.
 Sir JOHN COCKROFT, C.B.E., M.A., Ph.D.,
 F.R.S.

Sir CHARLES DARWIN, K.B.E., M.C., M.A.,
 Sc.D., F.R.S.
 N. FEATHER, Ph.D., F.R.S.
 G. I. FINCH, M.B.E., D.Sc., F.R.S.
 D. R. HARTREE, M.A., Ph.D., F.R.S.
 N. F. MOTT, M.A., F.R.S.
 M. L. OLIPHANT, Ph.D., D.Sc., F.R.S.
 F. E. SIMON, C.B.E., M.A., D.Phil., F.R.S.
 T. SMITH, M.A., F.R.S.
 Sir GEORGE THOMSON, M.A., D.Sc., F.R.S.

Papers for publication in the *Proceedings* should be addressed to the Hon. Papers Secretary,
 Dr. H. H. HOPKINS, at the Office of the Physical Society, 1 Lowther Gardens, Prince
 Consort Road, London S.W.7. Telephone : KENSington 0048, 0049.

Detailed Instructions to Authors were included in the February 1948 issue of
 the *Proceedings*; separate copies can be obtained from the Secretary-Editor.

BULLETIN ANALYTIQUE

Publication of the Centre National de la Recherche Scientifique, France

The *Bulletin Analytique* is an abstracting journal which appears in three parts, Part 1 covering scientific and technical papers in the mathematical, chemical and physical sciences and their applications, Part 2 the biological sciences and Part 3 philosophy.

The *Bulletin*, which started on a modest scale in 1940 with an average of 10,000 abstracts per part, now averages 35 to 45,000 abstracts per part. The abstracts summarize briefly papers in scientific and technical periodicals received in Paris from all over the world and cover the majority of the more important journals in the world scientific press. The scope of the *Bulletin* is constantly being enlarged to include a wider selection of periodicals.

The *Bulletin* thus provides a valuable reference book both for the laboratory and for the individual research worker who wishes to keep in touch with advances in subjects bordering on his own.

A specially interesting feature of the *Bulletin* is the microfilm service. A microfilm is made of each article as it is abstracted and negative microfilm copies or prints from microfilm can be purchased from the editors.

The subscription rates per annum for Great Britain are 4,000 frs. (£4) each for Parts 1 and 2, and 2,000 frs. (£2) for Part 3. Subscriptions can also be taken out to individual sections of the *Bulletin* as follows :

	frs.	
Pure and Applied Mathematics—Mathematics—Mechanics	550	14/6
Astronomy—Astrophysics—Geophysics	700	18/-
General Physics—Thermodynamics—Heat—Optics—Elec- tricity and Magnetism	900	22/6
Atomic Physics—Structure of Matter	325	8/6
General Chemistry—Physical Chemistry	325	8/6
Inorganic Chemistry—Organic Chemistry—Applied Chemistry—Metallurgy	1,800	45/-
Engineering Sciences	1,200	30/-
Mineralogy—Petrography—Geology—Paleontology ..	550	14/6
Biochemistry—Biophysics—Pharmacology	900	22/6
Microbiology—Virus and Phages	600	15/6
Animal Biology—Genetics—Plant Biology	1,800	45/-
Agriculture—Nutrition and the Food Industries	550	14/6

Subscriptions can be paid directly to the editors : Centre National de la Recherche Scientifique,
 18, rue Pierre-Curie, Paris 5ème (Compte-chèque-postal 2,500-42, Paris), or through Messrs. H. K.
 Lewis & Co. Ltd., 136, Gower Street, London W.C. 1.



Infra - red Photo - conductive cells

For Pyrometry, Spectroscopy, and the Detection of Radiant Heat

These lead sulphide cells are the fastest and most sensitive devices for the detection and measurement of infra-red radiation in the 1 to 3 micron wavelength

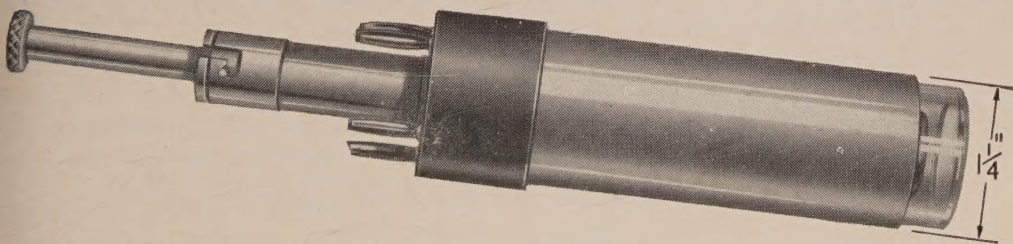
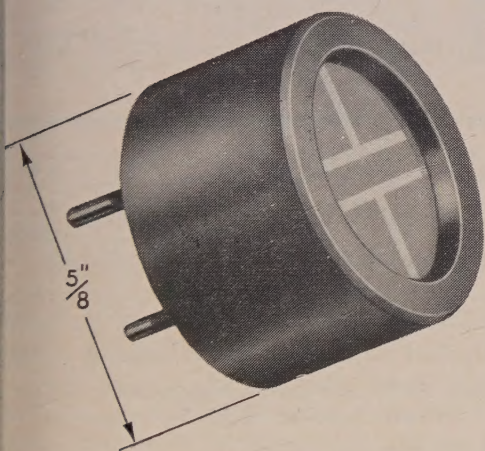
region of the spectrum. They are sensitive to source temperatures as low as 200°C, and they respond to temperature variations within 100 microseconds.

Left: Type "M", for detection and pyrometry, is of minimum dimensions and simple mechanical construction.

Below: Type "C.1", for detection and spectroscopy. This cell has provision for cooling by carbon dioxide, a feature which considerably increases its sensitivity.

Other BTH infra-red devices include: Nernst filaments (as infra-red sources), special infra-red transmitting glass, and semiconductor bolometers.

Full particulars on application.



BRITISH THOMSON-HOUSTON

THE BRITISH THOMSON-HOUSTON CO., LTD., RUGBY, ENGLAND

A 3986

PROCEEDINGS OF THE PHYSICAL SOCIETY

ADVERTISEMENT RATES

The *Proceedings* are divided into two parts, A and B. The charge for insertion is £18 for a full page in either Section A or Section B, £30 for a full page for insertion of the same advertisement in both Sections. The corresponding charges for part pages are :

$\frac{1}{2}$ page	£9	5	0	£15	10	0
$\frac{1}{4}$ page	£4	15	0	£8	0	0
$\frac{1}{8}$ page	£2	10	0	£4	5	0

Discount is 20% for a series of six similar insertions and 10% for a series of three.

The printed area of the page is $8\frac{1}{2}'' \times 5\frac{1}{2}''$, and the screen number is 120.

Copy should be received at the Offices of the Physical Society six weeks before the date of publication of the *Proceedings*.

★ NOW AGAIN IN PRINT ★

A new printing of a standard book with corrections and supplement.

The Physics of High Pressure

By P. W. BRIDGMAN

*Ph.D., Sc.D., For.Mem.R.S., Nobel Laureate,
Hollis Professor of Mathematics and Natural
Philosophy, Harvard University.*

This is a pioneer work (1931) that filled a serious gap in scientific literature, and whose author still occupies a foremost place in the important and fruitful field of High Pressure Research.

The book gives a summary of the author's work and a review of all other important work in this field to the time of original publication, and there are copious and conveniently arranged references to sources.

The supplement to the new printing summarises the more recent work.

100 text-figures and tables. 450 pp.

35s. net.

LONDON: G. BELL & SONS, LTD.

THE PHYSICAL SOCIETY VOLUME XIII of the REPORTS ON PROGRESS IN PHYSICS

This volume is now published. It is a comprehensive annual review by specialist authors. The contents are as follows :

- M. P. LORD and W. D. WRIGHT. The Investigation of Eye Movements.
- L. GOLDBERG. Recent Advances in Infra-Red Solar Spectroscopy.
- W. G. PENNEY and H. H. M. PIKE. Shock Waves and the Propagation of Finite Pulses in Fluids.
- E. C. STONER. Ferromagnetism: Magnetization Curves.
- M. RYLE. Radio Astronomy.
- G. P. KUIPER. Planetary and Satellite Atmospheres.
- A. H. COOKE. Paramagnetic Relaxation Effects.
- J. H. FREMLIN and J. S. GOODEN. Cyclic Accelerators.
- C. F. POWELL. Mesons.

The price is 50s. 0d. Members: One copy at 25s.
Postage and packing 1s.

Further information can be obtained from
THE PHYSICAL SOCIETY
1 Lowther Gardens, Prince Consort Road, London S.W.7

VITREOSIL MERCURY VAPOUR PUMPS



This new M.V. Fore Pump will operate from an ordinary water filter pump, and when used in conjunction with our Single-Stage or Two-Stage Pump, pressures less than 0.00002 mm. Hg are attained.

Write for descriptive leaflet

THE THERMAL SYNDICATE LTD.

Head Office: Wallsend, Northumberland
London Office: 12-14 Old Pye Street, S.W.1

The



NEPHELOMETER

This instrument is specially designed to estimate bacterial growth quickly and accurately. Since the measurements are made using the tubes in which the cultures are grown, their growth may be recorded and plotted with the minimum inconvenience.

THE 'EEL' NEPHELOMETER incorporates a $3\frac{1}{2}$ in. scale. Mains stabilisation is provided. Adjustment of controls enables a wide range of turbidity to be covered accurately.

Write for full details and price.

EVANS ELECTROSELENIUM LTD.

SALES DIVISION 310 HARLOW ESSEX

PHYSICAL SOCIETY SPECIALIST GROUPS

OPTICAL GROUP

The Physical Society Optical Group exists to foster interest in and development of all branches of optical science. To this end, among other activities, it holds meetings about five times a year to discuss subjects covering all aspects of the theory and practice of optics, according to the papers offered.

COLOUR GROUP

The Physical Society Colour Group exists to provide an opportunity for the very varied types of worker engaged on colour problems to meet and to discuss the scientific and technical aspects of their work. Five or six meetings for lectures and discussions are normally held each year, and reprints of papers are circulated to members when available. A certain amount of committee work is undertaken, and reports on Defective Colour Vision (1946) and on Colour Terminology (1948) have already been published.

LOW TEMPERATURE GROUP

The Low Temperature Group was formed to provide an opportunity for the various groups of people concerned with low temperatures—physicists, chemists, engineers, etc.—to meet and become familiar with each other's problems. The group seeks to encourage investigations in the low temperature field and to assist in the correlation and publication of data.

ACOUSTICS GROUP

The Acoustics Group was formed to meet the long-felt need for a focus of acoustical studies in Great Britain. The scope includes the physiological, architectural, psychological, and musical aspects of acoustics as well as the fundamental physical studies on intensity, transmission and absorption of sound. The Group achieves its object by holding discussion meetings, by the circulation of reprints and by arranging symposia on selected acoustical topics.

Further information may be obtained from the Offices of the Society :

1 LOWTHER GARDENS, PRINCE CONSORT ROAD, LONDON S.W.7.

RESONANT ABSORBERS AND REVERBERATION

Report of the
1947 SUMMER SYMPOSIUM
OF THE
ACOUSTICS GROUP
OF THE
PHYSICAL SOCIETY

together with the Inaugural Address
of the Group:

ACOUSTICS AND SOME ALLIED STUDIES

by ALEXANDER WOOD

57 pages. 7s. 6d.; by post 8s.

Orders, with remittances, to be sent to
THE PHYSICAL SOCIETY
1 Lowther Gardens, Prince Consort Road,
London S.W.7

SYMPOSIUM ON NOISE AND SOUND TRANSMISSION

Report of the
1948 SUMMER SYMPOSIUM
OF THE
ACOUSTICS GROUP
OF THE
PHYSICAL SOCIETY

200 pages. 17s. 6d.; by post 18s.

(Price 10s. 6d., by post 11s., to Fellows of
the Society and Members of the Acoustics
Group)

Orders, with remittances, to be sent to
THE PHYSICAL SOCIETY
1 Lowther Gardens, Prince Consort Road,
London S.W.7

Report of a Conference
on
**THE STRENGTH
OF SOLIDS**

held at the
H. H. WILLS PHYSICAL
LABORATORY, BRISTOL
in July 1947

162 pp. Price 25s., to Fellows 15s. 6d.;
postage and packing 8d.

Orders, with remittances, to
THE PHYSICAL SOCIETY
1 Lowther Gardens, Prince Consort Road,
London S.W.7

REPORT OF AN
INTERNATIONAL CONFERENCE
ON
FUNDAMENTAL PARTICLES
AND
LOW TEMPERATURES

HELD AT
*The Cavendish Laboratory,
Cambridge*
on 22-27 July 1946

Volume I 200 pages
FUNDAMENTAL PARTICLES

Volume II 184 pages
LOW TEMPERATURES

*Price of each volume (in paper covers) 15s.,
inclusive of postage*

Orders, with remittances, should be sent to
THE PHYSICAL SOCIETY
1 Lowther Gardens, Prince Consort Road,
London S.W.7

THE PROCEEDINGS OF THE PHYSICAL SOCIETY

Section B

VOL. 63, PART 10

1 October 1950

No. 370 B

The Influence of the Condenser on Microscopic Resolution

BY H. H. HOPKINS AND P. M. BARHAM

Imperial College, London

MS. received 13th April 1950

ABSTRACT. An expression is found for the distribution of light in the image of two small apertures which are illuminated by a condenser of numerical aperture equal to s times that of the imaging objective. The resolving power of the system is written $\rho = K\lambda/(N.A.)$, and K is found as a function of s . It is shown that precisely the same result obtains for both critical and Köhler illumination.

§ 1. INTRODUCTION

THE theory of the resolving power of a telescope is generally based on a consideration of the image of a double star. Optically this is represented as the image of two closely spaced incoherent point sources of the same intensity. Each source produces a diffraction pattern in the focal plane of the telescope objective. The image of the double star is then obtained as the sum of the separate intensities in the two diffraction patterns. The Rayleigh criterion of resolution requires that the minimum of intensity midway between the geometrical images is of the order of 20% smaller than the intensity at the maxima of the summed intensities. Conventionally the criterion is regarded as being satisfied when the geometrical image of one source falls on the first dark ring of the diffraction image of the other.

In the case of a slit shaped aperture the intensity distribution in the image of a point source has the form $I = \{\sin x/x\}^2$. This gives a decrease in intensity of 18.9% at the point midway between the geometric images. If a circular aperture is employed, the intensity distribution has the form $I = \{2J_1(z)/z\}^2$. The decrease in intensity is then found to be 26.4%. If α is the angular semi-aperture, and N a refractive index, the two sources will be 'resolved' when their geometrical images are separated by a distance ρ , where

$$\text{Slit shaped aperture:} \quad \rho = 0.50\lambda/N \sin \alpha. \quad \dots\dots(1)$$

$$\text{Circular aperture:} \quad \rho = 0.61\lambda/N \sin \alpha. \quad \dots\dots(2)$$

It is significant that the smaller resolvable separation (1) is associated with a smaller drop in intensity.

Disturbances from two distinct point sources are incoherent. In the case of a telescope imaging double stars, it therefore suffices to add the intensities of the separate diffraction patterns. This will not generally be true for the images

of, say, two illuminated pinholes in an opaque screen, for there some degree of phase correlation will obtain. In general, therefore, it will be necessary to take phase relationships into account when adding the disturbances in the image plane of a microscope.

Martin (1931) considered the problem of the image of two small illuminated apertures. His treatment was only approximate, but showed very clearly the physical processes involved. The case of critical illumination was considered. Firstly assuming a point source for the illuminant, and then extending the treatment qualitatively to consider an extended source imaged on the object by means of a perfectly corrected condenser of aperture equal to that of the objective, it was concluded that "the ultimate effect is likely to be similar to that characteristic of two independent elementary sources", the two apertures being at a separation given by (2). In the present paper it is shown that this is, in fact, exactly true for both critical and Köhler illumination. This accords with a result predicted by Zernike (1938).

In our case an expression is obtained for the disturbance in the final image plane associated with the image of two pinholes illuminated by a condenser of any given aperture when used in conjunction with a large source of uniform intensity. Circular apertures are assumed for both condenser and objective. The resolvable separation ρ is then written

$$\rho = K\lambda/N \sin \alpha \quad \dots\dots(3)$$

instead of (2). K is found as a function of s , the ratio (N.A. condenser)/(N.A. objective). N.A. denotes, as usual, the numerical aperture equal to $N \sin \alpha$.

Recently a criterion of resolution due to Sparrow (1916) has been employed (Ramsay, Cleveland and Koppius 1941, Françon 1950). If I is the intensity at the point midway between the two geometric images, and x is a coordinate measured along the line joining them, the images are said to be resolved when $\partial^2 I / \partial x^2 = 0$. It has been claimed that this gives a true 'limit' of resolution, since the intensity curve is then 'flat'. However, the criterion is not unique, since the equation $\partial^2 I / \partial x^2 = 0$ will frequently have an infinite number of roots. Moreover the 'resolution' indicated by this criterion is meaningless in some cases, notably in finding the limit of detection of the microscope. The diameter of that smallest particle that can be 'seen' is found to be zero. With increasing contrast sensitivity of the screen on which the image is received, the size of the smallest detectable particle does decrease indefinitely. In a sense, therefore, the result obtained using the criterion $\partial^2 I / \partial x^2 = 0$ is valid. Nevertheless it is of little practical value.

Because of this we have adopted a Rayleigh criterion of resolution which for circular apertures requires the decrease in intensity to be 26.4% of the maximum intensity. The analysis is based on a consideration of critical illumination. It is then shown that the same result obtains for Köhler illumination.

§ 2. CRITICAL ILLUMINATION WITH AN EXTENDED SOURCE

We have first to define an optical unit of length. Suppose a length ρ in the object plane has an image of length ρ' . Then the magnification is given by $m = \rho' / \rho$. If α , α' are the angles which a ray makes with the axis in the object and image spaces respectively, and these latter have refractive indices equal to

N and N' , the magnification is also given by $m = N \sin \alpha / N' \sin \alpha'$. Equation of these two expressions shows that the one coordinate length

$$z = \frac{2\pi}{\lambda} \rho N \sin \alpha = \frac{2\pi}{\lambda} \rho' N' \sin \alpha' \quad \dots\dots(4)$$

can be used to define equally ρ or ρ' . This is convenient since it is the variable (4) which appears in the functions expressing the amplitude in the diffraction distributions.

Consider now an opaque plane containing two small apertures, P_1, P_2 . The sizes of P_1 and P_2 will be assumed to be equal and both small compared with the Rayleigh resolution of the objective O , by means of which the two points are imaged at P_1', P_2' . Let α, α' in (4) refer to the objective O , and let $\rho_0 = P_1 P_2, \rho_0' = P_1' P_2'$. Then

$$z_0 = \frac{2\pi}{\lambda} \rho_0 (N.A.)_0 \quad \dots\dots(5)$$

is the optical separation of P_1 and P_2 . $(N.A.)_0 = N \sin \alpha$ is the numerical aperture of the objective.

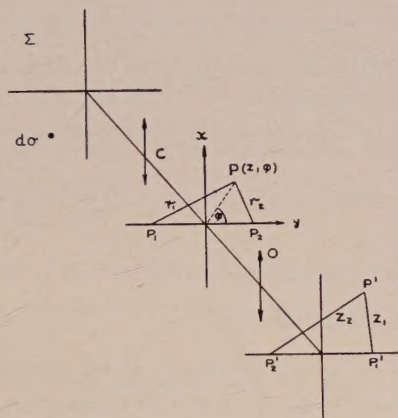


Figure 1.

If an element $d\sigma$ of the source Σ is imaged at $P(z, \phi)$ by the condenser C , the amplitude associated with the image of $d\sigma$ will be that in an Airy disc with centre at P . Let $\rho_1 = PP_1, \rho_2 = PP_2$. Then the amplitude at P_1 due to $d\sigma$ may be written

$$u_1 = \frac{J_1 \left\{ \frac{2\pi}{\lambda} \rho_1 (N.A.)_C \right\}}{\frac{2\pi}{\lambda} \rho_1 (N.A.)_C} = \frac{J_1(sr_1)}{sr_1}, \quad \dots\dots(6)$$

where $(N.A.)_C$ is the numerical aperture of the condenser, and $s = (N.A.)_C / (N.A.)_0$. The variable r_1 is defined by $r_1 = (2\pi/\lambda) \rho_1 (N.A.)_0$. It is the optical measure of ρ_1 for the objective. The amplitude produced by $d\sigma$ at P_2 is given by

$$u_2 = \frac{J_1(sr_2)}{sr_2}, \quad \dots\dots(7)$$

where r_2 is similarly defined for ρ_2 . The condenser is assumed to be free from aberration and perfectly focused.

The diffraction images of the points P_1, P_2 will be Airy discs centred on P_1', P_2' respectively. The amplitude produced at P' by disturbances originating at P_1, P_2 will therefore be given by

$$u = u_1 \frac{J_1(z_1)}{z_1} + u_2 \frac{J_1(z_2)}{z_2},$$

where z_1, z_2 are the optical distances $P_1'P', P_2'P'$. The disturbances u_1, u_2 are coherent, since they derive from the same element $d\sigma$ of the source. To find the intensity at P' due to the whole source requires the integration of u^2 over the domain Σ . That is

$$I(z_1, z_2) = \int_{\Sigma} \left\{ u_1 \frac{J_1(z_1)}{z_1} + u_2 \frac{J_1(z_2)}{z_2} \right\}^2 d\sigma. \quad \dots\dots (8)$$

Expanding the expression in brackets in (8),

$$I(z_1, z_2) = \left\{ \int_{\Sigma} u_1^2 d\sigma \right\} \frac{J_1^2(z_1)}{z_1^2} + \left\{ \int_{\Sigma} u_2^2 d\sigma \right\} \frac{J_1^2(z_2)}{z_2^2} + 2 \left\{ \int_{\Sigma} u_1 u_2 d\sigma \right\} \frac{J_1(z_1)}{z_1} \frac{J_1(z_2)}{z_2}. \quad \dots\dots (9)$$

Using the expressions (6) and (7) for u_1 and u_2 the integrals in (9) may be evaluated. To do this the domain Σ is assumed to be of infinite extent. Physically this requires that the geometrical image of the source shall be large compared with the distance P_1P_2 .

Let P_1, P_2 be at the points $(-y, 0), (+y, 0)$ where $2y = z_0$. (z, ϕ) are the coordinates of P . Then

$$r_1^2 = y^2 + z^2 + 2yz \cos \phi, \quad r_2^2 = y^2 + z^2 - 2yz \cos \phi$$

and the integral in the first term of (9) is

$$\int_{\Sigma} u_1^2 d\sigma = \int_0^{\infty} z dz \int_0^{2\pi} \left\{ \frac{J_1\{s(y^2 + z^2 + 2yz \cos \phi)^{1/2}\}}{s(y^2 + z^2 + 2yz \cos \phi)^{1/2}} \right\}^2 d\phi.$$

The domain of integration has been formally extended to the infinite plane. The integral remains unchanged if the origin is displaced to the point $(-y, 0)$. It is then given by

$$\int_{\Sigma} u_1^2 d\sigma = \int_0^{\infty} z \left\{ \frac{J_1(sz)}{sz} \right\}^2 dz \int_0^{2\pi} d\phi = \frac{\pi}{s^2} \quad \dots\dots (10)$$

since

$$\int_0^{\infty} \frac{J_1^2(t)}{t} dt = \frac{1}{2}.$$

By a similar procedure the integral in the second term of (9) is found to be

$$\int_{\Sigma} u_2^2 d\sigma = \pi/s^2. \quad \dots\dots (11)$$

There remains the integral in the third term.

This third integral is

$$\int_{\Sigma} u_1 u_2 d\sigma = \int_0^{\infty} z dz \int_0^{2\pi} \frac{J_1\{s(y^2 + z^2 + 2yz \cos \phi)^{1/2}\}}{s(y^2 + z^2 + 2yz \cos \phi)^{1/2}} \frac{J_1\{s(y^2 + z^2 - 2yz \cos \phi)^{1/2}\}}{s(y^2 + z^2 - 2yz \cos \phi)^{1/2}} d\phi$$

which may be written

$$\int_{\Sigma} u_1 u_2 d\sigma = \int_0^{\infty} z dz \int_0^{2\pi} \frac{J_1(sz)}{sz} \cdot \frac{J_1\{s(z_0^2 + z^2 - 2z_0 z \cos \phi)\}^{1/2}}{s(z_0^2 + z^2 - 2z_0 z \cos \phi)^{1/2}} d\phi \quad \dots\dots(12)$$

if the origin is displaced to the point $(-y, 0)$, and $2y$ is replaced by z_0 .

The integrand in (12) may be expanded with the aid of Neumann's addition theorem for the Bessel functions (Watson 1942). Thus, consider the differentiation

$$\frac{\partial}{\partial \phi} \{J_0(R)\} = -\frac{J_1(R)}{R} ab \sin \phi,$$

where $R = \{a^2 + b^2 - 2ab \cos \phi\}^{1/2}$. Neumann's theorem has the form

$$J_0(R) = J_0(a)J_0(b) + 2 \sum_{p=1}^{\infty} \cos p\phi J_p(a)J_p(b).$$

Differentiating this last with respect to ϕ , and substituting for $(\partial/\partial \phi)\{J_0(R)\}$, there is found the result

$$\frac{J_1(R)}{R} b = \frac{2}{a} \sum_{p=1}^{\infty} \frac{p \sin p\phi}{\sin \phi} J_p(a)J_p(b).$$

If $a = sz_0$, $b = sz$, substitution of this expression in (12) gives

$$\int_{\Sigma} u_1 u_2 d\sigma = \frac{2}{s^2 z_0} \int_0^{\infty} \frac{J_1(sz)}{z} dz \int_0^{2\pi} \sum_{p=1}^{\infty} \frac{p \sin p\phi}{\sin \phi} J_p(sz_0)J_p(sz) d\phi.$$

The integral in ϕ has the value 2π when p is odd, and is zero when p is even.

That is

$$\int_{\Sigma} u_1 u_2 d\sigma = \frac{4\pi}{s^2} \sum_{p=1, 3, \dots}^{\infty} p \frac{J_p(sz_0)}{sz_0} \int_0^{\infty} \frac{J_1(sz)J_p(sz)}{z} dz.$$

The remaining integral in z is one of Lommel's integrals (Watson 1942). It has the value zero for odd integral values of p , except $p=1$. In this case it is equal to $\frac{1}{2}$. Hence

$$\int_{\Sigma} u_1 u_2 d\sigma = \frac{\pi}{s^2} \frac{2J_1(sz_0)}{sz_0}, \quad \dots\dots(13)$$

the remaining terms in the p summation being zero.

Using (10), (11) and (13) in (9), the intensity at the point P' is found to be

$$I(z_1, z_2) = \frac{J_1^2(z_1)}{z_1^2} + \frac{J_1^2(z_2)}{z_2^2} + 2 \frac{2J_1(sz_0)}{sz_0} \frac{J_1(z_1)}{z_1} \frac{J_1(z_2)}{z_2} \quad \dots\dots(14)$$

from which the common factor π/s^2 has been omitted.

Some interesting conclusions follow at once from (14). If sz_0 is a root of $J_1(sz_0)=0$, other than $sz_0=0$, the product term is absent. The intensity $I(z_1, z_2)$ is then expressed by the sum of the separate intensities associated with P_1 and P_2 . P_1, P_2 are therefore incoherently illuminated. In particular, this will be so, if $s=1$, when z_0 is a non-zero root of $J_1(z_0)=0$: that is, when the points P_1, P_2 are separated by a distance equal to the radius of any dark ring of the Airy pattern associated with the objective aperture. When P_1, P_2 are on the limit of resolution (2), these points will therefore be incoherently illuminated if the numerical aperture of the condenser is equal to that of the objective. Under these conditions the resolution of two illuminated small apertures is given by the expression (2).

If the aperture of the condenser is made limitingly small, (14) becomes

$$I(z_1, z_2) = \left\{ \frac{J_1(z_1)}{z_1} + \frac{J_1(z_2)}{z_2} \right\}^2 \quad \dots\dots (15)$$

since $\lim_{s \rightarrow 0} \{2J_1(sz_0)\}/(sz_0) = 1$. The points P_1, P_2 are then coherently illuminated no matter what their separation, z_0 . The significance of this in practice is best seen by noting that $2J_1(sz_0)/sz_0 = 0.880$ when $sz_0 = 1$. If $s = \frac{1}{10}$, points in a circle of radius $z_0 = 10$ will be very nearly coherently illuminated. The diameter of this coherently illuminated area ($2z_0 = 20$) is approximately five times the limit resolution ($z_0 = 3.83$) of the objective for two incoherent point sources.

To investigate the intensity along the line $P_1'P_2'$, a coordinate x measured from the mid-point of $P_1'P_2'$ may be used. The intensity at $P'(x)$ is then given by

$$I(x) = \frac{J_1^2(x+y)}{(x+y)^2} + \frac{J_1^2(x-y)}{(x-y)^2} + 2 \frac{2J_1(sz_0)}{sz_0} \frac{J_1(x+y)}{x+y} \frac{J_1(x-y)}{x-y}, \quad \dots\dots (16)$$

where $y = \frac{1}{2}z_0$ as before.

It is a simple matter, using (16), to find the separations of P_1P_2 which give a decrease in intensity of 26.4% at O , when s has different values. In this manner the value of K has been found for the range $s = 0.0 - 2.0$. The curve of Figure 2

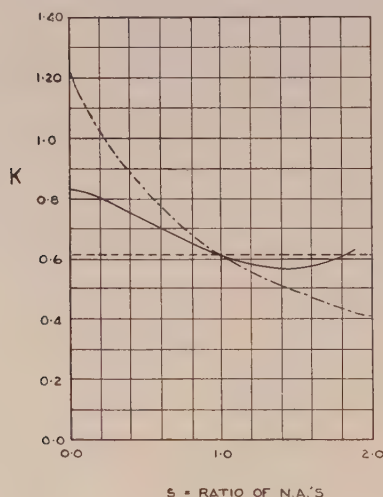


Figure 2.

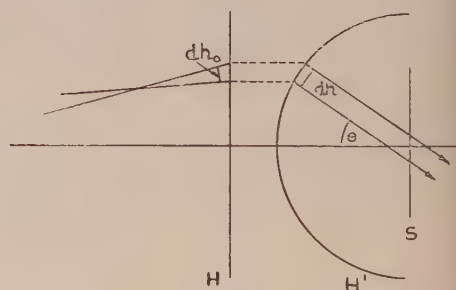


Figure 4.

shows the variation of K with s . If the influence of the aperture of the condenser on resolution is ignored, $K = 0.61$ for all values of s . This is the broken straight line in Figure 2. The broken curved line shows K as a function of s on the basis of the rule attributed to Abbé. According to this the effective aperture is the mean of the apertures of the condenser and the objective. It leads to an absurd result if the numerical aperture of the objective tends to zero. On the other hand it gives a rough approximation to the present result if $0.5 < s < 1.0$. When one remembers the other factors (such as scattered light, contrast in the object) which influence the resolution of the microscope, it is not surprising that the Abbé rule has been acceptable in practice.

§ 3. KÖHLER ILLUMINATION

In critical illumination coherent light from an element of the illuminant is found in the object plane as an Airy distribution of amplitude. Thus a single element of the illuminant illuminates any two points in the object co-phasally, but with different amplitudes. In Köhler illumination coherent light from an element of the illuminant illuminates two points in the object with light of the same amplitude but having a phase difference. The arrangement is shown diagrammatically in Figure 3.

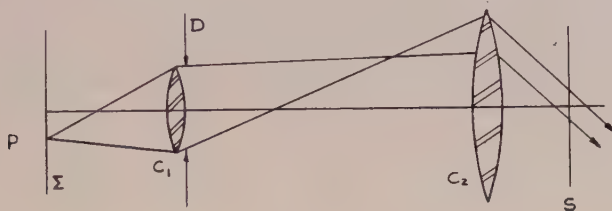


Figure 3.

The source Σ is imaged by a condenser C_1 in the focal plane of a second condenser C_2 , which is further arranged to image a diaphragm D in the plane of the object S . Light from an element P of Σ therefore results in a plane wave falling obliquely on the axial region of the object plane S . The object is illuminated by a set of plane waves whose normals lie within the cone subtended by C_2 at S . Let this cone be of semi-angle β , and write $N \sin \beta = s(\text{N.A.})_0$, $(\text{N.A.})_0$ being the numerical aperture of the objective, and N the refractive index of the space between C_2 and S .

Consider two points in the object S , such as P_1, P_2 in Figure 1. The plane wave falling on S whose normal makes an angle θ with the axis in the azimuth ϕ will have a phase retardation $ikN \sin \theta \cdot \rho \cos \phi$ at P_2 relative to the phase at P_1 . The disturbances at P_1 and P_2 are thus given by

$$\left. \begin{aligned} u_1 &= A, \\ u_2 &= A \exp(-ikN \sin \theta \cdot \rho \cos \phi), \end{aligned} \right\} \dots\dots(17)$$

where A is the real amplitude at these two points.

The condensers are assumed to be free from aberration. They therefore satisfy the sine condition, and in consequence the rear unit surface of C_2 will be a sphere with its centre at the axial point of S . If A_0 is the amplitude of the incident wave at the unit surface H (Figure 4) of C_2 , and A is the amplitude of the emergent wave at the other unit surface H' , then the conservation of energy requires that $A_0^2 dh_0 = A^2 dh$ where dh_0, dh are elements of area. Now $dh = dh_0 / \cos \theta$, hence

$$A = A_0 \cos^{1/2} \theta \dots\dots(18)$$

and the expressions (17) become

$$\left. \begin{aligned} u_1 &= A_0 \cos^{1/2} \theta, \\ u_2 &= A_0 \cos^{1/2} \theta \exp(-ikN \sin \theta \cdot \rho \cos \phi). \end{aligned} \right\} \dots\dots(19)$$

Let P_1', P_2' be the images of P_1, P_2 (as in Figure 1) and let P' be a point (z_1, z_2). Then the intensity at P' is given by

$$I(z_1, z_2) = \iint \left| u_1 \frac{J_1(z_1)}{z_1} + u_2 \frac{J_1(z_2)}{z_2} \right|^2 d\Omega \quad \dots\dots(20)$$

as in (8), but here u_1, u_2 have the values given in equation (19). $d\Omega$ is an element of solid angle equal to $\sin \theta d\theta d\phi$, and the limits of integration are $0-2\pi$ for ϕ and $0-\beta$ for θ . Further, since u_2 is complex, it is the squared modulus which appears in the integrand of (20). Hence corresponding to (9), (20) gives

$$\begin{aligned} I(z_1, z_2) = & \left\{ \int_0^\beta \int_0^{2\pi} \sin \theta \cos \theta d\theta d\phi \right\} \left\{ \frac{J_1^2(z_1)}{z_1^2} + \frac{J_1^2(z_2)}{z_2^2} \right\} \\ & + 2 \frac{J_1(z_1)}{z_1} \frac{J_1(z_2)}{z_2} \int_0^\beta \int_0^{2\pi} \cos(kN \sin \theta \cdot \rho \cos \phi) \cdot \sin \theta \cos \theta d\theta d\phi \end{aligned} \quad \dots\dots(21)$$

a constant factor A_0^2 being omitted.

The integral in the first term of (21) has the value $\pi \sin^2 \beta$. The integral in the second term is equal to

$$2\pi \int_0^\beta \sin \theta \cos \theta J_0(kN\rho \sin \theta) d\theta;$$

writing $x = kN\rho \sin \theta$, and $sz_0 = kN\rho \sin \beta$, this integral becomes

$$\frac{2\pi \sin^2 \beta}{s^2 z_0^2} \int_0^{sz_0} x J_0(x) dx = \pi \sin^2 \beta \frac{2J_1(sz_0)}{sz_0}.$$

Omitting the factor $\pi \sin^2 \beta$, (21) is now

$$I(z_1, z_2) = \frac{J_1^2(z_1)}{z_1^2} + \frac{J_1^2(z_2)}{z_2^2} + 2 \frac{2J_1(sz_0)}{sz_0} \frac{J_1(z_1)}{z_1} \frac{J_1(z_2)}{z_2} \quad \dots\dots(22)$$

which is identical with (14). Hence integrating the phases in Köhler illumination leads to precisely the same result as integrating the amplitudes in critical illumination.

This result is of considerable interest in practical microscopy. It shows that, given a broad source of uniform intensity, the appearance of the image will be independent of whether Köhler or critical illumination is employed. The Köhler system has, however, two distinct advantages in other respects. There is no difficulty in obtaining uniform illumination of the object, and the area of the object in which light falls may be controlled by the diaphragm D. By this means scattered light can be reduced with considerable improvement in the contrast of the image.

It is unfortunate that critical and Köhler illumination are designated in French by the terms 'éclairage incohérente' and 'éclairage cohérente' respectively. The identity of the expressions (14) and (22) shows that the coherence between points in the object plane in the two cases must be exactly the same when the condensers have the same numerical aperture.

REFERENCES

- FRANÇON, M., 1950, *Le contraste de phase* (Paris : Édit. Rev. Opt. Théor. Instrum.).
 MARTIN, L. C., 1931, *Proc. Phys. Soc.*, **43**, 186.
 RAMSAY, B. P., CLEVELAND, E. L., and KOPPIUS, O. T., 1941, *J. Opt. Soc. Amer.*, **31**, 26.
 SPARROW, C. M., 1916, *Astrophys. J.*, **44**, 76.
 WATSON, G. W., 1942, *Bessel Functions* (Cambridge : University Press), p. 134.
 ZERNIKE, F., 1938, *Physica*, **8**, 785.

Reflectivity of Thin Silver Films and their Use in Interferometry

By H. KUHN AND B. A. WILSON *

Clarendon Laboratory, Oxford

MS. received 31st March 1950

ABSTRACT. A direct photoelectric method allowed the reflectivity R and the transmissivity T of partially reflecting films to be measured to an accuracy of 0.3% of the incident light intensity. For a large number of silver films, deposited on glass by evaporation *in vacuo*, the values of R and T were measured for visible light of five different wavelengths, in the range of high reflectivities ($R > 0.7$). The change of R as a function of time was also studied. With only moderate control of the conditions of surface cleaning and evaporation, the values of R were nearly always found to lie close to a 'standard' curve giving R as a function of T , the wavelength, and the age of the film. Possible causes of scatter from this standard curve were investigated. T was found not to obey an exponential law as a function of the thickness.

On the basis of these results, resolving power and brightness of etalon fringes were plotted as functions of T . The conclusion is reached that, in most practical cases, the resolving power of etalons for visible light is limited by imperfections of the surfaces rather than by the reflectivity of the silver films, if their thickness is properly chosen.

§ 1. INTRODUCTION

IN instruments based on the interference of multiple beams, transparent silver films of high reflectivity are widely used. The Fabry-Perot etalon and interference filters are among the most important examples. The resolving power of these instruments is essentially proportional to $1/(1 - R)$, where R is defined as the ratio of the intensities of reflected and incident light. In increasing the value of R by increasing the thickness of the film, a practical limit is set by intensity requirements, since the transmission factor T decreases rapidly. Beyond a certain limit, the resolving power can only be increased at considerable sacrifice of intensity. The accurate knowledge of the value of R which can be obtained for a given value of T at a given wavelength is therefore of practical value in interferometry.

Though a number of observers have carried out direct measurements of reflectivities of silver films, our knowledge of the values of R and T in the range of high reflectivity ($R > 0.75$) is far from adequate.

The discrepancies between results of different observers and the scatter of the values obtained by any one observer are very large, and it is unknown how far these differences are caused by errors of the measurements, which are generally as great as 1% and often more.

Measurements of widths of interference fringes have given lower limits of reflectivities but, especially for high values of R , the results are considerably affected by imperfections of the plate surfaces.

In order to study not only the values of the reflectivity as a function of transmission and wavelength, but also the scatter of the values of R for films deposited under similar conditions and the change of R with ageing, it was necessary to make the errors of measurement considerably smaller than these variations. This

* Rhodes Scholar.

aim was achieved in the experiments described below. They were mainly intended to provide an answer to the following questions : (i) What value of R can be obtained for any given value of T between 0 and 0.2 and any given wavelength of visible light, if a good standard technique of surface cleaning and evaporation is used, and what is the amount of scatter about this 'standard' value of R ? (ii) How does the value of R change in the course of time, if the film is kept under the same conditions as in ordinary spectroscopic use ?

Regarding the influence of the numerous factors of surface conditions, vacuum and speed of evaporation, some useful information was obtained, but a comprehensive study of this question was not attempted.

§ 2. THE OPTICAL METHOD

The principle of the method employed is simple and well known, but the accuracy of the results depends on some details which are not quite obvious and will therefore be described (Figure 1).

The plate P , carrying the film whose reflectivity is to be measured, is mounted on a spectrometer table, with the axis of rotation passing through the reflecting surface. The metal plate holding P has a circular aperture Q of diameter 1.1 cm. The light source S is in a fixed position, 200 cm. from P . A photo-multiplier M is

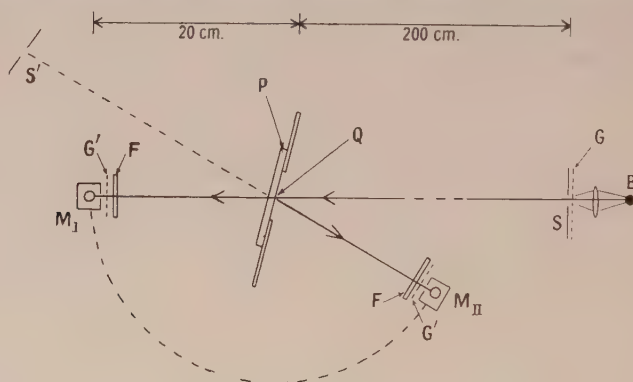


Figure 1. The optical system.

mounted on the movable arm of the spectrometer. In position M_I , the photo-multiplier receives light passing from S through Q directly when P is removed, or after passage through the plate P when this is inserted. In position M_{II} , it receives light reflected from P at a small angle of incidence (about 15°). This light can be regarded as coming from the virtual image S' of the source. The distance of S' from M_{II} is the same as that of S from M_I . The intensities observed in the three experiments are therefore in the ratio $1 : T : R$, provided the following conditions are fulfilled: (a) The light source and the aperture of the photocell must be so small that any ray passing from one to the other intersects the plane of P well inside the stop Q . (b) The light source must emit uniformly in all directions within the solid angle subtended by the aperture of the receiving system, and the latter must have an isotropic response. These conditions are especially important since S' is the mirror image of S , so that lack of uniformity in the angular distribution of the emitted light will have different effects in the two positions of M . (c) Light scattered by the mount of the reflecting plate, by the reflecting surface

itself, and by any other parts of the apparatus must be negligible. (d) The reflecting plate P must be sufficiently plane. (e) All geometrical adjustments have to be sufficiently accurate: the plane of P must pass through the axis of rotation, and the plane defined by S, M_I and M_{II} must be normal to the axis of rotation, and the lines SM_I and SM_{II} must pass approximately through the centre of Q.

In order to fulfil conditions (a) and (b), light from a 24-watt bulb B, connected to a large battery, was focused on a ground glass G which was fitted with a circular stop of diameter 5 mm. A similar ground glass G' and stop were fixed in front of the photo-multiplier.

The surface of the brass plate holding P was covered with black velvet paper. When M was set only slightly off the angle of reflection, the intensity fell to zero, showing practical absence of scattered light including light scattered from P itself. The intensity measured as a function of small horizontal or vertical displacements of M from the reflection position showed a symmetrical curve with a flat top whenever all adjustments had been carefully made.

The photo-multiplier, type R.C.A. I.P.21, was connected directly to a galvanometer. By varying the distance of the light source from the photocell and applying the inverse square law, it was found that the galvanometer deflection was not strictly proportional to the intensity, and all readings had to be corrected accordingly.

The effective wavelength range in each experiment was a function of the colour filter used, of the spectral intensity distribution of the source and of the response curve of the photosensitive layer. The latter has a maximum at about 4100 Å. and the sensitivity decreases rapidly in the near infra-red. From spectroscopic examination of the filters, the effective wavelength was estimated.

The Table gives a list of the filters used, the estimated limits of the effective wavelength bands, and the approximate centre of gravity of each band.

Ilford red	6400–7200 Å.	6800 Å.
Ilford green	5100–5400 Å.	5200 Å.
Ilford blue-green	4700–5200 Å.	4900 Å.
Wratten No. 48	4400–5000 Å.	4700 Å.
Wratten No. 35	3900–4500 Å.	4200 Å.

The violet, blue and blue-green filters were used in conjunction with a cell containing copper sulphate solution.

The colour filters F (Figure 1) were placed very close to the small aperture in front of the photo-multiplier. When they were placed further away, the small local variations of density of the filters were found to cause errors up to 0.5%.

When a measurement was repeated, after removal and re-setting of P and readjustment of the instrument, the value of R was generally reproduced to within 0.3%, and disagreements greater than 0.5% were practically never found. The estimated limits of error of a single measurement of R was thus about ± 0.003 . With the precautions described, all possible systematic errors should have been practically negligible, and the stated limits of error are believed to represent the absolute accuracy of the values of R . The accuracy of measurement of T is a little greater, so that the value of $R + T$ for each film should rarely be in error by more than ± 0.005 .

In the method described, the value of R was measured at an angle of incidence of 15° , whereas in the Fabry–Perot interferometer the angle of incidence is practically zero. For opaque metal films, the change of R with the angle of incidence can be

calculated from the values of the optical constants and is found to be of opposite sign for light polarized in the plane of incidence and at right angles to it. For the average of the two planes of polarization, the difference between the values of R for 0° and 15° is quite negligible (of the order of 0.001). For transparent films, the theoretical formulae are complicated, but for the comparatively low transmission used in our experiments, the dependence of R on the angle cannot differ much from that for thick films. This was indirectly confirmed by some measurements with plane-polarized light; the differences of the values of R for the different planes of polarization were small and close to the values predicted by the theory for thick films.

The error made in regarding the values of R measured at an angle of 15° as the reflectivity for normal incidence is below 0.002 for dense films, but it may arise to about 0.01 for the lowest reflectivities measured.

§ 3. THE PREPARATION OF THE FILMS

The evaporation chamber consisted of a large brass tank evacuated by means of a mercury diffusion pump of a rated speed of 25 litre/sec., but the liquid air trap and the duct to the chamber may have reduced the speed to about half this value. The pressure in the tank was measured by means of a Penning gauge. It was between 3 and 5×10^{-5} mm. Hg during the evaporation. These values refer to calibration with air.

Two tungsten filaments of thickness 0.7 mm., each carrying two beads of silver, could be heated independently. A few turns of thin platinum wire were wound round the V-shaped parts of the filaments, according to common practice, in order to cause the silver to adhere to the filaments. When a fairly good vacuum had been reached, air was admitted to a pressure of a few millimetres of mercury, and a discharge from a spark coil was passed through the tank for 5 to 10 minutes before the pumping was resumed. This treatment was repeated once or twice. The actual evaporation lasted about 5 minutes.

In each evaporation, three sets of two glass plates were used, at distances of 18, 20, and 22 cm. respectively from the filaments. This method allowed the comparison of films deposited under exactly the same conditions of evaporation.

The glass plates were of good optical quality, accurately plane and parallel, and of size 4.1 cm. \times 3.2 cm. Some of the plates were polished lightly with rouge before they were taken into use, so that the surfaces were similar to those of new plates, but this process was not repeated after the plates had once been covered with silver. The plates were washed in nitric acid, then rinsed with tap water and dried with cotton wool of good commercial quality. The surface was considered satisfactory when breathing produced a uniform film.

For the ageing tests, the plates were kept in a glass container, protected from dust by a loosely fitting cover. The container was left in a Laboratory room which was free from tobacco smoke, flames and chemical fumes.

§ 4. THE MEASURED VALUES OF R AND T

In the final set of experiments, the results of which are reported here, 18 glass plates were coated with silver in the way described and each plate was measured four times, first immediately after removal from the evaporation tank, then after intervals of 3, 8, and 22 days from the time of deposition. Each time the values of T and R were measured for five different wavelengths. Six plates

were left to be re-measured after 68 days, while the other 12 plates were cleaned, re-silvered and measured again when new and after 22 days.

For the measurements of these 30 films immediately after evaporation and after 22 days, the values of $R + T$ are plotted in Figure 2. Within the range of T

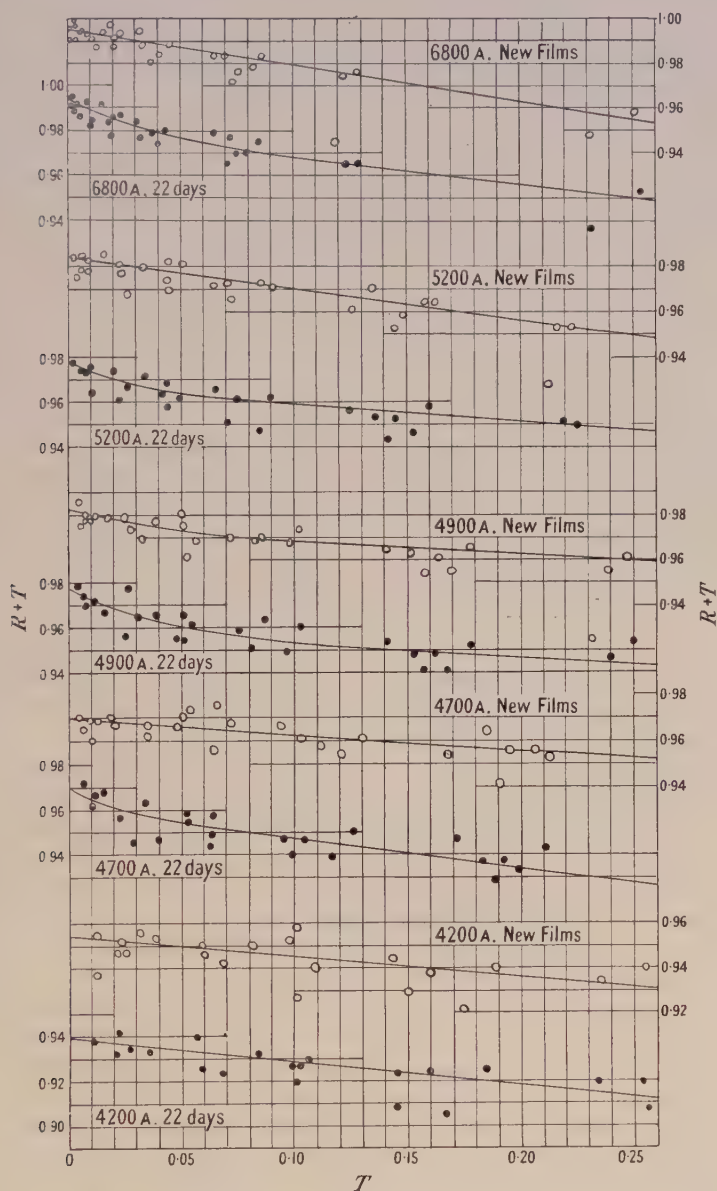


Figure 2. Measured values of $R + T$ as function of T .

plotted, these graphs contain all the measurements, without any selection. Only one film gave values so much below the curves (by about 5%) that they were not plotted for technical reasons, while for another film, for the same reasons, only the measurement in the red for the new film was included.

Since T changes with the wavelength, the same films do not appear at the same values of the abscissae for different curves. If this fact is taken into account, some groups of films can be seen to form similar 'constellations' of points in the graphs of different wavelengths. The group of 6 points which appears at 6800 Å. between $T=0.06$ and $T=0.09$ and at 5200 Å. between $T=0.12$ and $T=0.16$ forms an example of this fact which shows that the scatter of the points in the graphs is mainly due to genuine differences of the properties of the films, and only to a small extent to errors of measurement.

Most points lie quite close to a curve showing a decrease of $R+T$ with increasing transmission, i.e. decreasing thickness of the film. The absorption $A=1-R-T$ is thus found to increase with decreasing film thickness. Except for the violet where the scatter is somewhat larger, most points lie less than $\frac{1}{2}\%$ off the curve.

The curves of Figure 2 were used in plotting R as a function of T in Figures 3 (a) and 3 (b).

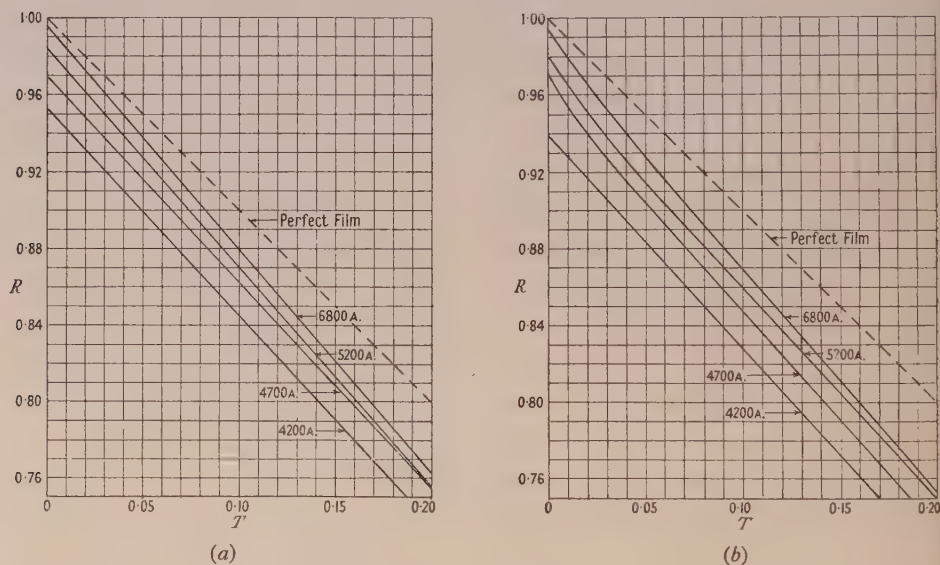


Figure 3. R as function of T .

(a) for new films, (b) for aged films (22 days).

The loss of reflectivity of the films as a result of ageing depends on the wavelength of the light and on the thickness of the film. Examination of Figure 2 and of other data shows that for dense films R decreases less rapidly than for thin films. In order to obtain a simplified picture of the process of ageing, on the basis of statistical evidence, the relative values of $R+T$ were averaged for the six films which were re-measured after 68 days, i.e. the average of $(R+T)/(R+T)_0$ for these six plates was plotted as a function of time in Figure 4, where $(R+T)_0$ is the value of $R+T$ for the new film. Since T changes little and is much smaller than R , this plot is almost identical with a plot of R/R_0 . The six films were of different thicknesses, but all of them, expressed in terms of interferometry, were fairly dense films for red, and fairly light films for violet light.

The values for red and green show that the rate of decrease of R becomes small after three weeks. The points for 4200 Å. cannot be fitted well by a simple curve;

examination of the individual results for the six plates and for others which were measured after 50 days makes it appear likely that the ageing curve for violet light is, in fact, not simple. In any case, it is certain that the reflectivity decreases with age more rapidly for shorter wavelengths.

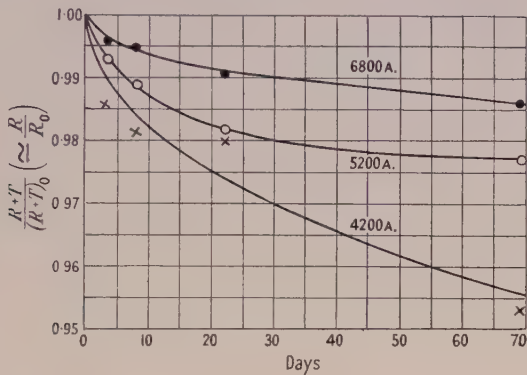


Figure 4. Relative change of R and $R+T$ with age.

A number of measurements made outside this systematic research confirms the conclusion that, in general, the rate of loss of reflectivity decreases with time ; one pair of etalon plates, whose properties had not been measured accurately immediately after deposition of the films, were found to have values of $R+T$ of

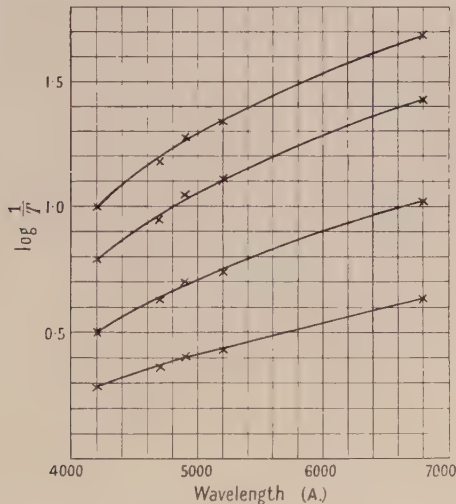


Figure 5. Optical density $D=\log 1/T$ as function of wavelength.

0.97 and 0.98 for red light after having been in use for over 6 months. In some films, the reflectivity was actually found to have increased after a few weeks, but in these cases, the initial values of $R+T$ had been abnormally low.

Figure 5 shows the optical density $D=\log 1/T$ plotted as function of the wavelength. The points forming each curve are averages of several films of very similar density.

§ 5. DISCUSSION OF THE RESULTS

Before this systematic research was undertaken, the instrument described in §2 had been used* for measuring the values of R and T for a considerable number of silver films deposited on etalon plates, most of which were made of fused silica. Most of these values agree well with the curves in Figure 2.

Since the scatter of the points in Figure 2 is much greater than the errors of the optical measurements and thus represents genuine differences in the properties of the films, it appeared desirable to establish the causes of these differences. But the large number of variables which might possibly influence the properties of the films allowed only tentative conclusions to be reached.

(i) Influence of conditions of evaporation. If vacuum conditions and speed of evaporation, within the range of variation in these experiments, had an important influence on the properties of the films, any two films deposited simultaneously at the same distance would tend to be more similar to one another than to other films of similar density. No effect of this kind was apparent. However, in comparing films of approximately equal density, but deposited at different distances from the target, some evidence was found for the smaller distance to produce slightly higher reflectivity. This effect, if real, could be interpreted as due to different speeds of evaporation.†

(ii) Influence of the type of glass. Of the 18 glass plates used, some consisted of glass appearing distinctly green when viewed end-on, while others appeared quite colourless. The results obtained with these two kinds of glass did not show any systematic differences. Silica plates, as mentioned before, also gave similar results.

(iii) Influence of surface conditions. Of six pairs of glass plates, each pair was coated together at the same distance, and the properties of the films were measured several times. The films were then removed with acid and the plates re-coated in the same way; in one case this procedure was repeated a third time. In six of these seven repeats, the plate which gave the higher value of R , compared with the 'standard' curve of Figure 2, in the first coating, also gave the higher value in the subsequent coating. The differences in question were of the order of 0.01. It thus appears that some surface conditions which are not effected by the cleaning process, are often responsible for producing a 'better' or 'worse' coating. In a few cases, imperfect cleaning was, no doubt, the cause of too low values of R , and on rare occasions even of much too low values.

Previously published direct measurements of reflectivities of transparent films (Romanowa, Robzow and Pokrowsky 1934, Goos 1936, Krautkrämer 1938, Strong and Dibble 1940) show so much more scatter than the values reported here that only rough comparison is possible.

The work of Strong and Dibble (1940) covers mainly the range of low and medium reflectivity and their measurements of R are only relative and hardly accurate enough for application to interferometry. The existence of two different types of silver films below a certain thickness, as reported by these authors, may be connected with our observation that thinner films are less stable than thicker

* These measurements were carried out in conjunction with Mr. L. C. Bradley and Dr. G. W. Series, and the results were reported at the International Conference on Optical Properties of Thin Films in Marseilles in April 1949.

† Note added in proof. R. S. Sennett and G. D. Scott (*J. Opt. Soc. Amer.*, 1950, **40**, 203) report a marked increase of reflectivity with increase of speed of evaporation.

ones. Our measurements do not extend to sufficiently thin films to allow direct comparison.

The measurements by Krautkrämer (1938) fall into the range of higher reflectivities, but were made with a small number of films only. Within their limits of error, stated as ± 0.01 , they are compatible with our results.

Among others, Tolansky (1946) and Dufour (1948) have given values of reflectivities, but lack of details does not allow comparison.

The reflectivity of opaque silver films, made by evaporation, was measured by Edwards and Petersen (1936). Their values for yellow and green light ($R=0.985$) are in very good agreement with our results in the limit of $T=0$ (see Figure 2).

Values of the reflectivity of silver films were derived from measurements of the width of interference fringes produced with etalons of very small spacings (Bright, Jackson and Kuhn 1949). This indirect method gave lower limits of $R+T$ which are perfectly consistent with our direct measurements. The increase of $R+T$ with increasing thickness of the films was, in these indirect measurements, disguised by the imperfections of the etalon plates, an effect which becomes more important as R increases.

For opaque films, the reflectivity can be calculated from the optical constants, but the results of such calculations have generally been found to be too low. If the values from the latest measurements of the optical constants of freshly deposited silver (Hass 1946) are compared with our limits of R for $T=0$, this discrepancy still exists. The measured values of R exceed the derived values by amounts increasing from 0.02 in the red to 0.06 in the violet.

For transparent films, the formulae of the theory are rather complicated. Calculations by Barns and Czerny (1931) show a rate of decrease of $R+T$ with increasing T which is similar to that found in our experiments, but their absolute values are consistently lower.

Though the thickness of the films was not measured, the results plotted in Figure 5 show that the intensity of the transmitted light does not vary exponentially with the thickness of the film; if the exponential law of absorption were valid, the ratio of the optical densities for any two films would be the same for different wavelengths. Figure 5 shows that these ratios are quite different for red and violet. Some indication of this fact was found by Bright, Jackson and Kuhn (1949).

One can demonstrate this effect, which is, of course, theoretically not unexpected, by a simple qualitative experiment; a pile of glass plates, each carrying a thin silver film, shows a deep violet colour in transmission, very different from the blue of a single, dense film.

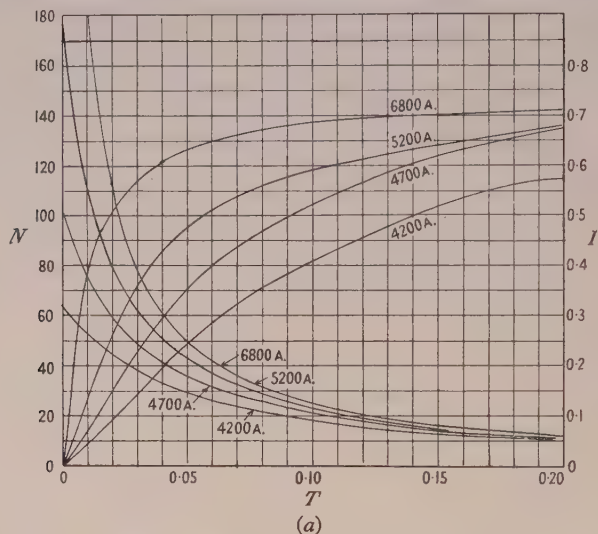
§ 6. APPLICATION TO INTERFEROMETRY

The resolving power of the Fabry-Perot etalon can be defined in various ways, and a number of authors have tabulated it as a function of R . A very convenient definition (Bright, Jackson and Kuhn 1949) considers two lines as just resolved if their distance is equal to the instrumental half-value width; the resulting intensity curve shows a depression of about 20% for lines of equal intensity, as in the Rayleigh condition for gratings and prisms. A simple expression for the resolving power can then be derived if in Airy's formula the sine of the phase angle is replaced by the angle itself, near the maxima of the intensity. This approximation is accurate enough, as long as the reflectivity is not much below 0.8. If the resolving power is expressed, in the usual way, as the product of the order of

interference n and a factor N which can be considered as the effective number of interfering beams, the latter is found to be

$$N = \pi \sqrt{R/(1-R)}.$$

With the use of the measurements described above, the value of N is plotted as a function of T , for new and for 22 days old silver films, in Figures 6(a) and 6(b).



5200 Å. refers to second curve, not first.

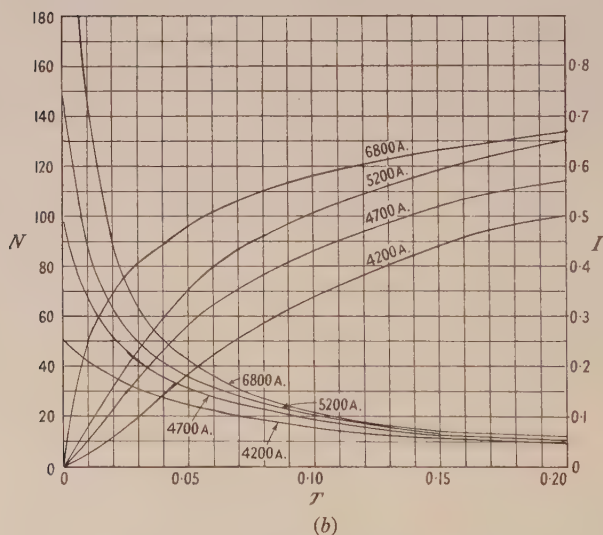


Figure 6. Effective number of beams N and intensity I of etalon fringes.
(a) for new films, (b) for aged films (22 days).

In the same Figures, the intensity of the maxima, $I = \{T/(1-R)\}^2$, is plotted. These graphs make it possible to find the value of T , for a given colour, which gives the best compromise of the requirements of resolving power and intensity. If, for example, an intensity of the fringes of 0.3 of that without any etalon is required, for a several weeks old film, Figure 6(b) shows that for red light 1/110 of one order can be

resolved, and for green light $1/40$ of one order, provided the etalon plates are perfect. The required transmission factors are 0.015 and 0.04 respectively, for these two colours. If the value of T is to be measured with light of any other colour, the curves in Figure 5 allow the necessary conversion to be made.

It must be remembered that the formula $I = \{T/(1-R)\}^2$ gives the correct intensity only for monochromatic light. If the spectral width of the line under investigation is comparable with the instrumental width, the intensity is lower.

The surfaces of commercially obtainable etalon plates are generally not good enough to allow a smaller fraction than $1/50$ of one order to be resolved, and less than this for plates of large size. Our measurements show that, certainly for wavelengths of over 5000 Å., a considerable increase in resolving power could be achieved with ordinary silver films, if etalon plates with more perfect surfaces were available.

ACKNOWLEDGMENT

The authors wish to acknowledge the contribution due to Mr. L. C. Bradley and Dr. G. W. Series, especially in the earlier stages of this work.

REFERENCES

- BARNES, R. B., and CZERNY, M., 1931, *Phys. Rev.*, **38**, 338.
BRIGHT, R. J., JACKSON, D. A., and KUHN, H., 1949, *Proc. Phys. Soc. A*, **62**, 225.
DUFOUR, CH., 1948, *Le Vide*, **3**, 480.
EDWARDS, H. W., and PETERSEN, R. P., 1936, *Phys. Rev.*, **50**, 871.
GOOS, F., 1936, *Z. Phys.*, **100**, 95.
HASS, G., 1946, *Optik*, **1**, 8.
KRAUTKRÄMER, J., 1938, *Ann. Phys., Lpz.*, (5) **32**, 537.
ROMANOWA, M., ROBZOW, A., and POKROWSKY, G., 1934, *Phys. Z. Sowjet*, **5**, 746.
STRONG, J., and DIBBLE, B., 1940, *J. Opt. Soc. Amer.*, **30**, 431.
TOLANSKY, S., 1946, *Physica*, **12**, 649.

The Absorption Spectra of Solid Lead Sulphide, Selenide and Telluride

By A. F. GIBSON

Telecommunications Research Establishment, Ministry of Supply

Communicated by R. A. Smith; MS. received 6th March 1950

ABSTRACT. Recent interest in lead sulphide, selenide and telluride as photoconductors makes information on their absorption spectra valuable. It is found that the absorption spectrum of each material is characterized by strong absorption in the visible and ultra-violet region, with a further band in the infra-red. The effects of temperature and oxidation are also studied.

In PbS the forbidden energy region between the filled and empty bands is found to be about 1.3 ev. in width, not 0.4 ev. as previously suggested. Hence photoconductivity in PbS cannot be associated with the main lattice. The corresponding energy gaps in PbSe and PbTe are found to be about 1.05 ev. and 0.9 ev. respectively.

§ 1. INTRODUCTION

THE absorption spectra of insulators and semiconductors are usually characterized by very strong absorption at short wavelengths (usually in the ultra-violet region) with a sharp edge on the long wavelength side. This absorption is generally assumed to be due to electronic transitions between the highest filled energy band and the lowest empty energy band of the solid. The absorption coefficient is usually of the order of 10^5 or 10^6 cm⁻¹.

The lattice absorption edge is often followed on the long wavelength side by an absorption band or tail of much lower absorption coefficient, of the order of 10 cm⁻¹. This absorption is generally dependent on the conditions of sample preparation and is thought to be due to impurities, cracks and other defects in the crystal lattice.

The absorption spectra of PbS, PbSe and PbTe are not exceptions to these general conditions, though the long wavelength tail absorption bands have considerably larger absorption coefficients and bandwidths than those usually encountered in sulphides.

The photoconductive properties of PbS and its associated compounds are well known (Sosnowski *et al.* 1947, Moss 1949, Chasmar 1948). The spectral response of all three materials is characterized by a sharp cut-off at long wavelengths occurring at about 3μ for PbS and about 5μ for PbSe and PbTe. In all cases the long wavelength limit moves to longer wavelengths on cooling. Early theoretical work (Sosnowski *et al.* 1947) suggested that the photoconductivity of PbS was due to absorption in the bulk lattice. This implies that the minimum energy difference between the highest filled band and the conduction band of PbS is about 0.4 ev., and less for the selenide and telluride.

The photoconductivity of PbS and its associated compounds is largely determined by suitable treatment with oxygen (Sosnowski *et al.* 1947, Schwarz 1948). Recent work in this laboratory (Gibson and Moss 1950) together with other unpublished work by Mr. A. S. Young, has shown that oxygen treatment has very marked effects on the photosensitivity spectrum. Thus in the case of PbTe photoconductivity is limited to wavelengths less than 3μ without oxygen treatment, moving to 5μ on oxidation. This and similar work suggests that photosensitivity in these materials is not primarily a property of the bulk lattice.

§ 2. EXPERIMENTAL METHODS

Lead sulphide and lead selenide layers may be prepared by two methods: evaporation *in vacuo* or chemical deposition from colloidal solution (Kicinski 1948). Layers of PbTe have not, as yet, been successfully deposited chemically and hence only evaporated PbTe layers have been examined. Layers were mounted on discs of polished quartz, artificial sapphire or KRS5 (a mixed crystal of thallium bromo-iodide) depending on the wavelength range under examination. Chemical methods of deposition gave layers of the greater reproducibility and uniformity of thickness. Within the limits of chemical analysis (1%), PbS layers deposited chemically are pure PbS.

The chief errors in absorption measurements on thin films are as follows: Firstly the layers consist of small microcrystals (of the order of 1000 Å. in size) and transmission between grains may be more important than transmission through grains. This effect is easily detected as an apparently constant absorption with wavelength and may be eliminated by careful layer preparation. In particular, chemical layers are superior in this respect to evaporated layers. A second important source of error is due to scattering of light by individual grains of the layer. This effect may be eliminated by collecting the transmitted radiation in a spherical mirror of high aperture.

The third remaining error is due to reflection. As the refractive index of PbS, PbSe and PbTe is very high (about 4.0 for PbS and over 5.0 for PbTe) the reflection coefficient is high and reflection represents a most serious source of error. When the absorption within the specimen is large (say 99% or greater) the error due to reflection can be ignored. When the percentage absorption falls to low values, however, on the long wavelength side of the lattice absorption edge, reflection introduces an apparent absorption which may be greater than the true absorption.

To eliminate reflection errors two specimen layers were prepared simultaneously under exactly similar conditions, except that one layer was arranged to be thicker than the other. The transmission through each layer was measured concurrently at each wavelength. The chief reflection, which occurs at the air-specimen interface, is the same for both layers. Errors due to reflections at the specimen-mount interface and mount-air interface are only equal in each layer if the absorption in the specimen is zero, but this is where reflection errors would otherwise be most serious. When the layers differ in transmission by a factor of five, the remaining reflection error is about 1%.

If the two layers have thicknesses d_1 and d_2 respectively, the absorption coefficient being α , then

$$J_1 = J_0(1 - R) \exp(-\alpha d_1) \quad \text{and} \quad J_2 = J_0(1 - R) \exp(-\alpha d_2)$$

where J_1 and J_2 are the intensities of the transmitted beams, J_0 the intensity of the incident beam and R the reflection coefficient of the air-specimen interface.

Hence
$$\alpha = \frac{\ln J_1/J_2}{(d_2 - d_1)}.$$

In the presentation of the results $\log J_1/J_2$ has been plotted. To obtain the absolute value of α the difference in layer thickness must be known. This is obtained by weighing, but high accuracy is not possible. Values of α are indicated alongside those of $\log J_1/J_2$.

The errors inherent in this method that are not accounted for are as follows:

(i) Interference between reflected and incident beams. This effect would lead to an apparent absorption varying cyclically with wavelength. In fact no such effect was observed. This was thought to be due to the corrugated nature of the specimen surfaces.

(ii) If both the mount and specimen absorb at any particular wavelength, then the amount absorbed by each mount is not equal. This error can be arranged to be negligible.

(iii) In spite of identical preparation conditions a pair of layers may not, in fact, be identical. Tests showed that this source of error was unimportant in chemical layers, but occasionally evaporated specimens had to be abandoned because of this feature.

Another method of eliminating reflection errors was also examined. This consisted of measuring the transmission through a 'black body' type cone of Pyrex glass coated with PbS and collecting the transmitted radiation in a spherical mirror of large aperture. The absorption curve obtained over the limited wavelength range available, (0.3μ to 3.4μ) was the same as that obtained by the difference method. The cone method was not very suitable for evaporated layers and was later abandoned.

The absorption measurements were made using a double prism monochromator with interchangeable quartz, LiF and NaCl prisms, using a thermocouple, a PbTe cell or a photomultiplier as detector. A wavelength resolution of 0.05μ or better was generally employed.

To study the absorption spectra at low temperatures both layers of each pair were totally immersed in liquid nitrogen in an unsilvered quartz dewar vessel. For some measurements layers were deposited directly on to the inner surface of the dewar vessel. The accuracy of these measurements at low temperatures was not high, say 20%, due to the constant boiling of the coolant and water condensation.

EXPERIMENTAL RESULTS

§ 3. THE ABSORPTION SPECTRUM OF LEAD SULPHIDE

3(i) *General Results*

The absorption spectrum in the range 0.2μ to 7.0μ of a typical chemically deposited layer of PbS is given in Figure 1. If care is taken to use a standard deposition method the layers are quite reproducible. Deviations from the standard method cause small changes in the absorption spectrum, particularly around 0.9μ . Layers may be prepared with a very marked dip at this wavelength which separates the lattice absorption and the tail into two distinct bands.

Evaporated layers of PbS give very similar absorption spectra to those of chemical layers. The chief differences occur (a) in the long wavelength tail band which may differ in magnitude by as much as a factor of 3 and (b) in the wavelength region around 0.6μ . The original PbS available for the preparation of evaporated layers is, however, of doubtful purity. Thus two samples of 'pure PbS' available commercially have been found to contain 45% and 55% of PbSO_4 respectively. The chemically deposited layers probably represent the purest specimens available.

The chief characteristics of the absorption spectrum of PbS are easily distinguished, the lattice edge being very marked. The absorption coefficient in this region is about $2 \times 10^5 \text{ cm}^{-1}$, which is a reasonable value for any semiconductor (Mott and Gurney 1940). The most surprising feature of the absorption spectrum is the marked tail band which extends beyond 6μ . The absorption coefficient in this band is about 10^4 cm^{-1} and is therefore much larger than that found in semiconductors. The significance of this result will be discussed later.

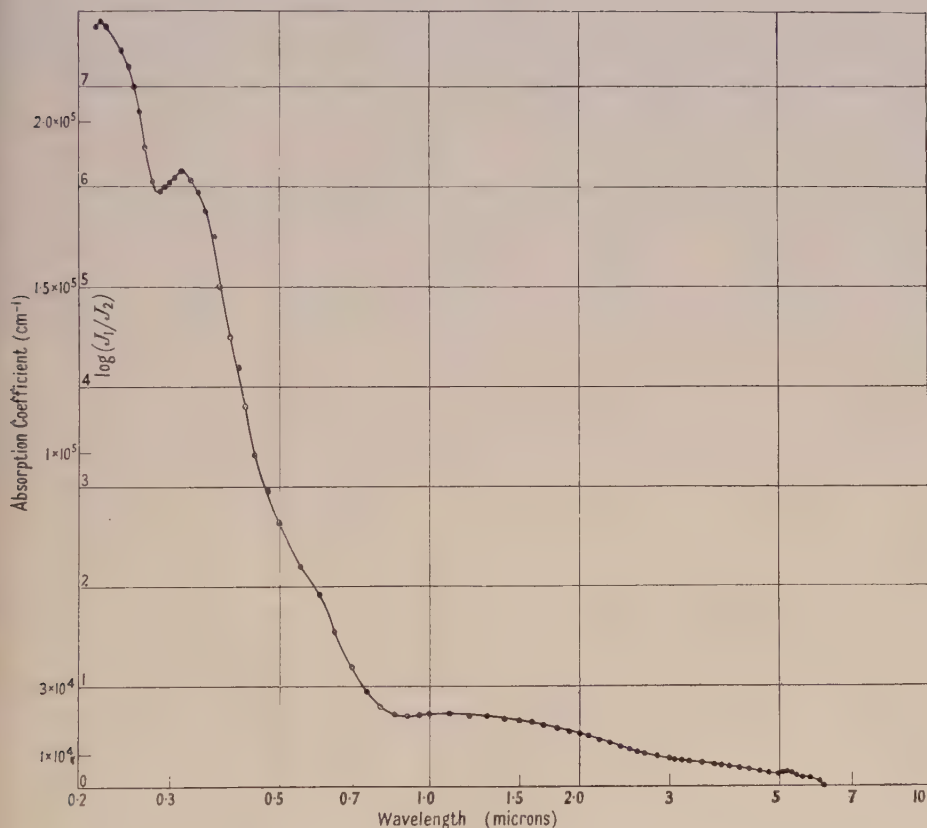


Figure 1. The absorption spectrum of chemically deposited lead sulphide.

3(ii) The Effect of Oxygen Impurity

The importance of treatment with oxygen to obtain photosensitive layers of PbS is well known.

Oxygen may be introduced either (a) during the preparation of the original material, or (b) during evaporation, or (c) after the layer has been deposited. Generally speaking only processes (b) and (c) have marked effects on the photosensitivity.

Chemical layers of PbS are normally baked in air for about 30 minutes at about 150°C . in order to produce photosensitivity. This corresponds to oxidation process (c) above. Initial measurements indicated that such treatment made no significant change in the absorption spectrum. Bakes up to 16 hours

duration were tried. This result was not altogether unexpected as von Hippel *et al.* (1946) have reported the same result for thallium sulphide, another material normally sensitized by baking in air or oxygen.

A significant effect due to oxygen was observed when care was taken to reduce all extraneous effects to a minimum. In particular the layers were not removed from the monochromator mounting for baking. Evaporated layers were prepared *in vacuo* and their transmission measured at each wavelength before air at atmospheric pressure was admitted by breaking a small glass seal.

The change in absorption observed was very small (about 3% or less) but almost doubled on baking in air. The magnitude of the change was wavelength dependent, being most marked at the wavelengths 1.0μ and 2.3μ in the tail band. In the tail absorption band the absorption decreased on admission of oxygen.

In view of the small change in absorption to be observed the errors in this measurement are large, but the reality of the effect is beyond doubt. The most surprising feature is that the absorption coefficient in the tail absorption band decreases on oxidation, when an increase would be expected if new impurity bands are being introduced. It may be significant that previous workers (Sosnowski *et al.* 1947) have noticed peaks in the photoconductivity spectrum of PbS at about 1μ and 2μ which they ascribe to oxygen treatment. These wavelengths agree fairly well with the figures given above.

It has been stated by Wilman (1948) and others that as much as 10% of PbO.PbSO_4 may be formed on the oxidation of PbS films. It is almost certain that the main absorption band of this material lies in the far ultra-violet outside the range of measurement.

3 (iii) *The Effect of Temperature*

The absorption spectrum of PbS at room temperature and at 77°K . is shown in Figure 2, the abscissa being the reciprocal of the wavelength. The most obvious effect of cooling is to shift the lattice absorption edge to longer wavelengths. A number of determinations of the magnitude of the shift have been made, the mean value indicating a shift of about $6 \times 10^{-4} \text{ eV}/^\circ\text{K}$. This compares with the measured shift in the spectral limit for photoconductivity of $4.8 \times 10^{-4} \text{ eV}/^\circ\text{K}$., and is in the same direction (Moss 1949).

A lattice edge shift to longer wavelengths on cooling is not usual in semiconductors. There are, in general, two factors which determine the shift of the lattice edge with temperature. As the lattice contracts on cooling ions move closer together, interaction increases and allowed energy bands broaden. In addition, however, electron interaction with the thermal vibrations of the lattice decreases on cooling and allowed energy bands narrow (Radkowsky 1948). It is not possible without detailed calculation to determine which effect will be the more important in PbS. The energy change due to contraction is very approximately proportional to energy bandwidth, whereas the shift due to lattice vibration effects is independent of bandwidth. As the former effect appears to be the more important in PbS it is concluded that the allowed energy bands in PbS are very wide. In general this would be expected in a sulphide of high dielectric constant.

The long wavelength tail absorption band of PbS also undergoes a change on cooling. The band appears to narrow appreciably, at least on the long wavelength side, and the peak of the band moves to longer wavelengths. The

total area under the tail band is not appreciably altered. It should be pointed out that measurements at 77° K. could not be made at wavelengths greater than 4.2 μ because of absorption in the quartz dewar vessel. In addition measurements around 2.7 μ were impossible due to the condensation of water on the cooled surfaces of the dewar vessel. Thus the accuracy in the 3 μ and 4 μ region is not very high.

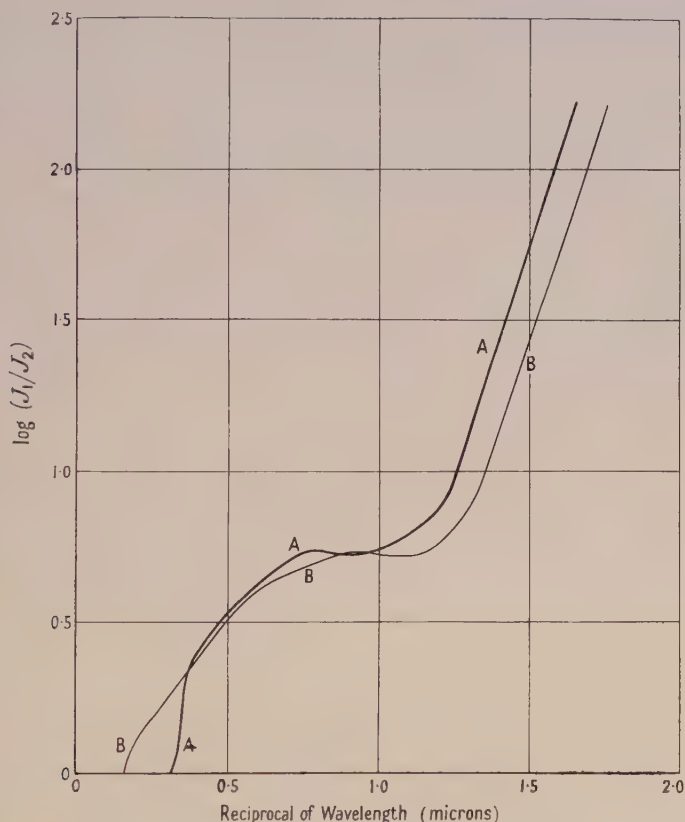


Figure 2. The absorption spectrum of lead sulphide.
A at 77° K., B at 290° K.

3(iv) Other Measurements on PbS

(a) In view of the lack of marked effects due to the exposure of evaporated PbS films to the air, layers were prepared *in vacuo* on KRS5 discs and subsequently opened to the air. As KRS5 is transparent to very long wavelengths (to about 40 μ) it was possible to examine the absorption of PbS out to 16 μ (the limit set by the monochromator and detector). No major absorption bands in the region 7 μ to 16 μ were observed. The measurements set an upper limit to the 'Reststrahlungsfrequenz' in PbS.

(b) Attempts have been made to measure the absorption spectra of single crystals of natural galena. These experiments were not very successful as it was impossible to obtain crystal specimens sufficiently thin and yet free from holes. The measurements obtained indicated a similar structure to that shown in Figure 1, the lattice edge being easily observable.

Due to the above difficulties it was not possible to observe changes in absorption with crystal direction by transmission measurements. As an alternative method crystals were split and polished and mounted on a table rotatable through 270° . The reflectivity of the specimens was then measured with plane-polarized infra-red radiation at various crystal angles. No significant changes in reflectivity with crystal direction were observed.

§ 4. THE ABSORPTION SPECTRUM OF LEAD SELENIDE

The absorption spectrum of a chemically deposited layer of this material is given in Figure 3 where the absorption coefficient is plotted against the

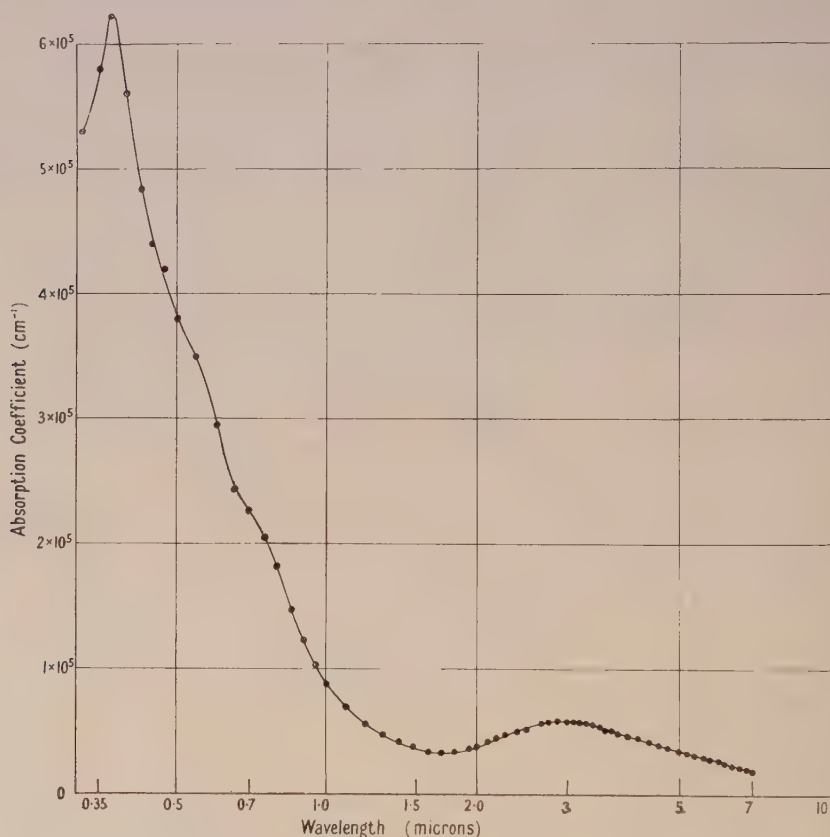


Figure 3. The absorption spectrum of chemically deposited lead selenide.

logarithm of the wavelength. The spectrum is similar to that of PbS except that it is shifted bodily to longer wavelengths. The shift is about 0.4 e.v. in the region of lattice absorption.

The lattice edge of PbSe, like that of PbS, moves to longer wavelengths on cooling. The shift is about the same as, or rather less than, that of PbS. The expansion coefficients of PbS and PbSe are almost identical but the allowed energy bands are likely to be somewhat narrower in PbSe. According to Moss (1949) the shift in spectral limit of photoconductivity of PbSe is exactly the same as that of PbS.

§ 5. THE ABSORPTION SPECTRUM OF LEAD TELLURIDE

This material cannot be obtained by chemical deposition and hence only evaporated films may be studied. PbTe can, however, be prepared by heating the elements in sealed and evacuated quartz tubes and hence a product of high purity (particularly as regards oxygen) obtained. This represents an important advantage over PbS and PbSe.

The absorption spectrum of a layer of PbTe prepared by the evaporation *in vacuo* of a powder sample manufactured *in vacuo* is given in Figure 4. The general features are similar to those of the sulphide and selenide.

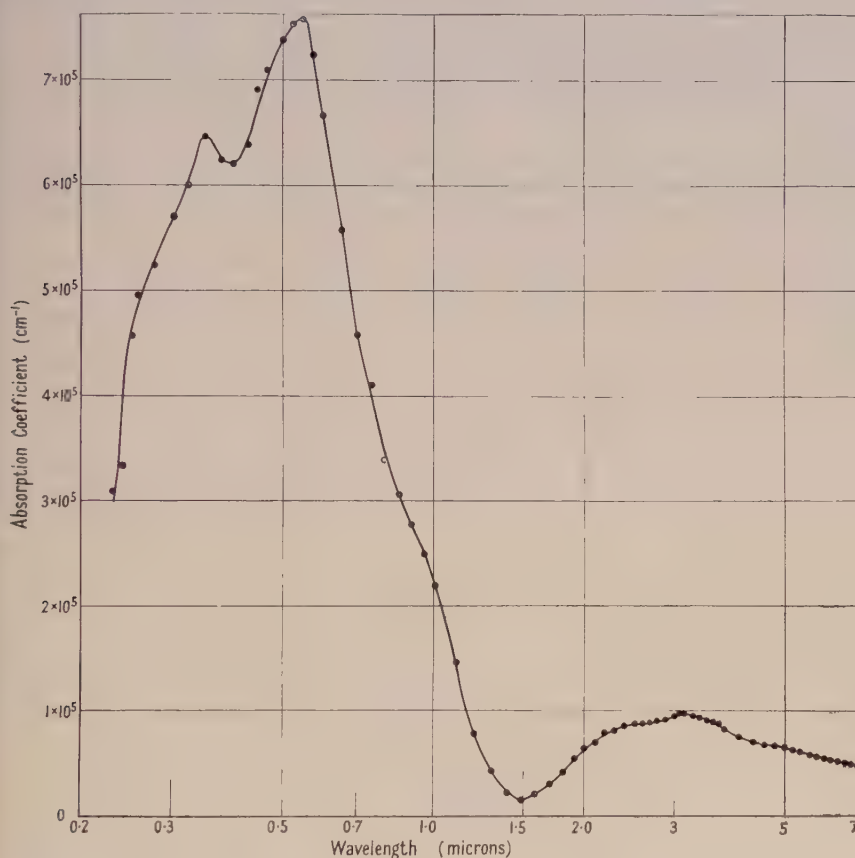


Figure 4. The absorption spectrum of lead telluride (material prepared in high vacuum).

The effect of oxygen on the absorption spectrum of this material can be studied both in the bulk material and in films. As for PbS, the absorption in the long wavelength tail band decreases slightly when air is admitted to vacuum-prepared films but the effect is smaller than that in the sulphide and too small for adequate measurement.

To study the effect of oxygen on the bulk material, specimens of PbTe have been prepared by heating the elements in low pressures of air and in open crucibles. The effect of such treatment is illustrated in Figures 5 and 6. The absorption at short wavelengths is not appreciably affected (the main peak at 0.55μ remains entirely unchanged in position or magnitude) but marked changes occur at longer wavelengths. A new absorption peak appears at about 0.9μ and the

tail absorption decreases in magnitude on its short wavelength side. The latter effect results in an apparent shift to longer wavelengths of the tail band maximum and the minimum between the main bands.

This comparatively violent oxidation (the material examined in Figure 6) was heated to over $1,000^{\circ}\text{C.}$ in air) is clearly similar, except in magnitude, to oxidation of sulphide and telluride films by exposure to the air. Similar though less marked effects can be obtained by evaporation of unoxidized PbTe samples in low pressures (of the order of 10^{-2} mm.Hg) of air. It seems likely that all

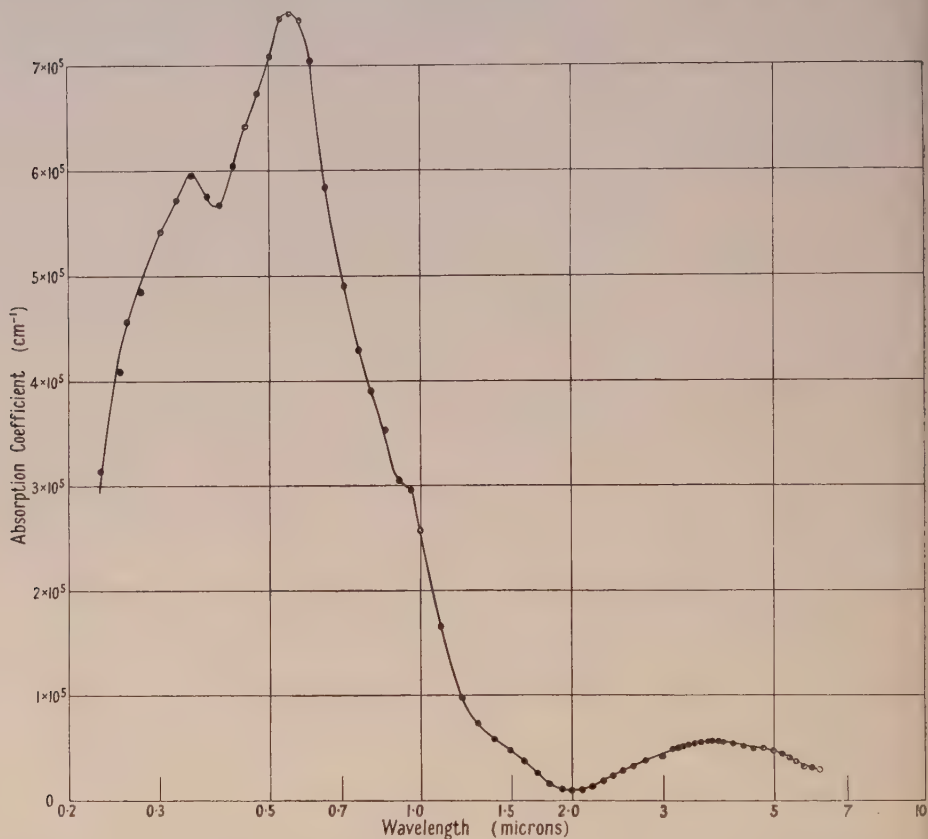


Figure 5. The absorption spectrum of lead telluride (material prepared in low pressure of air).

the more marked differences in absorption spectra between PbS, PbSe or PbTe samples of different origin are due to oxidation effects.

Very intense oxidation of PbTe results finally in complete decomposition and the formation of a grey-white product. By analogy with PbS, the material is thought to be PbO.PbTeO_4 . The only marked absorption of this material commences about 2800 Å. and extends below the limit of measurement. It seems likely that the absorption bands of PbO.PbSO_4 would be at even shorter wavelengths.

The shift in the lattice absorption edge in PbTe on cooling is even less than that of the selenide and its magnitude proportionately uncertain. A reasonable value would appear to be a $1.5 \times 10^{-4} \text{ eV}/^{\circ}\text{K.}$ According to Moss the shift in photoconductive limit is the same as for the sulphide and selenide but recent work in this laboratory by Mr. A. S. Young has shown that any shift between 2 and $7 \times 10^{-4} \text{ eV}/^{\circ}\text{K.}$ may be obtained in PbTe, depending on sample preparation.

§ 6. THE ABSORPTION SPECTRA OF PbS, PbSe AND PbTe: GENERAL DISCUSSION

6 (i) Lattice Absorption

The lattice absorption bands of each material almost certainly correspond to electronic transitions between the highest filled energy band and the lowest empty band, that is, the transfer of an electron from S, Se or Te ions to Pb ions. The long wavelength part of this band may correspond to exciton transitions (Mott and Gurney 1940), but there is no evidence in favour of this view.

Extrapolation indicates that the lattice absorption coefficient of PbS will reach zero at about 0.9μ , corresponding to a minimum energy of about 1.3 or 1.4 ev. This value is considerably greater than the value of 0.4 ev. suggested by Sosnowski *et al.* (1947) and suggests that these authors were mistaken in

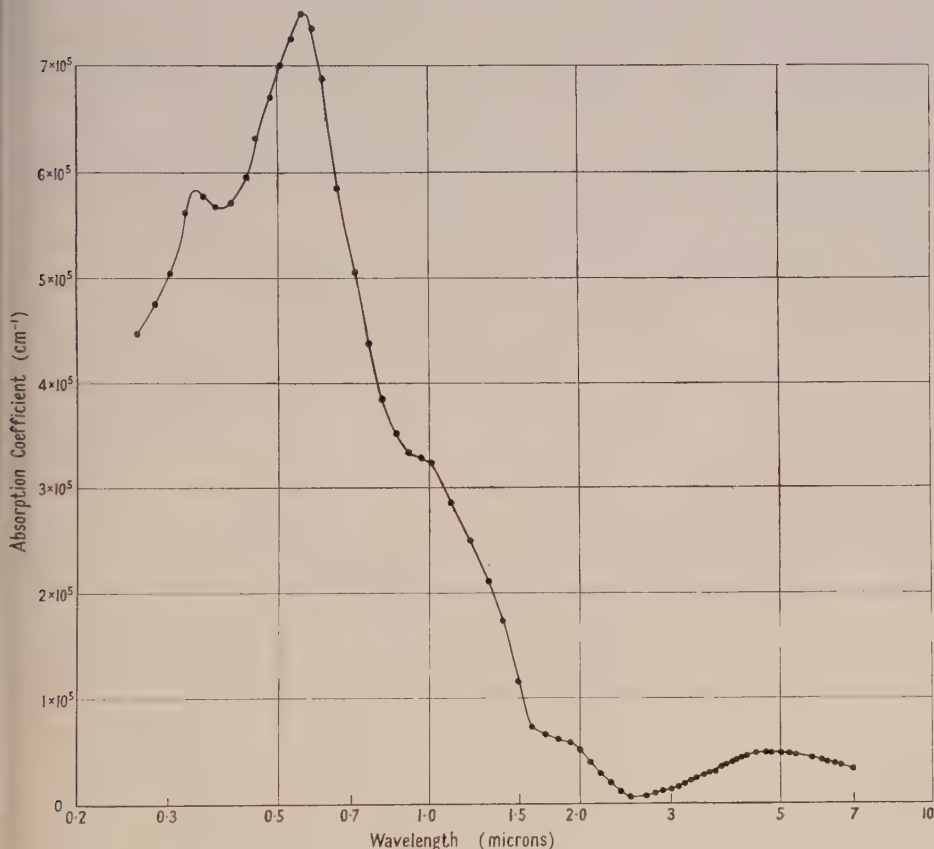


Figure 6. The absorption spectrum of lead telluride (material prepared in air).

associating photoconductivity with lattice absorption. It would appear that the photoconductive spectrum is in fact determined by impurities or other effects.

It is of interest to note that the sensitization spectrum of optically sensitized PbS layers (Gibson 1949) is almost exactly coincident with the main lattice absorption. Previously sensitization was thought to take place at specks of free sulphur but the similarity between the sensitization spectrum and the photoconductivity of free sulphur is not very close. It is now clear that a more likely

explanation of optical sensitization involves absorption in the main lattice and the subsequent filling of electron traps lying just below the conduction band of the solid.

The threshold energy for lattice absorption falls progressively from the sulphide to the telluride, as might be expected. The magnitude of the absorption coefficient increases through the series. The latter effect must be associated with decreasing energy bandwidths as the spectra move to longer wavelengths. Due to this progression almost all the main absorption band of PbTe lies within the limits of measurement and an estimate of the bandwidth may be made. The half width of the absorption band is about 4 eV., which must be approximately equal to the sum of the widths of the two allowed energy bands involved.

6(ii) *The Long Wavelength Tail Absorption Band*

By analogy with other photoconductors and semiconductors this band may be ascribed to impurities in interstitial or substitutional lattice positions. There are, however, a number of reasons for rejecting this explanation, as follows.

(a) The absorption coefficient is too large, being about 10^4 cm^{-1} in PbS and larger in PbTe. Absorption bands of the magnitude and width observed would correspond to an impurity concentration of the order of 10^{20} per cm^3 . PbS, PbSe and PbTe are highly polarizable materials and therefore it may be argued that they are capable of taking up very large amounts of impurity without serious lattice distortion. Notwithstanding this, it seems unlikely that a chemically deposited film of PbS, which is never heated, should contain about 100 times as many impurities as are usually found in other sulphides.

(b) If photoconductivity is associated with impurities and the excitation of electrons from impurity levels, the absorption bands observed cannot correspond to such transitions, as the absorption spectra and photoconductivity spectra are not the same. At room temperature absorption in PbS extends to 6 or 7 μ , while photoconductivity to 3 μ .

An alternative explanation is to ascribe the observed absorption band to transitions of electrons in the conduction band of the solid, the transition involved being to the next highest empty band, which probably overlaps the conduction band. The measurements of Eisenmann (1940) and others suggest that the concentration of electrons in the conduction band of PbS is of the order of 10^{19} or 10^{20} at room temperature. This number appears to be largely invariant with temperature (Dunaer 1947). Thus, PbS, PbSe and PbTe are semi-metallic (Chasmar 1948). These electrons would give rise to an absorption band at long wavelengths of about the magnitude observed. The area under the band would be largely unaltered on cooling, though the energy distribution of the electrons may alter. No photoconductivity would arise from this type of transition and hence the lack of photoconductivity at 6 μ is accounted for. The effect of oxygen in diminishing the absorption band may be interpreted as the capture of electrons by oxygen atoms on the surface of the crystallites.

If this explanation is correct, photoconductivity cannot arise from an increase in the number of electrons in the conduction band as the efficiency would be too low. Schwarz (1949) has suggested that photoconductivity is a surface phenomenon arising from adsorbed films of oxygen. A theory of this type has been considered for some time in this laboratory. Each crystallite of PbS (n-type) is assumed to have oxygen atoms adsorbed on its surface which capture electrons from the

interior of the crystallite and produce a negative surface charge. Illumination may eject electrons from the surface oxygen states, the surface charge would be reduced and conduction facilitated. There is increasing experimental evidence in favour of this view but conclusive evidence is still lacking.

ACKNOWLEDGMENTS

I am indebted to my colleagues at the Telecommunications Research Establishment for much help, advice and criticism, and particularly to those to whom reference has been made in the text. I am indebted to the Chief Scientist, Ministry of Supply and the Controller, H.M. Stationery Office, for permission to publish this work.

REFERENCES

- CHASMAR, R. P., 1948, *Nature, Lond.*, **161**, 281.
- DUNAER, J. A., 1947, *C. R. Acad. Sci., URSS.*, **55**, 21.
- EISENMANN, L., 1940, *Ann. Phys., Lpz.*, **38**, 121.
- GIBSON, A. F., 1949, *Nature, Lond.*, **163**, 321.
- GIBSON, A. F., and MOSS, T. S., 1950, *Proc. Phys. Soc. A*, **63**, 176.
- VON HIPPEL, A., *et al.*, 1946, *J. Chem. Phys.*, **14**, 355, 370.
- KICINSKI, F., 1948, *Chem. and Ind.*, **17**, 54.
- MOSS, T. S., 1949, *Proc. Phys. Soc. B*, **62**, 741.
- MOTT, N. F., and GURNEY, R. W., 1940, *Electronic Processes in Ionic Crystals* (Oxford: Clarendon Press).
- RADKOWSKY, A., 1948, *Phys. Rev.*, **73**, 749.
- SCHWARZ, E., 1948, *Nature, Lond.*, **162**, 614; 1949, *Proc. Phys. Soc. A*, **62**, 530.
- SOSNOWSKI, A., *et al.*, 1947, *Nature, Lond.*, **159**, 818.
- WILMAN, H., 1948, *Proc. Phys. Soc.*, **60**, 117.

Note on the Electron Velocity Distribution in Low Voltage Arcs

By M. S. B. CHAGHTAI

Queen's University, Belfast

Communicated by K. G. Emeléus; MS. received 20th March 1950

ABSTRACT. An analysis has been made of a large number of hot cathode low voltage arc-type discharges in mercury vapour and hydrogen at low pressure by the cold probe methods of Langmuir and Mott-Smith. It has been verified that the space potential in the plasma near the filament is positive relative to anode potential, and it has been shown that consistent data for the space potential and concentrations of the slow (ultimate) electrons are obtainable from analyses of probe characteristics in both retarding and accelerating fields for electrons. The way in which the fast (primary) electrons develop a random motion has been traced by progressively confining them within the main discharge, firstly by using a cylindrical gauze anode with open ends, secondly by using a solid anode with open ends and lastly by using a solid anode with end caps.

§ 1. INTRODUCTION

IN an hot cathode arc discharge at low pressure electrons from the cathode are accelerated through a double space-charge sheath and produce a highly conducting plasma further out. The collision processes occurring in the plasma have been investigated in detail by Langmuir and Jones (1928), who have studied how the primary electrons have their directions altered and give up energy in various types of collisions with the gas molecules. They were able to distinguish three main groups of electrons in the plasma; the primary electrons from the filament, the secondary electrons ejected from atoms and produced by loss of energy of the primary electrons, and the slow 'ultimate' electrons which are mainly responsible for the high conductivity. The tube used had a straight filament cathode mounted axially in a closed cylindrical metal box, with the end caps insulated from the curved wall. By varying the gas pressure, Langmuir and Jones made an investigation* of the transition from the velocity distribution principally studied, which can be approximately described by the three groups, to the velocity distribution which is encountered under many other conditions (Langmuir and Mott-Smith 1924), in which a single group is present, often with a Maxwellian distribution of velocities. The present author has found that some simple modifications of the electrode system used by Langmuir and Jones permit the demonstration of the transition in another way. The modifications consist in the use of different types of anode, which progressively confine the faster electrons more within the general body of the arc plasma. This shows rather directly how the overall velocity distribution tends to become Maxwellian, although both the atomic process involved and the current voltage characteristics of the collectors are too complex to permit full theoretical analysis.

* See particularly Figure 13 of their paper.

§ 2. APPARATUS AND EXPERIMENTAL METHODS

Most of the experiments were performed in mercury vapour saturated at a temperature of approximately 20°C . A few experiments performed with hydrogen at the same pressure gave similar results. No allowance has been made for thermal effusion. The tubes had an axial tungsten filament cathode 0.2 mm. in diameter, used as a bright emitter. The length of the filament between its supporting leads varied from 6.0 to 6.5 cm. as replacements of it were made. The fall of potential along the filament was approximately 8 volts. The anode of the first tube (Figure 1) was made of nickel gauze (with 25 wires/cm. , each wire 0.15 mm. diameter) of length 4.2 cm. and diameter 2.3 cm. In the second tube the nickel gauze was replaced by nickel sheet of the same dimensions, and in the third tube the nickel sheet was furnished with two flat end caps through which the filament and probe leads passed. Two cylindrical molybdenum probes were used. The first F_1 was situated at about the middle of the filament, and the second F_2 at one end in such a position that its exposed length always lay within the perpendicular from the corresponding end of the anode on the filament. Both probes were 0.1 mm. in diameter, F_1 being 0.8 cm. long and F_2 0.4 cm. long. They were

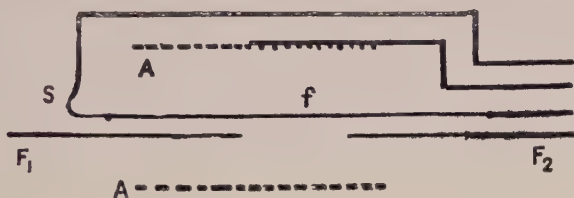


Figure 1. Diagram of electrodes and leads for tube 1. Gauze anode, AA; filament, f , held taut by sprung metal strip, S , at left-hand end; probes, F_1 and F_2 , with glass shields omitted. The four leads on the right passed to a common pinch. The lead to F_1 passed through a separate seal at the left.

shielded by fine glass tubes except at the exposed ends. The probes were parallel to the filament, and about 3 mm. from it. They were put close to the filament in order to minimize complications from plasma oscillations, which do not usually become pronounced until farther out (Neill 1949). By reversing the direction of the current through the filament, information could be obtained about the discharge at four different regions along its length from the negative end. The electrodes were mounted axially in a glass tube 4.5 cm. in diameter and 15 cm. long, with an appendix containing a drop of pure mercury. The tube was kept continuously evacuated by a diffusion pump.

Most measurements were made with the tubes passing temperature-limited currents from the whole of the filament. A few were made with the current not quite saturated. No significant differences were found between the two sets of results. With tubes 1 and 2 the plasma could be seen to bulge beyond the open ends of the anode, in some instances filling the whole of the tube. With tube 3 there was occasionally a small penetration of plasma past a filament lead. The characteristic curves were obtained using standard circuits as described, for example, by Greeves and Johnston (1936); any runs in which variation of probe potential caused a detectable change in anode current were rejected. The general shape of the characteristic curves was that described by Langmuir and Jones. For sufficiently negative voltages of the probes a small positive ion current was received which did not vary much with voltage. When the probe voltage was

raised to that of the neighbouring part of the filament a rapid change in current occurred, due to the reception of primary electrons. With increasing positive voltages more primary electrons were received. On approaching the anode potential a further rapid increase of electron current to the probe occurred, due to the reception of the ultimate electrons. In no case was it possible to distinguish clearly between primary and secondary groups.

§ 3. ANALYSIS OF RESULTS

As the probes were situated close to the filament it was essential to know that they were actually in the plasma. This was considered likely, from the appearance of the discharge and from the fact that the cathode sheath was probably much nearer the cathode (Druyvesteyn and Penning 1940). It was confirmed by the analysis of the electron currents received by the probes when their potential was near that of the anode. Since the ultimate electrons were present in much greater numbers than the primary electrons, the latter could be allowed for on this part of the probe characteristic by approximate graphical extrapolation. The residual currents of ultimate electrons were analysed in two ways, first, by plotting the currents on a semi-logarithmic scale against the probe voltage (i.e. $(\log i, V)$ graph), and second, by plotting their squares against the probe voltage, on a linear scale (i.e. (i^2, V) graph). Both methods permit the determination of the space potential and of the electron concentration (Langmuir and Mott-Smith 1924). In the second method it is necessary to apply two corrections: first, for the position of the space potential, using a value for the mean electron energy obtained by the first method, and second, for the distortion of the linear $[(\text{current})^2, \text{potential}]$ graph through incomplete orbital motion near the space potential. Reasonably consistent results were obtained by the two methods, as is shown by some typical data given in the Table. In all cases the space was positive with respect to the anode.

Plasma Data

Tube and probe	Pressure (10^{-8} mm.)	Arc current (ma.)	Space potential (volts)		Ultimate electron concentration ($10^9/\text{cm}^3$)	
			from $(\log i, V)$	from (i^2, V)	from $(\log i, V)$	from (i^2, V)
1, F ₁	1.35	160	7.5	7.4	25.6	20.9
1, F ₂	1.35	176	7.0	7.1	0.3	0.2
2, F ₁	1.24	220	5.0	5.0	21.2	18.8
2, F ₂	1.24	200	2.2	2.0	1.1	0.8
3, F ₁	1.04	347	4.5	4.5	18.6	16.8
3, F ₂	1.04	340	1.7	1.7	0.4	0.4

The arc voltage drop was 25, and the filament current 4.85 amp. in each case.

The distribution analysis outlined above suggested that if the primary electrons were progressively confined within the inter-electrode space by partial reflection from the surface of suitably designed anodes, the overall distribution would tend to become more nearly Maxwellian. Tubes 1, 2 and 3 (see §2) were designed and used one after the other with this end in view. In tube 1 a number of the faster electrons were being lost to the main body of the plasma because they passed out through the wires of the gauze. In tube 2 there was no penetration of the anode by fast electrons, although not all were reflected from the metal (Langmuir and Jones 1928). In tube 3, loss of electrons through the ends of the anode was prevented in addition. Results of the type anticipated were obtained.

Consideration was given to the possibility that the space potential was near the cathode potential, corresponding to a point on the $(\log i, V)$ graph at which the rate of increase of primary electron current with increase of probe voltage begins to diminish rapidly. This alternative interpretation of the $(\log i, V)$ graph has been rejected from the close analogy between the discharges studied in this investigation, and those studied by Langmuir and Jones (1928) and Compton and Eckart (1925) in which the space potential was near that of the anode.

An attempt has been made to determine the velocity distribution amongst the primary electrons from analysis of the $(\log i, V)$ curves with the probe potential not far from that of the cathode. Qualitatively the distribution, particularly for tube 1, clearly consists of a large component of drift motion with a superimposed

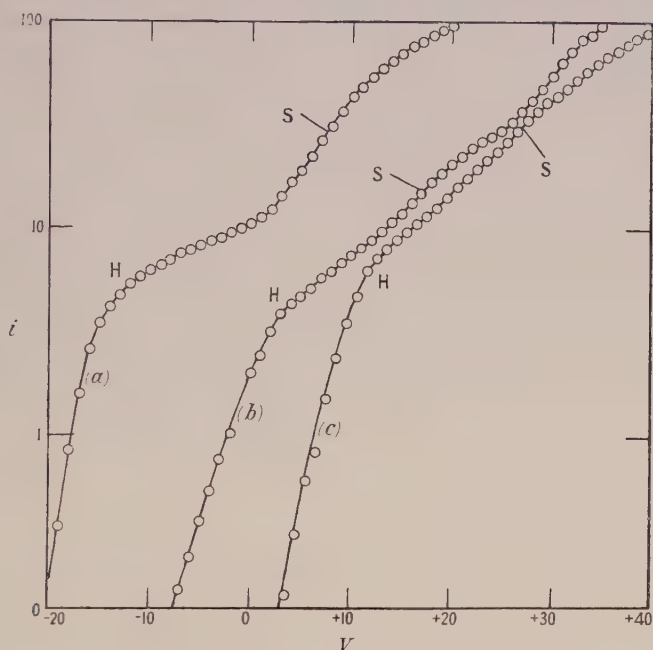


Figure 2. Semi-logarithmic plots of electron current i on arbitrary scale against probe voltage V relative to anode. Curve (b) is displaced 12.5 volts to the right and curve (c) 22.5 volts to the right. The space potentials are at S.

smaller random motion. Methods for analysing such curves have been developed by Langmuir and Mott-Smith (1926). Three complete semi-logarithmic plots of electron current against probe voltage are shown in Figure 2, for tube 1 (curve *a*), tube 2 (curve *b*) and tube 3 (curve *c*). The discharge conditions were: for curve *a*, pressure 1.35×10^{-3} mm., arc current 160 ma.; for curve *b*, pressure 1.24×10^{-3} mm., arc current 220 ma.; for curve *c*, pressure 1.04×10^{-3} mm., arc current 347 ma. In each case the arc voltage drop was 25.0, and the filament current 4.85 amp. Further data are included in the Table. The curves show a transition from the form in which the primary electrons are well separated (*a*) towards a form in which the semi-logarithmic plot is more nearly straight over the greater part of its length negative to the space potential. This type of transition has been found consistently in some 100 characteristic curves for F_1 ; it occurs in all cases by simultaneous flattening of the left-hand hump H, and extension towards more negative voltages

of the approximately straight part corresponding to the ultimate electrons near the space potential. Since the existence of a straight-line curve for $(\log i, V)$ shows that the electrons concerned have a Maxwellian distribution of velocities, we appear to have here an example of the degeneration of the separate groups towards a single group having an overall Maxwellian distribution and equivalent temperature. This is what would be expected through the progressive enclosure of the discharge, with diminishing leakage from the cylinder of primary electrons, and, possibly to a less extent, of ultimate electrons. The characteristic curves have proved to be too complex to permit quantitative analysis, but it does appear that not only is there a modification of the primary group, but in addition, an extension towards higher energies of the ultimate group, and that, could the discharge conditions be varied widely enough to follow these processes still further, a single group with a definite temperature (much above the gas temperature because of the presence of electric fields) would be obtained.

Confirmation of the essential correctness of this interpretation of the data for F_1 is afforded by the results obtained with F_2 . When this was at the negative end of the filament, the characteristic curves for tubes 1 and 2 were similar to one another, whilst with tube 3 only a slight straightening occurred. The similarity of the characteristic curves for tubes 1 and 2 is due to the magnetic field of the filament current. This bends the electron beam emerging from the filament sheath into the cylinder, and therefore robs the region surrounding this end of a considerable number of primary electrons. This bending occurs with both tubes, and although the laws of electron reflection are unknown in detail and probably vary considerably, the increased reflection from the solid anode in tube 2 can scarcely result in the redirection of many electrons towards the negative end. Hence the overall velocity distribution there remains practically unchanged. In tube 3, again, little alteration of the characteristic curves would be expected because the axial component of the velocity of the primary electrons is small.

When F_2 was at the positive end of the filament the probe characteristics were found to change in type much as they did with F_1 , for all three tubes. This again is to be expected, because at this end the magnetic field tends to make the primary electrons pass out of the cylinder.

ACKNOWLEDGMENTS

The experiments described are part of an investigation of low voltage arcs made by the author whilst a research student of the Government of Pakistan at Queen's University, Belfast. The author wishes to express his thanks to the Pakistan Government, and to Professor K. G. Emel us, in whose laboratory the work was done.

REFERENCES

- COMPTON, K. T., and ECKART, C., 1925, *Phys. Rev.*, **25**, 139.
 DRUYVESTEYN, M. J., and PENNING, F. M., 1940, *Rev. Mod. Phys.*, **12**, 87.
 GREEVES, F. D., and JOHNSTON, J. E. McF., 1936, *Phil. Mag.*, **21**, 659.
 LANGMUIR, I., and JONES, H. A., 1928, *Phys. Rev.*, **31**, 357.
 LANGMUIR, I., and MOTT-SMITH, H. M., 1924, *Gen. Elect. Rev.*, **27**, 449 etc.; 1926, *Phys. Rev.*, **28**, 727.
 NEILL, T. R., 1949, *Nature, Lond.*, **163**, 59.

The Determination of the Viscosity of Molten Metals

By M. R. HOPKINS AND T. C. TOYE

The British Iron and Steel Research Association, Swansea

MS. received 16th February 1950

ABSTRACT. A method is described for the measurement of the viscosity of molten metals at temperatures up to about 900° C. The metal is contained in a cylindrical crucible which is allowed to oscillate about its axis under the control of the torsion in a suspension wire. The theory of the method is considered.

The viscosity of zinc has been determined in the temperature range 430° C. to 480°C. and the results are given.

§ 1. INTRODUCTION

THERE is not a great deal of information available on the coefficients of viscosity of molten metals. Still less is known of the viscosities of alloys and the effect, upon the viscosity of one metal, of the addition of small quantities of another.

Most of the well-known methods for the determination of the viscosity of substances which are liquid at room temperature are unsuitable for measurements on liquid metals. The use of the oscillating disc method, in which a solid of revolution such as a disc, suspended by a wire, is allowed to oscillate about its axis in the liquid, against the restoring torque provided by the torsion in the wire, has been described in some detail by Stott (1933) who applied it to the investigation of the viscosity of molten tin. The chief disadvantage of this method is that contamination of the surface of the liquid, by oxide or otherwise, leads to a serious dragging effect on the rod connecting the disc to the suspension wire. It is difficult to eliminate this contamination in experiments on substances such as molten zinc. The method of enclosing the liquid inside a hollow sphere attached to a bifilar suspension and allowed to execute torsional oscillations has been developed and used with success by Andrade and Chiong (1936).

They discuss the calculation of the coefficient of viscosity from the observed damping of the oscillations and show that the method can be made to yield accurate results. Andrade and Rotherham (1936) give an alternative method of determining the viscosity by observing the forces necessary to maintain the oscillations at a constant amplitude.

The choice of material for the construction of the hollow sphere presents problems when it has to contain molten metal at high temperatures. The material must be immune to attack by the molten metal, and must be capable of being formed to the required shape without too much difficulty. Sintered alumina is a substance which withstands high temperatures and resists chemical attack, but hollow spheres which can be sealed with the metal inside are not easily made from this material. Accurately made cylindrical crucibles of sintered alumina are, however, readily available, and it seemed desirable that an investigation should be made of the possibility of determining the viscosity of molten metals by observing the oscillations of a cylindrical containing vessel left open at the top end. This method has been suggested by Knappwost (1948).

For a cylinder it is more difficult than in the case of a sphere to obtain a manageable expression from which the viscosity can be calculated in terms of the dimensions of the apparatus. It is possible, nevertheless, to use the method for absolute determinations. The theoretical considerations outlined below indicate how this may be done, and also provide the basis for a calibration formula, which can be determined by using liquids of known viscosity.

§ 2. THEORY OF THE METHOD

The oscillation of a closed cylinder of length short in comparison with its diameter has been considered by Meyer (1891), and viscosity determinations made on the basis of his analysis by Mutzel (1891).^{*} We shall consider here the case of a long cylinder open at one end. Let the cylinder, containing liquid, execute rotational oscillations about its axis (which we take to be the z -axis, in the vertical direction). Let (u, v, w) be the velocities of the liquid at the point (x, y, z) in the (x, y, z) directions, and let $p(x, y, z)$ be the pressure. Then, if (X, Y, Z) are the components of the body forces and ν the kinematic viscosity η/ρ where η is the coefficient of viscosity and ρ the density, the general equations of viscous flow are

$$\left. \begin{aligned} \frac{\partial u}{\partial t} + u \frac{\partial u}{\partial x} + v \frac{\partial u}{\partial y} + w \frac{\partial u}{\partial z} &= X - \frac{1}{\rho} \frac{\partial p}{\partial x} + \nu \nabla^2 u, \\ \frac{\partial v}{\partial t} + u \frac{\partial v}{\partial x} + v \frac{\partial v}{\partial y} + w \frac{\partial v}{\partial z} &= Y - \frac{1}{\rho} \frac{\partial p}{\partial y} + \nu \nabla^2 v, \\ \frac{\partial w}{\partial t} + u \frac{\partial w}{\partial x} + v \frac{\partial w}{\partial y} + w \frac{\partial w}{\partial z} &= Z - \frac{1}{\rho} \frac{\partial p}{\partial z} + \nu \nabla^2 w, \end{aligned} \right\} \dots\dots(1)$$

to which must be added the continuity equation

$$\frac{\partial u}{\partial x} + \frac{\partial v}{\partial y} + \frac{\partial w}{\partial z} = 0. \dots\dots(2)$$

Assuming that there is no motion in the z direction, that there are no body forces, and that the velocities are small enough to enable us to neglect the non-linear terms, the equations reduce to

$$\left. \begin{aligned} \frac{\partial u}{\partial t} &= -\frac{1}{\rho} \frac{\partial p}{\partial x} + \nu \nabla^2 u, \\ \frac{\partial v}{\partial t} &= -\frac{1}{\rho} \frac{\partial p}{\partial y} + \nu \nabla^2 v, \end{aligned} \right\} \dots\dots(3)$$

$$\frac{\partial u}{\partial x} + \frac{\partial v}{\partial y} = 0. \dots\dots(4)$$

Let us assume now that each particle of fluid moves in a circle with a velocity depending only on the distance r from the axis, on z and on t , and put

$$u = -\psi y, \quad v = \psi x,$$

where ψ is a function of r, z and t . The tangential velocity at a distance r is then $r\psi$ and the radial velocity zero; ψ is in fact the angular velocity of the liquid.

^{*} We are indebted to the referee for pointing out that work on the determination of viscosity by observing the oscillations of a closed cylinder containing liquid has been done by Okaya and Hasegawa (1933) and Okaya (1936).

Multiplying the first of equations (3) by y , the second by x and subtracting, we have, in cylindrical polar coordinates, when there is no azimuthal variation of ψ

$$\frac{\partial^2 \psi}{\partial r^2} + \frac{3}{r} \frac{\partial \psi}{\partial r} + \frac{\partial^2 \psi}{\partial z^2} = \frac{1}{\nu} \frac{\partial \psi}{\partial t} \quad \dots\dots(5)$$

We suppose that the system has settled down so that the liquid has the same period and decay as the containing vessel.

Then $\psi = \Phi e^{\alpha t}$

and if a is the radius of the cylinder, c the height of the liquid in the cylinder, and the origin is taken at the centre of the base of the cylinder,

$$\begin{aligned} \psi &= \Phi e^{\alpha t} \text{ at } z=0 \text{ and at } r=a, \\ \frac{\partial \psi}{\partial z} &= 0 \text{ at } z=c. \end{aligned}$$

Equation (5) then becomes

$$\frac{\alpha}{\nu} \phi = \frac{\partial^2 \phi}{\partial r^2} + \frac{3}{r} \frac{\partial \phi}{\partial r} + \frac{\partial^2 \phi}{\partial z^2}, \quad \dots\dots(6)$$

with the boundary conditions

$$\left. \begin{aligned} \phi &= \Phi \text{ at } z=0 \text{ and at } r=a, \\ \frac{\partial \phi}{\partial z} &= 0 \text{ at } z=c. \end{aligned} \right\} \quad \dots\dots(7)$$

α is complex; in fact $\alpha = -\beta + i\gamma$, where $\beta = 2\delta/T$ and $\gamma = 2\pi/T$, δ being the logarithmic decrement and T the period of oscillation. The solution of (6) satisfying the boundary conditions (7) is

$$\phi = \frac{a\Phi J_1(mr)}{r J_1(ma)} + \frac{2\Phi}{r} \sum \frac{J_1(k_n r) m^2 \cosh l_n(z-c)}{J_0(k_n a) k_n (k_n^2 - m^2) \cosh l_n c}, \quad \dots\dots(8)$$

where $-m^2 = \alpha/\nu$ and J_0 and J_1 are Bessel functions of order 0 and 1 respectively. The summation is taken over the positive roots k_n of $J_1(k_n a) = 0$, l_n being given by $l_n^2 = m^2 - k_n^2$. The damping torque on the system due to the viscous drag of the liquid on the walls of the cylinder is

$$G = 2\pi\eta \left\{ a^3 \int_0^c \left(\frac{\partial \psi}{\partial r} \right)_{r=a} dz - \int_0^a \left(\frac{\partial \psi}{\partial z} \right)_{z=0} r^3 dr \right\}, \quad \dots\dots(9)$$

where $\frac{\partial \psi}{\partial r} = e^{\alpha t} \frac{\partial \phi}{\partial r}$ and $\frac{\partial \psi}{\partial z} = e^{\alpha t} \frac{\partial \phi}{\partial z}$,

which, on evaluating with reference to (8), becomes

$$G = 2\pi\eta \left\{ -\frac{mca^3 J_2(ma)}{J_1(ma)} + 2m^4 a^2 \sum \frac{\tanh l_n c}{l_n k_n^2 (k_n^2 - m^2)} \right\} \Psi^*, \quad \dots\dots(10)$$

where $\Psi^* = \Phi e^{\alpha t}$ is the angular velocity of the cylinder containing the liquid. We can write $\Psi^* = d\theta/dt$ and $\theta = \Phi e^{\alpha t}/\alpha$ where θ is the angle through which the cylinder has turned from some zero position.

Equation (10) can be expressed as

$$G = L \frac{d\theta}{dt} \quad \dots\dots(11)$$

and the equation of motion of the oscillating system, assuming that the external damping due to causes other than the viscous drag is small, is

$$I \frac{d^2\theta}{dt^2} + L \frac{d\theta}{dt} + f\theta = 0, \quad \dots\dots(12)$$

where I is the moment of inertia, and f the restoring torque per unit angle of rotation.

As is shown by Andrade and Chiong (1936), (12) may be written as follows on putting $L = M + iN$ and remembering that $\alpha = -\beta + i\gamma$.

$$I\alpha^2 + (M + iN)\alpha + f = 0,$$

$$I(\beta^2 - \gamma^2) - \beta M - \gamma N + f = 0,$$

$$-2I\beta\gamma - \beta N + \gamma M = 0,$$

i.e.
$$M = \beta \left\{ \frac{f}{\beta^2 + \gamma^2} + I \right\}; \quad N = \gamma \left\{ \frac{f}{\beta^2 + \gamma^2} - I \right\}.$$

Since $\beta = 2\delta/T$, $\gamma = 2\pi/T$, $f = 4\pi^2 I/T_0^2$ where T and T_0 are the periods of the full and empty cylinder respectively.

$$\left. \begin{aligned} M &= \frac{2I\delta}{T} \left(\frac{T^2}{T_0^2} \frac{1}{\Delta^2 + 1} + 1 \right), \\ N &= \frac{2\pi I}{T} \left(\frac{T^2}{T_0^2} \frac{1}{\Delta^2 + 1} - 1 \right), \end{aligned} \right\} \quad \dots\dots(13)$$

where $\Delta = \beta/\gamma = \delta/\pi$.

Since Δ is small, the expressions for M and N become

$$M = \frac{2I\delta}{T} \left(\frac{T^2}{T_0^2} + 1 \right); \quad N = \frac{2\pi I}{T} \left(\frac{T^2}{T_0^2} - 1 \right). \quad \dots\dots(14)$$

These equations contain only measurable quantities, so that M and N are known. Simple considerations show that if the external damping is small but not negligible, it is approximately accounted for by subtracting the logarithmic decrement observed when the cylinder is empty from that observed when the cylinder contains liquid, to obtain the value δ in the expression for M . The apparatus should, however, be designed to keep the external damping as low as possible.

The value of the coefficient of viscosity η in terms of the logarithmic decrement δ can theoretically be obtained by combining equations (10), (11) and (14) to give

$$\begin{aligned} \frac{2I\delta}{T} \left(\frac{T^2}{T_0^2} + 1 \right) &= \text{Real part of} \left[2\pi\eta \left\{ -mca^3 \frac{J_2(ma)}{J_1(ma)} \right. \right. \\ &\quad \left. \left. + 2m^4 a^2 \sum \frac{\tanh l_n c}{l_n k_n^2 (k_n^2 - m^2)} \right\} \right] \quad \dots\dots(15) \end{aligned}$$

In order to use this, it is necessary to simplify the right-hand side. This we now proceed to do.

$$m^2 = -\frac{\alpha}{\nu} = \frac{1}{\nu} (\beta - i\gamma) = -\frac{i\gamma}{\nu} \left(1 + \frac{i\beta}{\gamma} \right).$$

Therefore

$$m = \left(\frac{\pi}{T\nu} \right)^{1/2} (1 - i) \left(1 + \frac{i\beta}{\gamma} \right)^{1/2}.$$

To a first approximation therefore

$$m = \left(\frac{\pi}{T\nu}\right)^{1/2} - i \left(\frac{\pi}{T\nu}\right)^{1/2}$$

and

$$ma = a \left(\frac{\pi}{T\nu}\right)^{1/2} (1-i) = \mu(1-i) \text{ say.}$$

It is convenient to put $\zeta = \mu(1-i)$ and observe that

$$\frac{J_2(\zeta)}{J_1(\zeta)} = \frac{2}{\zeta} - \frac{J_0(\zeta)}{J_1(\zeta)}.$$

Since, in our experiments μ is large, we can use the well-known asymptotic expansions for $J_0(\zeta)$ and $J_1(\zeta)$, viz.

$$J_0(\zeta) \sim \left(\frac{2}{\pi\zeta}\right)^{1/2} \left\{ \left(1 - \frac{9}{128\zeta^2}\right) \cos\left(\zeta - \frac{\pi}{4}\right) + \frac{1}{8\zeta} \sin\left(\zeta - \frac{\pi}{4}\right) \right\},$$

$$J_1(\zeta) \sim \left(\frac{2}{\pi\zeta}\right)^{1/2} \left\{ \left(1 + \frac{15}{128\zeta^2}\right) \sin\left(\zeta - \frac{\pi}{4}\right) + \frac{3}{8\zeta} \cos\left(\zeta - \frac{\pi}{4}\right) \right\}.$$

Now $\cos(\zeta - \pi/4) = e^{\mu} e^{i(\mu - \pi/4)/2}$ and $\sin(\zeta - \pi/4) = e^{\mu} e^{i(\mu - \pi/4)/2} i$ on neglecting $e^{-\mu}$ compared with e^{μ} , so that

$$\begin{aligned} \frac{J_0(\zeta)}{J_1(\zeta)} &= \frac{1 - \frac{9}{128\zeta^2} + \frac{1}{8\zeta i}}{\frac{1}{i} \left(1 - \frac{15}{128\zeta^2}\right) + \frac{3}{8\zeta}} \\ &= \frac{1 + 8\zeta i}{8\zeta + 3i} \text{ neglecting terms in } \frac{1}{\zeta^2} \end{aligned}$$

which reduces to

$$\frac{2 + i(8\mu - 1)}{8\mu - 3} \text{ again neglecting terms in } \frac{1}{\mu^2} \text{ compared with unity.}$$

Hence

$$\zeta \frac{J_0(\zeta)}{J_1(\zeta)} = \mu \left(\frac{8\mu + 1}{8\mu - 3}\right) + i\mu$$

and

$$\begin{aligned} \zeta \frac{J_2(\zeta)}{J_1(\zeta)} &= 2 - \zeta \frac{J_0(\zeta)}{J_1(\zeta)} \\ &= 2 - \mu \left[\frac{8\mu + 1}{8\mu - 3}\right] - i\mu. \end{aligned}$$

Equation (15) may now be written

$$\frac{2I\delta}{T} \left(\frac{T^2}{T_0^2} + 1\right) = 2\pi\eta \left[-ca^2 \left\{ 2 - \mu \left(\frac{8\mu + 1}{8\mu - 3}\right) \right\} + K(\mu) \right], \dots\dots(16)$$

where $K(\mu) = \text{Real part of } 2\zeta^4 \Sigma \frac{\tanh l_n c}{l_n k_n^2 [(ak_n)^2 - \zeta^2]}.$

If the height of the liquid in the cylinder is not small compared with the diameter of the cylinder, $K(\mu)$ is much smaller than the other term on the right-hand side of (16). Physically, this means that most of the viscous drag takes place at the

curved surface of the cylinder as compared with the end. We can proceed now by using (16) to find an approximate value of η and of course μ , neglecting $K(\mu)$, and then using the approximate value of μ to evaluate $K(\mu)$ and so by a process of successive approximation arrive at a value of η satisfying the equation. It is found in practice that, after first obtaining an approximate value of μ , it does not involve much extra labour to compute $J_0(\xi)/J_1(\xi)$ without neglecting terms in $1/\xi^2$, and thus to obtain numerically a more accurate expression than that given by the term containing $\{2 - \mu(8\mu + 1)/(8\mu - 3)\}$ in (16).

Calculation of $K(\mu)$ for various values of μ shows that it is very nearly a linear function of μ . It is worth tabulating this function if the apparatus is to be used unchanged for a large number of determinations.

An alternative procedure is to write (16) in the form

$$\delta \left(\frac{T^2}{T_0^2} + 1 \right) = A\eta T + B\mu\eta T + C \frac{\eta T}{\mu} \\ = A\eta T + B(\eta\rho T)^{1/2} + C \left[\frac{(\eta T)^3}{\rho} \right]^{1/2}$$

and to determine the constants A , B and C by observations on liquids of known viscosity. The cubic equation in $\eta^{1/2}$ can be solved by the usual methods.

§ 3. APPARATUS

The apparatus is described with reference to the sectional diagram of Figure 1.

The silica furnace tube K, 3 ft. 6 in. long and 5 in. internal diameter, is wound at E. The winding is arranged so as to ensure that a uniform temperature can be maintained over a length of the furnace safely in excess of that occupied by the sintered alumina crucible H which contains the molten metal under investigation. The dimensions of the crucible are : height 10 cm., internal diameter 3.9 cm., wall thickness 1 mm. Below the crucible are heat insulating bricks F which are supported by means of a long steel tube which rests on the lower steel endplate T of the furnace. The temperature of the furnace is controlled by a Cambridge regulator, and measured by means of a carefully calibrated platinum-platinum-rhodium thermocouple, used in conjunction with a potentiometer graduated in hundredths of a millivolt, but capable of being read by estimation to a tenth of this value. For the type of thermocouple used, one millivolt corresponds roughly to 100°C. The regulator is used to connect one or other of two alternative sources of current to the furnace winding. By careful adjustment of the relative magnitudes of the currents available from these two sources, and by maintaining the cold junction of the thermocouple at 0°C. in a vacuum flask containing melting ice, it is found that the temperature can be controlled to $\pm \frac{1}{2}^\circ\text{C}$. This variation takes place over a period which is long compared with that required to make a determination of the viscosity. The furnace tube is surrounded by the lagging J.

The crucible H is supported in a light steel cradle attached to a steel rod which passes through the steel tube supporting the bricks F in the upper half of the furnace. At its upper end the steel rod carries an aluminium disc D, having a graduated flange, which can be observed through a glass window in the brass cover G. The whole oscillating system consisting of the crucible, the connecting rod and aluminium disc is suspended by a phosphor bronze wire,

ten inches long and one hundredth of an inch in diameter, fastened to a brass rod L which fits closely into a brass sleeve, the joint being lubricated with vacuum grease. The suspended system is located vertically by the brass bush R clamped to the rod L. Slight rotation of R starts the oscillations.

The upper part of the apparatus, consisting of the brass cover G, the upper endplate T of the furnace, the upper insulating bricks F and the whole of the suspension system, can be removed as one integral part, the only vacuum seal to be broken being that between the silica tube and the furnace endplate. This seal is made with vacuum wax. The lower endplate is similarly sealed to the silica tube, so that this can be evacuated. The viscosity determinations are carried

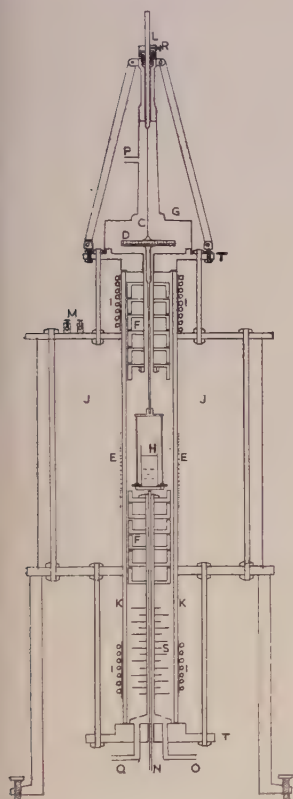


Figure 1.

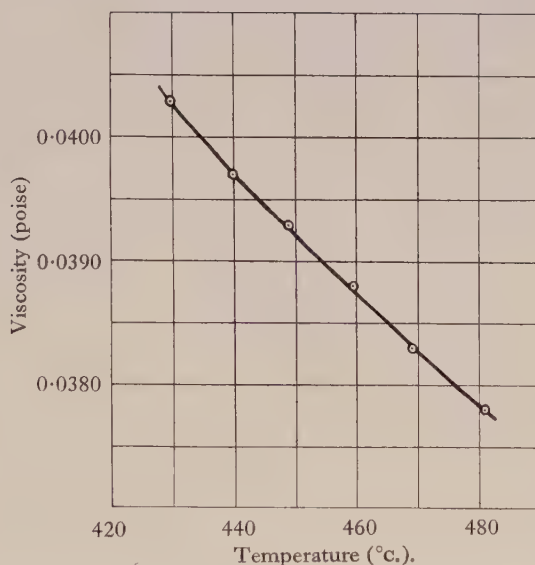


Figure 2.

out in an atmosphere of hydrogen, which after purification by passing through chromous chloride and potassium hydroxide, is dried and admitted through the side tube P in the brass cover G, and allowed to escape through the outlet tube Q at the bottom of the tube. Before the hydrogen is admitted the furnace tube is evacuated through the tube O in the bottom endplate.

In order to ensure that the phosphor bronze suspension wire be kept at a low constant temperature, and that the wax seals be kept cool, water cooling is provided at both ends of the silica tube.

Measurements of amplitudes and times of oscillation are made by observing the graduated aluminium disc D through a telescope placed a few feet away from the apparatus.

§ 4. EXPERIMENTAL PROCEDURE

A check determination was made of the viscosity of molten tin, the viscosity being calculated from the constants of the apparatus by the first of the methods described in § 2, that is without reference to observations on any other liquid. The value obtained was 0.01182 poise at 496.8° c. which agrees closely with the value 0.01187 obtained by Stott (1933).

In order to be able to use the second method given in § 2, the apparatus was calibrated, using liquids of known viscosity and density. The results are given in the next section. In all experiments the depth of liquid in the crucible was maintained the same, the amount of liquid necessary to ensure this being weighed beforehand.

The viscosity of molten zinc was then determined over a range of temperatures between 430° c. and 480° c. The material used was high purity zinc, for which we are indebted to The National Smelting Co., Ltd. The analysis gave the following quantities of impurities: Pb < 0.001% (probably 0.0005%), Cd 0.0001%, Cu 0.0001%, Fe 0.0005%, Ca a trace. The metal was melted in a separate furnace under a layer of wood charcoal, cooled and washed, first with 2% acetic acid solution to remove surface oxide and then with boiling distilled water. It was then placed in the viscometer and the temperature raised to 480° c. After 24 hours at this temperature, the logarithmic decrement was determined and further readings taken 12 hours and 24 hours later. Constant readings having been obtained corresponding to 480° c., the temperature was lowered to 470° c., and after an interval of 24 hours at this temperature the logarithmic decrement was again determined. Measurements were made, following the same procedure at 460°, 450°, 440° and 430° c. Trouble was at first experienced due to the vaporization of the zinc, but it was found that this could be eliminated by having a layer of powdered wood charcoal on the surface of the melt. Experiments on molten tin and molten zinc with and without such a layer of charcoal showed that the logarithmic decrement was not affected by its presence.

§ 5. RESULTS

(i) Calibration

The constants in the equation

$$\delta \left[\frac{T^2}{T_0^2} + 1 \right] = A\eta T + B(\eta\rho T)^{1/2} + C \left(\frac{(\eta T)^3}{\rho} \right)^{1/2}$$

were determined using five liquids: chloroform, water, carbon tetrachloride, benzene and tin, for which accurate values of η and ρ at various temperatures are available. The relevant data are given in Table 1. The value of δ given in the fourth column represents the observed value less the value of the logarithmic decrement obtained with the crucible empty at room temperature. This value was 0.003659 for the first four liquids and 0.001644 for the fifth. Each value given represents the mean of six separate observations.

The values of η and ρ for the first four liquids given in the table are obtained from *International Critical Tables*. The values for tin are taken from Stott's paper. Calculation of A , B and C from the above data by the method of least squares gives $A = -0.0362$, $B = 0.0438$, $C = 0.0306$. On using these values of A , B and C and the observed values of δ to calculate the viscosities η of the

calibrating liquids from the calibration formula, the greatest discrepancy between calculated and actual values is found to be 0.0002 poise. The values of δ , ρ and T in the case of zinc (see below) are such that the determination of the viscosity using the calibration formula is an interpolation and not an extrapolation process.

(ii) The Viscosity of Zinc

Using the above values of A , B and C the viscosity of zinc was determined at various temperatures. The results are given in Table 2. The logarithmic decrements δ given in the table were obtained by subtracting from the observed values the logarithmic decrement with the crucible empty at 455° c. This value was 0.001644. The values of the density were taken from a paper by Pascal and Journiaux (1914).

Table 1

Substance	Temperature (° c.)	Viscosity η (poise)	Density ρ (gm/cm ³)	Logarithmic decrement δ	Time of oscillation T (sec.)
Chloroform	23.00	0.005460	1.483347	0.007318	19.85
Water	23.75	0.009216	0.99738	0.007286	19.86
Carbon tetrachloride	19.75	0.009743	1.594539	0.009678	19.90
Benzene	19.75	0.006495	0.879012	0.005692	19.87
Tin	496.8	0.01187	6.785	0.023824	20.09

Time of oscillation of empty crucible = 19.81 seconds.

Table 2

Temperature (° c.)	Period (seconds)	Density (gm/cm ³)	Logarithmic decrement δ	Viscosity η (poise)
480.8	20.26	6.833	0.03929	0.0378
468.8	20.26	6.847	0.03955	0.0383
459.3	20.26	6.860	0.03981	0.0388
448.7	20.28	6.876	0.04008	0.0393
439.8	20.30	6.888	0.04027	0.0397
429.6	20.31	6.903	0.04056	0.0403

The relation between the viscosity η and the temperature is shown in the graph of Figure 2.

Andrade (1934) has suggested a relationship between the viscosity of a liquid and temperature of the form

$$\eta v^{1/3} = A e^{c/v\theta},$$

where v is the specific volume, θ the absolute temperature, and A and c are constants. On fitting this relation to the results for molten zinc it was found that with $A = 0.009533$ and $c = 81.266$ the calculated values of η agreed with the observed values to within 0.1%.

(iii) Absolute Determinations

The constants of the apparatus which enter into an absolute determination of the viscosity are the diameter of the crucible, the depth of the liquid in it, and the moment of inertia of the oscillating system. We have calculated the

viscosity of zinc using equation (16) and obtained the following values given in Table 3, the values of δ and ρ being those of Table 2.

Table 3

Temperature ($^{\circ}$ C.)	480.8	468.8	459.3	448.7	439.8	429.6
Viscosity (poise)	0.0380	0.0385	0.0390	0.0396	0.0400	0.0406

The greatest difference between these values and those of Table 2 amounts to 3 in the last decimal place, i.e. about three-quarters of one per cent.

(iv) Comparison with Previous Determinations

The only previous work on the viscosity of zinc of which we are aware is that of Gering and Sauerwald (1935), who determined the coefficients of viscosity of a number of metals by observing the motion of small quantities of the metal along a capillary tube under the influence of gas pressure. They obtained values for zinc in the temperature range 450° to 700° C. These values varied from 0.03168 poise at the lower to 0.01865 poise at the higher temperature. The results of the present paper are higher than this, e.g. our value at 448.7° C. is 0.0393 (Table 2), which may be compared with Gering and Sauerwald's 0.03168 at 450° C.

§ 6. CONCLUSION

The viscosity of pure zinc has been determined for various temperatures in the range 430° C to 480° C. by the oscillating cylinder method. It is intended to investigate the effect of adding small quantities of other metals such as aluminium to the zinc, and some preliminary measurements have already been carried out.

ACKNOWLEDGMENTS

The thanks of the authors are due to Sir Charles Goodeve, Director of The British Iron and Steel Research Association, who suggested the programme of which the work described in this paper forms part, for his continued interest, and to Mr. I. E. Thomas for valuable assistance in the construction of the apparatus.

REFERENCES

- ANDRADE, E. N. DA C., 1934, *Phil. Mag.*, **17**, 698.
 ANDRADE, E. N. DA C., and CHIONG, Y. S., 1936, *Proc. Phys. Soc.*, **48**, 247.
 ANDRADE, E. N. DA C., and ROTHERHAM, L., 1936, *Proc. Phys. Soc.*, **48**, 261.
 GERING, K., and SAUERWALD, F., 1935, *Z. anorg. allg. Chem.*, **223**, 204.
 KNAPPWOST, A. Z., 1948, *Metallkunde*, **39**, 314.
 MEYER, O. E., 1891, *Ann. Phys. Chem.*, **43**, 1.
 MÜTZEL, K., 1891, *Ann. Phys. Chem.*, **43**, 15.
 OKAYA, T., 1936, *Proc. Phys.-Math. Soc., Japan*, **18**, 268.
 OKAYA, T., and HASEGAWA, M., 1933, *Jap. J. Phys.*, **11**, 23.
 PASCAL, P., and JOUNIAUX, A., 1914, *Rev. Metall.*, **1**, 469.
 STOTT, V. H., 1933, *Proc. Phys. Soc.*, **45**, 530.

High Frequency Permeability of Ferromagnetic Materials

By R. MILLERSHIP* AND F. V. WEBSTER

Physics Department, University of Leeds

Communicated by R. Whiddington; MS. received 20th March 1950

ABSTRACT. Methods are described for the measurement of resistive and inductive permeabilities over a range of frequencies from 150 to 10,000 Mc/s. The measurements of the resistive permeabilities were carried out by comparing the attenuation of a coaxial transmission line with the ferromagnetic as the inner conductor with that of a coaxial line having a non-ferromagnetic as inner conductor. The inductive permeabilities were obtained from the wavelength in a coaxial line having the ferromagnetic as the inner conductor. The results show that at all frequencies the resistive permeability is greater than the inductive, and both decrease to unity at very high frequencies. The effective permeability, which is assumed to be complex, is deduced as a function of resistive and inductive permeabilities and plotted against frequency for a variety of materials. The experimental values are compared with theoretical values derived from two formal treatments.

§ 1. INTRODUCTION

THE process of magnetization of ferromagnetics under the influence of ultra-high-frequency fields has until recently received very little attention, probably because of the difficulty of producing an oscillatory field of sufficiently high frequency, but, as a result of extensive advances in ultra-high-frequency technique during the war, this difficulty has been largely removed. Unfortunately most of the previous investigations have been confined to very restricted frequency ranges; in fact, many have consisted of isolated determinations of permeability at a single frequency. Furthermore, the materials used in the past have often been of ill-defined composition. As the low field properties of magnetic materials are so strongly structure sensitive, it is only by using the same material (and preferably the same specimen) over the whole frequency range of interest that the character of the variation of permeability with frequency can be determined with any certainty.

A complete and critical account of the various methods which have been employed has been given by Allanson (1945). The methods fall into two distinct groups: those in which the permeability is determined from a measurement of the resistive losses of a circuit containing the ferromagnetic material, and those which are dependent upon the effective reactance of a similar circuit. The permeability deduced from measurements in the former category is usually denoted by μ_R , and that from measurements in the second category by μ_L . Of these two coefficients μ_R is always larger than μ_L , the difference between the two being covered formally by treating the permeability as a complex quantity. It is necessary to determine both μ_R and μ_L at the same frequency in order to calculate the complex permeability. This has not been generally realized, and, as a consequence, almost all the previous investigations have consisted of measurements of either μ_R or μ_L alone.

* Now with the National Coal Board.

In order to provide conditions under which the field may be introduced into the specimen it is convenient to use a transmission-line system incorporating the ferromagnetic material. The parameters of a transmission line which contains μ_R are the attenuation constant, the Q factor, and the characteristic impedance, whilst the wave velocity in the line gives the information necessary for the calculation of μ_L . Most of the measurements obtained by earlier workers were at frequencies of the order of 100 Mc/s., employing the open Lecher wire type of transmission line. Such a system would be unsuitable at higher frequencies as considerable power would be lost through radiation, and hand-capacity effects would also become significant. At these higher frequencies coaxial lines and waveguides have proved to be more satisfactory. One very accurate method would involve the use of a waveguide constructed partly of the ferromagnetic material: the disadvantages of this are that the magnetic properties of the material may be affected by machining, and that the waveguide could only be used over a limited range of frequencies.

One of the earlier theoretical treatments of magnetization at high frequencies was that developed by Arkadiew (1926) in which the permeability was introduced as a complex quantity. This theory contained much that is incompatible with the modern theory of ferromagnetism, and a theory based on more modern concepts was developed by Becker (1938, 1939), who assumed that the decrease in permeability was caused by a reduction of the field in the ferromagnetic due to microscopic eddy currents induced by domain boundary movements. Kittel (1946) attributed the reduction in the permeability to a reduced effective field across the domain boundary caused by the small penetration of the applied field due to the skin effect. Earlier Landau and Lifshitz (1935), considering the change of magnetization as due to the change in direction of the magnetic vector in the crystalline anisotropic field, predicted the occurrence of a resonance effect when the frequency of the applied field is equal to the Larmor frequency for gyroscopic rotation of the electron spins about the crystalline field direction. In metallic ferromagnetics, whether the magnetization change is due to translational boundary movements or to rotations of domain magnetization vectors, or both, the damping caused by microscopic eddy currents must be mainly responsible for the general decrease of permeability with frequency. These questions are further considered below (§ 4(iv)).

§ 2. METHOD

(i) *Measurement of the Resistive Permeability*

The method used for the measurement of μ_R has been described in detail in a previous paper (Hodsman, Eichholz and Millership 1949), and hence only a general outline will now be given. A coaxial-line system is employed with the specimen as the centre conductor. This arrangement has the advantage that radiation can be propagated down the line in the fundamental mode over an infinite range of frequencies and so the introduction of the oscillatory field presents little difficulty. As the specimen is in the form of a wire, accurate machining to conform with the geometry of the system is eliminated. Furthermore, as the outer conductor is earthed, radiation is prevented from entering and leaving the system, which is consequently immune from external interference and instability due to hand-capacity effects.

The permeability is determined from the attenuation constant of the system, which is given by (see, for example, Jackson 1945, p. 50)

$$\alpha = \frac{9.95 \times 10^{-6} f^{1/2}}{\log(b/a)} \left[\frac{1}{a} \left(\frac{\mu_a}{\sigma_a} \right)^{1/2} + \frac{1}{b} \left(\frac{\mu_b}{\sigma_b} \right)^{1/2} \right] \text{ db/metre, } \dots\dots(1)$$

where a , μ_a , and σ_a , are the radius, permeability, and conductivity respectively of the inner conductor, b , μ_b and σ_b are those of the outer conductor, and f is the frequency of oscillation in megacycles per second. If a line of length l is used and the attenuation is measured with the inner conductor firstly of ferromagnetic wire and secondly of non-ferromagnetic wire, then the difference in attenuation is given by

$$\Delta(\alpha l) = (\alpha_1 - \alpha_2)l = \frac{9.95 \times 10^{-6} l f^{1/2}}{a \log(b/a)} \left[\left(\frac{\mu_1}{\sigma_1} \right)^{1/2} - \left(\frac{1}{\sigma_2} \right)^{1/2} \right] \text{ db. } \dots\dots(2)$$

where μ_1 and σ_1 refer to the ferromagnetic specimen and σ_2 to the non-ferromagnetic.

In this way the effect of the outer conductor and of any other residual attenuation is eliminated. Measurements on the standing wave pattern in the line are transformed into values of input impedance for different terminations and plotted as circle diagrams of impedance, from which the attenuation constants are derived.

(ii) Measurement of the Inductive Permeability

It is apparent from the results of previous investigators that the dispersion in μ_L takes place at frequencies considerably below those at which the change in μ_R is most rapid. Preliminary investigations indicated that, at 1,500 Mc/s., μ_L was equal to unity for all the materials employed. Apparatus for the measurement of μ_L was therefore designed to cover the range from 150 to 1,500 Mc/s. only.

In order to measure μ_L under the same conditions as μ_R , a section of coaxial line was used in preference to the more easily constructed Lecher line, which ensured that the field configurations were precisely the same in both cases. The method employed is similar to that described by Glathart (1939), being based on the measurement of the wavelength in a coaxial line having the specimen as its centre conductor. Writing d_0 and d for the free space and measured half-wavelengths respectively the permeability is expressed as (Glathart 1939, p. 834)

$$\mu_L = 1.256 \left(\frac{a^2}{\rho} \right) \left(\log \frac{b}{a} \right)^2 \frac{(d_0^2 - d^2)}{d_0 d^4} \times 10^{13}, \dots\dots(3)$$

where ρ is the resistivity of the inner conductor. Equation (3) may be solved for Δd giving

$$\Delta d = d_0 - d = d_0 \left[1 - \left\{ \frac{3.544 \times 10^6 a \log(b/a)}{(\mu \rho d_0)^{1/2} + 3.544 \times 10^6 a \log(b/a)} \right\}^{1/2} \right]. \dots\dots(4)$$

By suitable choice of the dimensions of the system, the half-wavelength shortening $d_0 - d$ may be made sufficiently large to allow an accurate practical determination of μ_L to be made; this is so when $a \rightarrow 0$, and $b \rightarrow a$. Having regard to mechanical stability, accurate centring of the inner conductor and convenient operating conditions, a fairly large diameter outer tube containing a very fine inner conductor wire was designed. A schematic diagram of the apparatus is shown in Figure 1.

The wavelength is determined by altering the length of the line by means of a short-circuiting piston until two successive resonance peaks have been located. The distance moved by the piston between the resonance positions is then half the wavelength in the line. Resonance is observed by extracting a fraction of the power in the line by means of a small loop introduced through a slot at the input end of the outer conductor. The high-frequency current induced in the loop is rectified by a crystal and the output displayed directly on a meter. Figure 2 shows some typical resonance curves.

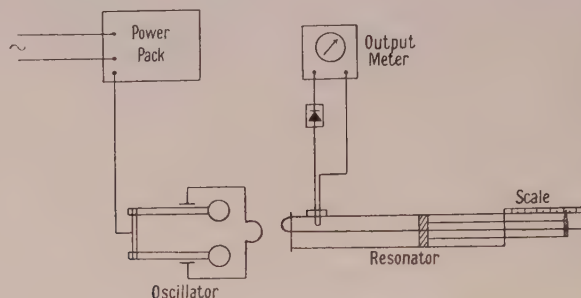


Figure 1. Layout of apparatus for measurement of μ_L .

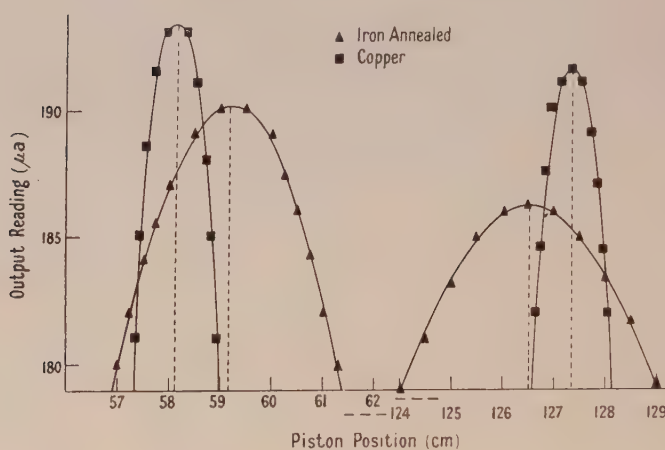


Figure 2. Typical resonance curves.

For the calculation of the free space half-wavelength equation (4) may be written

$$\Delta d_0 = d_0 \left[1 - \left(\frac{k}{(\rho d_0)^{1/2} + k} \right)^{1/2} \right], \quad \dots\dots(5)$$

where Δd_0 is the difference between the free space half-wavelength and the measured half-wavelength for a non-magnetic inner conductor and $k = 3.544 \times 10^6 a \log(b/a)$. As Δd_0 is always small, d_0 in the above equation may be replaced by the measured half-wavelength.

The free space half-wavelength is then obtained as the sum of Δd_0 and the measured half-wavelength for a non-magnetic inner conductor, i.e.

$$d_0 = d \left[2 - \left(\frac{k}{(\rho d)^{1/2} + k} \right)^{1/2} \right]. \quad \dots\dots(6)$$

§ 3. RESULTS

The following materials have been investigated, all in wire form: Swedish charcoal iron, white annealed and bright; 50/55 carbon steel, white annealed and bright; mumetal 6, hard drawn.

The percentage compositions and treatments of the specimens were as follows:

Iron: C, 0.03; Mn, 0.05; S, 0.002; Si, P, Cr, Ni, Co negligible.

Steel: C, 0.50-0.55; Mn, 0.5-0.6; S, 0.03; Si, 0.1; P, 0.02; Ni, 0.2; Cr nil.

Mumetal: Ni, 77; Fe, 15; Cu, 5; Cr, 2; Mn, 0.8; Si, 0.1.

The iron and steel specimens were hard drawn with 90% cold work. The white annealed specimens were annealed with a wet surface at a temperature of 700°C. in an inert atmosphere of town gas (CO , CO_2 , N_2) and the bright specimens were left unannealed.

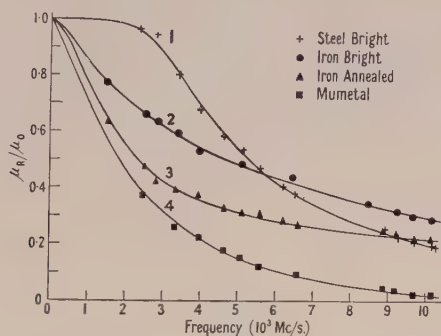


Figure 3. Relative resistive permeabilities.

Curve 1: Steel bright. Curve 2: Iron bright. Curve 3: Iron annealed. Curve 4: Mumetal.

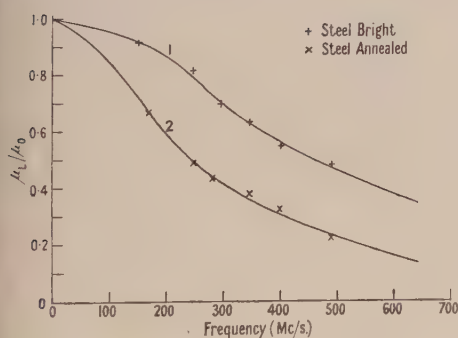


Figure 4. Relative inductive permeabilities.

Curve 1: Steel bright.
Curve 2: Steel annealed.

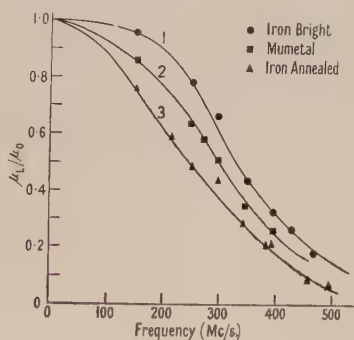


Figure 5. Relative inductive permeabilities.

Curve 1: Iron bright.
Curve 2: Mumetal.
Curve 3: Iron annealed.

In order to provide a firmer basis for comparison the results are shown as relative values, i.e. μ_R/μ_0 and μ_L/μ_0 in Figures 3, 4 and 5. The values of the initial permeability μ_0 are: iron annealed, 180; iron bright, 102; steel annealed, 103; steel bright, 65; mumetal, 440.

At any given frequency μ_R is greater than μ_L for all the materials employed. Both μ_R and μ_L appear to decrease to unity, although the frequency range

employed was not sufficiently great to obtain such a value for μ_R . No values below unity have been obtained, such as those reported by Birks (1948) for finely divided ferromagnetic compounds in paraffin wax. Owing to the lack of suitable oscillators it has not, as yet, been possible to obtain a sufficient number of readings to cover adequately the range where μ_L approaches unity.

§ 4. DISCUSSION OF RESULTS

(i) *Introduction*

An estimate of the strength of the high-frequency field that is applied to the specimen may be obtained from the equation for the power flowing down the line,

$$P = \pi \left(\frac{\mu_0}{\epsilon_0} \right)^{1/2} H_0^2 \log(b/a), \quad \dots\dots(7)$$

which is derived by integrating the time average Poynting vector over the cross section of the line. Assuming all the power produced by the oscillator is dissipated in the line an upper limit of 0.1 oersted is obtained for the field strength. The experimental values for the permeability therefore refer to magnetization in the reversible portion at the commencement of the magnetization cycle.

Any theory of the effects must explain the general decrease in the permeability, and also the difference which exists in the values obtained by resistive and inductive experimental methods.

(ii) *Effect of the Surface Condition*

It is apparent that the permeability for a high-frequency field is a property of the surface layer of the material and consequently will depend to some extent on the nature of the surface. It has in fact been suggested by Wien (1931), Michels (1931), and Procopiu and d'Albon (1937) that the general decrease in permeability with increasing frequency of the field is due to the existence of a thin surface layer (35–70 $\mu\mu$) of non-ferromagnetic material. Since the thinnest truly ferromagnetic films obtained by Sorenson (1924) and Tyndall (1924) are of the order of 20 $\mu\mu$, the existence of such a non-ferromagnetic layer appears to be unlikely. It is probable, however, that the domain structure in the surface layer will be different from that in the main body of the material: hence, if boundary movements are responsible for the magnetization at high frequencies, the magnetic properties will vary considerably for different skin depths and therefore for different frequencies.

Unfortunately, the permeability and conductivity always appear together as a ratio, i.e. μ/σ , in the equations for the attenuation and wavelength in a coaxial line. It is known that a change in conductivity takes place for non-ferromagnetics when the surface is etched or scratched and it is expected that a similar change takes place for ferromagnetics. If the surface is roughened the increased conducting path gives rise to a decreased conductance and permeance. These quantities are both dependent on the length of the conducting path and are reduced equally. Due to the reduction in the effective values of conductance and permeance the skin depth increases and brings about a corresponding increase in these quantities, the ratio μ/σ in the equations always remaining the same for different surface conditions. Thus it is very difficult to relate the permeability alone with surface condition, although it is intended to carry out experiments in this field in the future.

(iii) Difference between μ_R and μ_L

The most satisfactory approach to this problem was proposed by Arkadiew (1932) who treated the permeability as a complex quantity, i.e. of the form $\mu = \mu_1 - i\mu_2$. Considering a wire of ferromagnetic material, μ_R may be regarded as that value of μ which satisfies the theoretical equation for the resistance. Similarly μ_L emerges from the equation for the inductance.

The high-frequency resistance of an isolated conductor of radius r_0 per unit length is given by Jackson (1945, p. 38) as

$$R = \frac{1}{2\pi r_0} \left(\frac{\pi f \mu}{\sigma} \right)^{1/2}, \quad \dots\dots(8)$$

which gives (in C.G.S. units)

$$\frac{R}{R_0} = \frac{r_0}{2c} \left(\frac{2\pi\omega\mu_R}{\rho} \right)^{1/2}, \quad \dots\dots(9)$$

where R_0 is the D.C. resistance of the wire and ρ is the resistivity. Similarly

$$\frac{\omega L}{R_0} = \frac{r_0}{2c} \left(\frac{2\pi\omega\mu_L}{\rho} \right)^{1/2}. \quad \dots\dots(10)$$

Maxwell's equations for the specimen are

$$\left. \begin{aligned} -\frac{\partial H}{\partial r} &= \frac{4\pi E}{c\rho} \\ \frac{\partial E}{\partial r} &= i\frac{\omega\mu H}{c} \end{aligned} \right\}, \quad \dots\dots(11)$$

where r is the radial axis perpendicular to the direction of the wire.

Eliminating H ,

$$\frac{\partial^2 E}{\partial r^2} = i\omega \frac{4\pi\mu}{c^2\rho} E. \quad \dots\dots(12)$$

Substituting a complex permeability, $\mu = \mu_1 - i\mu_2$, gives

$$E = C \exp \left[\left\{ \frac{4\pi\omega}{c^2\rho} (\mu_2 + i\mu_1) \right\}^{1/2} r \right], \quad \dots\dots(13)$$

$$\text{and} \quad \frac{\partial E}{\partial r} = \left\{ \frac{4\pi\omega}{c^2\rho} (\mu_2 + i\mu_1) \right\}^{1/2} E. \quad \dots\dots(14)$$

The effective resistance R and inductance L are obtained from (Abraham and Becker 1932, p. 199)

$$\frac{R + i\omega L}{R_0} = i\frac{r_0}{2} \frac{4\pi\omega\mu}{c^2\rho} \left(\frac{E}{\partial E/\partial r} \right)_{r=r_0} \quad \dots\dots(15)$$

$$= \frac{r_0}{2} \left\{ \frac{4\pi\omega}{c^2\rho} (\mu_2 + i\mu_1) \right\}^{1/2} \quad \dots\dots(16)$$

$$= \frac{r_0}{2c} \left(\frac{2\pi\omega}{\rho} \right)^{1/2} \{ [(\mu_1^2 + \mu_2^2)^{1/2} + \mu_2]^{1/2} + i[(\mu_1^2 + \mu_2^2)^{1/2} - \mu_2]^{1/2} \} \quad \dots\dots(17)$$

$$\text{and therefore} \quad \left. \begin{aligned} \mu_R &= (\mu_1^2 + \mu_2^2)^{1/2} + \mu_2 \\ \mu_L &= (\mu_1^2 + \mu_2^2)^{1/2} - \mu_2 \end{aligned} \right\}, \quad \dots\dots(18)$$

from which

$$\left. \begin{aligned} \mu_1 &= (\mu_R \mu_L)^{1/2} \\ \mu_2 &= \frac{1}{2}(\mu_R - \mu_L) \end{aligned} \right\} \dots\dots (19)$$

These equations enable us to calculate μ_1 and μ_2 from the experimental values of μ_R and μ_L .

(iv) Theoretical Treatments

(a) Becker theory.

Becker (1938) considered the damping effect of microscopic eddy currents, associated with the movement of the domain walls, to be responsible for the general decrease in permeability with increasing frequency. As the domain wall moves, eddy currents, which are proportional to the velocity of movement, are induced in the surrounding medium. The eddy current field will be opposed to the change in magnetization and may thus be interpreted as a braking field which reduces the effective field acting on the wall. The displacements will therefore be reduced, resulting in a reduction of the permeability. This treatment leads to an expression of the form

$$\mu - 1 = \frac{\mu_0 - 1}{1 + i(\omega/\omega_1)}, \dots\dots (20)$$

where μ_0 is the D.C. initial permeability and ω_1 is a 'critical frequency' which, for a cubic domain of side l embedded in a ferromagnetic medium of susceptibility κ_0 , is expressed as

$$\omega_1 = \frac{3c^2}{4\pi^3 \sigma \kappa_0 l^2}. \dots\dots (21)$$

The high-frequency field is considered to be constant over the whole volume of the domain; owing to the small skin depth, however, the applied field may not even penetrate to the extent of the individual domains in the surface layer for centimetre waves. As the domain model assumed is over-simplified the equation for ω_1 is of doubtful validity, although equation (20) will still hold. Such an expression will result from any consideration of a damping force which is proportional to the velocity of movement of the boundary; and it is reasonable to suppose that these damping forces arise from the action of microscopic eddy currents.

Separating the real and imaginary parts of equation (20) we get

$$\left. \begin{aligned} \mu_1 - 1 &= \frac{\mu_0 - 1}{1 + (\omega/\omega_1)^2} \\ \mu_2 &= \frac{(\mu_0 - 1)(\omega/\omega_1)}{1 + (\omega/\omega_1)^2} \end{aligned} \right\}, \dots\dots (22)$$

the equations for the components of the complex permeability.

(b) Kittel theory.

A theory developed by Kittel (1946) relies on a more thorough consideration of the skin effect in a film one domain thick. The effective field acting on the domain boundary is the mean value of the applied field taken over the entire wall which moves as a rigid whole under its influence. The reduced permeability is thus accounted for in terms of the small effective field.

The theoretical curves are similar to those derived by Becker for frequencies beyond 3,000 Mc/s. but at lower frequencies they are very much steeper, and a

resonance peak appears on the initial part of the μ_R curve: of this there is no suggestion in the experimental curves. It seems therefore that the reduced penetration of the field due to the skin effect cannot be the sole cause of the ferromagnetic dispersion.

(c) Damped resonance considerations.

The results of experiments performed by Griffiths (1946) and Birks (1950), with a static field imposed on the specimen in addition to the transverse high-frequency field, indicate the existence of damped resonance phenomena. Resonance due to gyroscopic rotation of the electron spins about the field direction may occur when the frequency of the oscillating field is equal to the natural frequency of gyration given by the Larmor precession frequency, $\omega_0 = eH/4\pi mc$, where H is the strength of the field along the axis of rotation. With a superimposed static field the electron spins may be aligned throughout the material and a sharp resonance condition is obtained. A fuller treatment has been given by Kittel (1947, 1948) who showed that the resonance frequency depends on the shape of the specimen, and for a plane surface is given by $\omega_0 = \gamma(BH)^{1/2}$ (rather than $\omega_0 = \gamma H$), where $\gamma = e/4\pi mc = 2.80$ Mc/s/oersted.

Landau and Lifshitz (1935) were the first to consider resonance in the absence of an external biasing field, and deduced that it would occur about the anisotropy field direction. In an unmagnetized polycrystalline material the internal field will vary in direction throughout the volume and if strains are present there will also be a variation in magnitude; hence each domain will resonate at a different frequency and a broad flat resonance will be obtained instead of a sharp one.

In the experiments under discussion no static field was applied to the specimen and so the experimental results may be interpreted in terms of a damped resonance occurring about the crystal anisotropy field direction, the damping being caused by microscopic eddy currents.

The resonance dispersion equation for an oscillatory field transverse to the internal field is given by (Frenkel 1945)

$$\frac{\mu - 1}{\mu_0 - 1} = \frac{\omega_0^2}{\omega_0^2 - \omega^2 + 2i\omega\omega_1}, \quad \dots\dots(23)$$

where ω_0 is the 'resonance' frequency and ω_1 is the 'damping' frequency. Separating the real and imaginary parts of equation (23) we get

$$\left. \begin{aligned} \frac{\mu_1 - 1}{\mu_0 - 1} &= \frac{\omega_0^2(\omega_0^2 - \omega^2)}{(\omega_0^2 - \omega^2)^2 + 4\omega^2\omega_1^2} \\ \frac{\mu_2}{\mu_0 - 1} &= \frac{2\omega_0^2\omega_1\omega}{(\omega_0^2 - \omega^2)^2 + 4\omega^2\omega_1^2} \end{aligned} \right\}, \quad \dots\dots(24)$$

for the components of the complex permeability.

(d) Summary of theories.

The three methods of attack presented above may be summarized as follows:

(1) *Becker theory.* This theory is based entirely on damping produced by eddy currents on domain boundary movements. The formal treatment gives for μ the equation

$$\mu - 1 = \frac{\mu_0 - 1}{1 + i(\omega/\omega_1)}, \quad \dots\dots(20)$$

which contains one parameter that can be adjusted to give as close a fit to the experimental curves as possible.

(2) *Kittel theory*. Damping is not taken into account in this theory, the dispersion being wholly attributed to a reduction of the effective field acting on the domain wall because of the very small skin depth.

(3) *Damped resonance*. Rotations only are considered here and the formal treatment gives for μ

$$\frac{\mu - 1}{\mu_0 - 1} = \frac{\omega_0^2}{\omega_0^2 - \omega^2 + 2i\omega\omega_1}, \quad \dots\dots (23)$$

an equation with two parameters, both of which are adjusted to give the best fit to the experimental curves. It seems probable that these effects are present, not alone but all together in varying degrees, and, therefore, it is not to be expected that a perfect fit to the experimental curves will be obtained by considering any one effect. The aim is to obtain a general fit which may give some indication of the type of mechanism responsible for the magnetization at high frequencies, e.g. rotational movements of the spins or translational movements of the domain walls.

(v) *Comparison of the Experimental Results with Theories*

(a) *Becker theory*.

A comparison of the experimental results for the complex permeability with values of μ_1 and μ_2 calculated from equation (22) are given in Figures 6, 7 and 8.

The theoretical curves are fitted to the experimental results by making ω_1 (in equation (22)) approximately equal to the frequency at which the experimental value of μ_2 reaches a maximum. From the values of ω_1 the sizes of the domains are calculated using equation (21). These are: iron annealed $l = 1.7 \times 10^{-4}$ cm.; steel annealed $l = 1.4 \times 10^{-4}$ cm.; mumetal $l = 1.6 \times 10^{-4}$ cm. These values are of the right order of magnitude although little reliance can be placed on them because of the over-simplification of the domain model. It has been pointed out by Landau and Lifshitz (1935) and Néel (1944) that the domains in the body of the material will most likely be in the form of plane parallel sheets, whereas the surface layer will consist of small domains of triangular cross section which provide 'closures of flux' for the main internal domains and thus prevent the appearance of free poles at the surface.

Although the general forms of the experimental and theoretical curves are similar, the frequency at which μ_1 is equal to μ_2 is in all cases lower than that at which μ_2 is a maximum, whereas the theory shows that the μ_1 curve should pass through the maximum of the μ_2 curve. Also, the real part of the permeability decreases more rapidly than the theory indicates; this was observed by Johnson and Rado (1949) who experimented at frequencies of 200 and 975 Mc/s. with a superimposed static field applied to the specimen. The theory gives a much larger and sharper maximum for μ_2 than the experimental curve suggests.

(b) *Damped resonance*.

Theoretical values of the complex permeability are derived from equation (24) and are plotted against frequency together with experimental values in Figures 9, 10 and 11.

The curves are fitted to the experimental values by choosing ω_0 and ω_1 to produce a μ_2 curve which has a maximum approximating to the experimental maximum. The condition for a maximum in μ_2 is

$$3\omega^4 - 2\omega^2(\omega_0^2 + 2\omega_1^2) - \omega_0^4 = 0. \quad \dots (25)$$

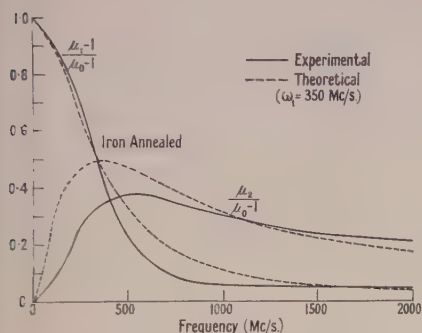


Figure 6. Comparison of experimental results with the Becker theory—Iron annealed.

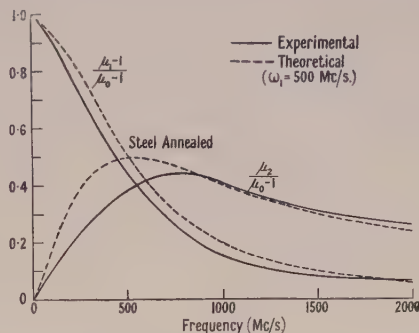


Figure 7. Comparison of experimental results with the Becker theory—Steel annealed.

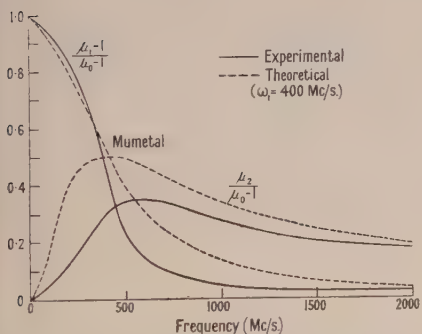


Figure 8. Comparison of experimental results with the Becker theory—Mumetal.

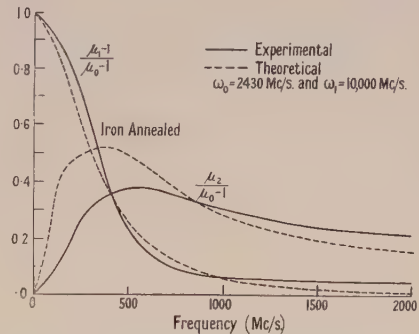


Figure 9. Comparison of experimental results with the damped resonance theory—Iron annealed.

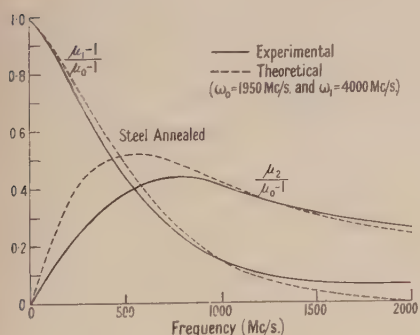


Figure 10. Comparison of experimental results with the damped resonance theory—Steel annealed.

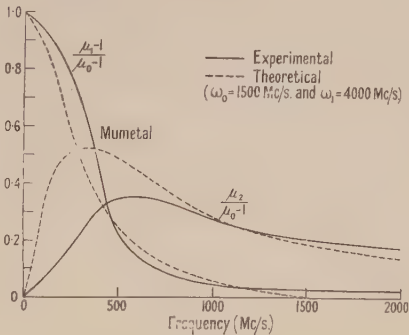


Figure 11. Comparison of experimental results with the damped resonance theory—Mumetal.

Due to a lack of suitable oscillators covering the range of frequencies between 500 and 1,000 Mc/s. the exact location of the maximum on the experimental curve for μ_2 cannot be obtained without further results for μ_2 in this range.

In some respects the type of curve obtained from considerations of a damped resonance expression approximates more closely to the experimental results than that drawn from an expression of the Becker type. The μ_1 and μ_2 theoretical curves intersect at a frequency slightly lower than that at which μ_2 is a maximum, which is in better agreement with experiment. Also, the μ_1 curve is nearer to the experimental results than the Becker μ_1 curve.

There are certain points, however, in which the experimental and theoretical curves do not agree. Firstly, the theory indicates that μ_1 becomes unity at a frequency equal to ω_0 and becomes less than unity at frequencies greater than ω_0 . Secondly, the theoretical curve (like the Becker curve) has a much larger and sharper maximum than the experimental points suggest.

A comparison of the resonance frequency with that which would be obtained for a resonance of the spins about the anisotropy field may be made by substituting the value of the field in the Larmor expression. The anisotropy field is given (Birks 1950) by $H=2K/I_0$, where K is the anisotropy constant and I_0 is the saturation magnetization. For iron, this is approximately 500 oersteds, which would give a Larmor frequency of 1,400 Mc/s. The resonance frequency for iron obtained from the experimental curves is therefore of the same order of magnitude as the Larmor frequency for the electron spins about the anisotropy field. The Larmor frequencies for steel and mumetal are approximately 1,400 and 120 Mc/s. respectively, which, especially in the case of mumetal, is not in very good agreement with the value of ω_0 substituted in the equation for μ . It is unlikely that an entirely different mechanism is operative for mumetal, and seems to indicate that more than one process is involved, e.g. a combination of boundary movements and spin rotations, both being damped by microscopic eddy currents.

§ 5. CONCLUSION

Experimental values of the permeability have been obtained from both resistive and inductive measurements on a circuit containing the ferromagnetic. The values of μ_R and μ_L , both decrease to unity as the frequency of the applied field is increased and μ_R is always greater than μ_L , the difference between them being covered formally by supposing the permeability to be complex.

The experimental values of the components of the complex permeability are compared with values obtained from two theoretical treatments, one based on boundary movements and the other on rotations; a fairly good fit is obtained in each case. The resonance frequency for iron calculated from damped resonance considerations approximates to the Larmor precession frequency of the electron spins about the anisotropy field, but the divergence for mumetal suggests the existence of more than one mechanism. It seems probable that the magnetic dispersion is due to eddy current damping of translational and rotational movements to approximately the same degree, the situation being further complicated by the possibility that skin depth effects of the type suggested by Kittel are responsible in some measure for the dispersion.

ACKNOWLEDGMENTS

We are greatly indebted to Professor R. Whiddington, under whose direction the work has been carried out, and to Professor E. C. Stoner for his continued interest and valuable advice. We wish to thank the Captain Superintendent, Admiralty Signal Establishment, for the generous loan of equipment, Messrs. John

Rigby & Sons Ltd., who provided the iron and steel specimens, Messrs. Telephone Construction & Maintenance Co. Ltd., who provided the mumetal wire and Mr. K. S. Driver for help with the proofs. One of us (F.V.W.) wishes to express his indebtedness to the Department of Scientific and Industrial Research for a grant.

REFERENCES

- ABRAHAM, M., and BECKER, R., 1932, *The Classical Theory of Electricity and Magnetism* (London: Blackie).
- ALLANSON, J., 1945, *J. Instn. Elect. Engrs.*, **92**, Pt. III, 247.
- ARKADIEW, W., 1926, *Ann. Phys., Lpz.*, **81**, 649; 1932, *Z. Phys.*, **74**, 5-6, 396.
- BECKER, R., 1938, *Phys. Z.*, **39**, 856; 1939, *Ann. Phys., Lpz.*, **36**, 340.
- BIRKS, J. B., 1948, *Proc. Phys. Soc.*, **60**, 282; 1950, *Proc. Phys. Soc. B*, **63**, 65.
- FRENKEL, J., 1945, *J. Phys., U.S.S.R.*, **9**, 299.
- GLATHART, J. L., 1939, *Phys. Rev.*, **55**, 833.
- GRIFFITHS, J. H. E., 1946, *Nature, Lond.*, **158**, 670.
- HODSMAN, G. F., EICHOLZ, G., and MILLERSHIP, R., 1949, *Proc. Phys. Soc. B*, **62**, 377.
- JACKSON, W., 1945, *High Frequency Transmission Lines* (London: Methuen).
- JOHNSON, M. H., and RADO, G. T., 1949, *Phys. Rev.*, **75**, 841.
- KITTEL, C., 1946, *Phys. Rev.*, **70**, 281; 1947, *Ibid.*, **71**, 270; 1948, *Ibid.*, **73**, 155.
- LANDAU, L., and LIFSHITZ, E., 1935, *Phys. Z. Sowjet*, **8**, 153.
- MICHEL, R., 1931, *Ann. Phys., Lpz.*, **8**, 877.
- NÉEL, L., 1944, *J. Phys. Radium*, **5**, 241.
- PROCOPIU, S., and D'ALBON, G., 1937, *C. R. Acad. Sci., Paris*, **205**, 1373.
- SORENSEN, A. J., 1924, *Phys. Rev.*, **24**, 658.
- TYNDALL, E. P. T., 1924, *Phys. Rev.*, **24**, 439.
- WIEN, M., 1931, *Ann. Phys., Lpz.*, **8**, 899.

The Production of Pulsed Magnetic Fields using Condenser Energy Storage

By K. S. W. CHAMPION

Electron Physics Department, University of Birmingham

Communicated by J. Sayers; MS. received 21st March 1950

ABSTRACT. An economical way of producing a pulsed magnetic field is to use condensers as the energy source and an air-cored magnet coil which, with the storage condensers, forms an oscillatory circuit. By means of a switch the coil is connected to the charged condensers and then disconnected precisely at the end of one cycle. In this way all the stored energy is used to produce the field, while most of it is recovered at the end of the pulse, the only appreciable losses being due to the resistance of the coil and switch.

The design of coils for use in the way described above is considered in detail. Expressions and curves are presented which enable the field produced by a specified coil and condenser combination to be readily calculated. Conversely, the data can be used to design the most satisfactory coil for any practical application. An example is given of the design and construction of an air-cooled coil.

§ 1. INTRODUCTION

TO investigate certain fundamental properties of low pressure arcs it became necessary to study the effect on them of strong magnetic fields. As the arcs in question were to be pulsed and the field required was inconveniently large for a conventional iron electromagnet, it was decided to pulse the magnetic field. The most satisfactory sources of the current pulse for such fields are

suitable generators or condensers. The design of coils for use with generators has been considered very fully by Cockcroft (1928).

However, very often condensers are a more satisfactory source of energy when such considerations as maintenance are taken into account, and, in the following, the design of suitable coils for use with a condenser energy source is considered. It is hoped that these data will be of use when it is necessary to design efficient coils for producing strong pulsed magnetic fields, for example, those for use with cloud chambers.

§ 2. THEORY OF PULSED MAGNETIC FIELD

If it is not necessary that the magnetic field pulse be square, a convenient and economical way of producing it is as follows. With the circuit as in Figure 1 the switch is closed when a pulse is desired and opened again precisely at the end of one cycle. By this means all the stored energy is used to produce the magnetic field, while most of it is returned to the condenser at the end of the cycle, the only appreciable losses being due to the resistance of the coil and switch. In practice it is usually found that an electronic switch is much more satisfactory than a mechanical switch.

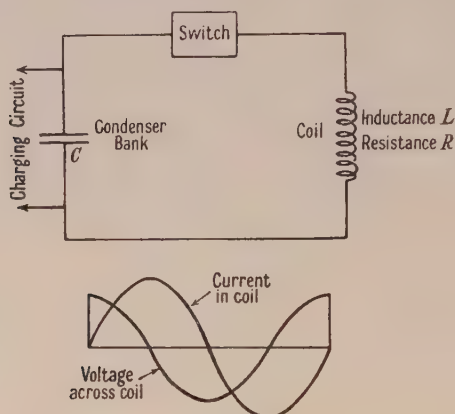


Figure 1. If R is not negligible the phase of the current is shifted and the waves are damped.

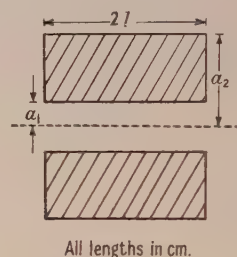


Figure 2.

If it were possible to convert all the energy stored in the condenser into a uniform magnetic field H_0 within the cylinder enclosed by the inner diameter of the coil, then the following relation would hold

$$\frac{H_0^2}{8\pi} \pi a_1^2 2l = \frac{1}{2} CV^2 \cdot 10$$

$$\text{i.e. } H_0 = \left(\frac{20C}{l} \right)^{1/2} \frac{V}{a_1} \quad \dots\dots(1)$$

where H_0 is in gauss, C in μF . and V in volts and it is assumed that the permeability is unity. The symbols representing the coil dimensions are defined in Figure 2.

Thus the actual magnetic field H at the centre of a coil can be expressed by

$$H = \left(\frac{20C}{l} \right)^{1/2} \frac{V}{a_1} K \quad \dots\dots(2)$$

where K is a positive quantity less than one. It is convenient to split K into the product of two quantities S and J where S depends only on the shape of the

coil and arises from the fact that the field is not uniform and not all contained in the cylinder enclosed by the inner diameter of the coil. J , on the other hand, is a factor to correct for the reduction in the first current peak (and, hence, the maximum magnetic field) due to the finite resistance of the coil. The values of S and J each lie between zero and one.

$$H = \left(\frac{20C}{l} \right)^{1/2} \frac{V}{a_1} SJ. \quad \dots\dots(3)$$

The value of the magnetic field at the centre of a coil may be expressed in the form

$$H = \frac{2\pi nI}{10(a_2 - a_1)} \cdot \ln \frac{a_2 + (l^2 + a_2^2)^{1/2}}{a_1 + (l^2 + a_1^2)^{1/2}} \quad \dots\dots(4)$$

where n is the number of turns in the coil (assumed to be uniformly distributed)

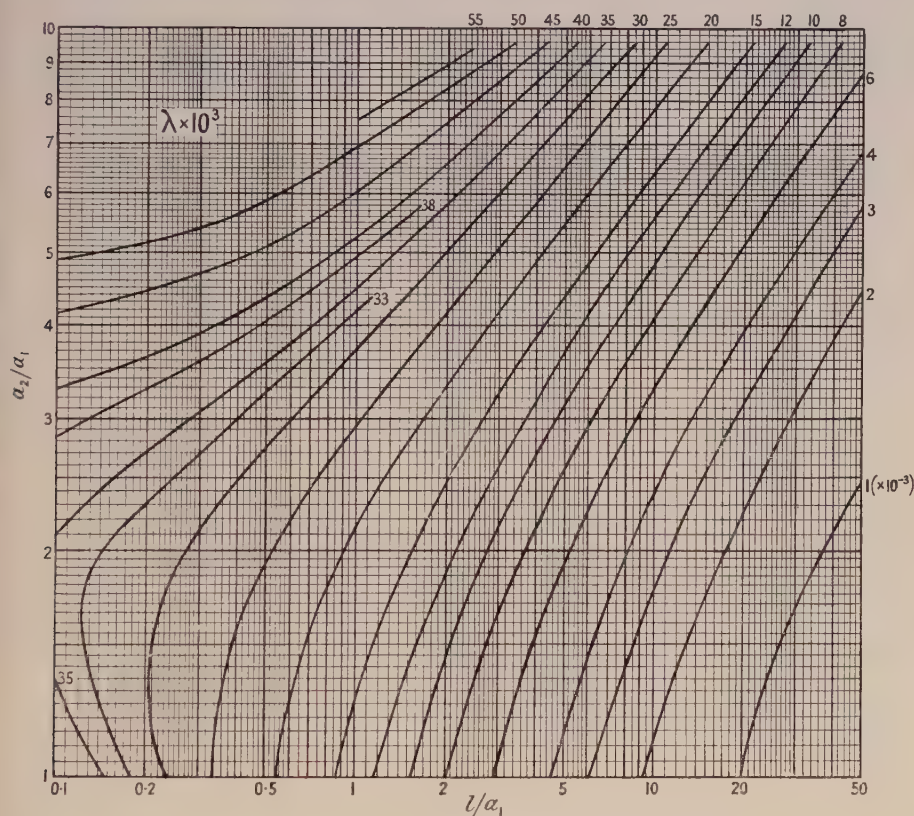


Figure 3. $L = n^2 a_1 \lambda$ or $n = (L/a_1 \lambda)^{1/2}$ L in $\mu\text{H.}$, a_1 in cm.

and I is the current in amperes. Now $n = (L/a_1 \lambda)^{1/2}$, as indicated by the curves for inductance* (Figure 3), and the maximum value of I is

$$I = \frac{V e^{-RT/8L}}{(R^2 + L^2 \omega^2)^{1/2}},$$

$$\text{where } \omega^2 = \frac{1}{LC} - \frac{R^2}{4L^2} \quad \text{and} \quad T = \frac{2\pi}{\omega}.$$

* These curves were calculated from data in a paper by Grover 1922.

Now

$$\frac{I}{V} \left(\frac{L}{C} \right)^{1/2} = \frac{e^{-RT/8L} \cdot \left(\frac{L}{C} \right)^{1/2}}{\left(R^2 + \frac{L^2 4\pi^2}{T^2} \right)^{1/2}}$$

$$= \frac{e^{-RT/8L} \left(1 + \frac{R^2 T^2}{16\pi^2 L^2} \right)^{1/2}}{\left(1 + \frac{R^2 T^2}{4\pi^2 L^2} \right)^{1/2}}.$$

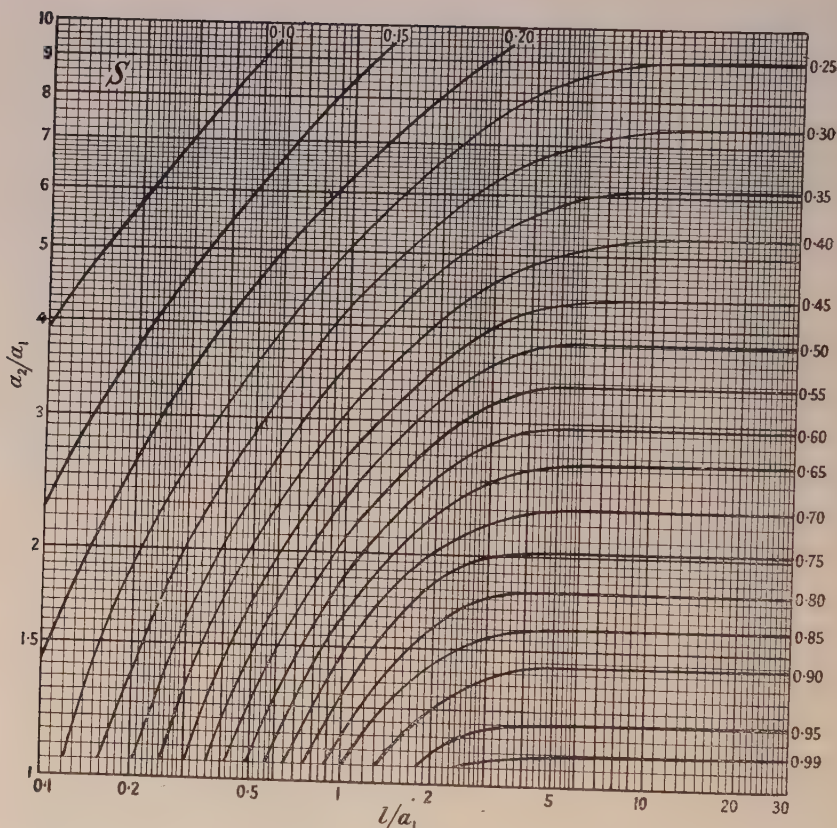


Figure 4.

$$H = \left(\frac{20C}{l} \right)^{1/2} \frac{V}{a_1} S J \quad H \text{ in gauss, } C \text{ in } \mu\text{F., } l \text{ and } a_1 \text{ in cm., } V \text{ in volts.}$$

This quantity, related to the first peak value I of the current, depending only on RT/L and such that its value is unity when R is zero, is the quantity J defined above.

$$J = \frac{I}{V} \left(\frac{L}{C} \right)^{1/2} = \frac{e^{-RT/8L} \left(1 + \frac{R^2 T^2}{16\pi^2 L^2} \right)^{1/2}}{\left(1 + \frac{R^2 T^2}{4\pi^2 L^2} \right)^{1/2}}. \quad \dots\dots (5)$$

If we substitute for n and I in (4) we obtain

$$H = \frac{2\pi L^{1/2} V J C^{1/2}}{10(a_2 - a_1) a_1^{1/2} \lambda^{1/2} L^{1/2}} \ln \frac{a_2 + (l^2 + a_2^2)^{1/2}}{a_1 + (l^2 + a_1^2)^{1/2}}.$$

From comparison of this expression and (3)

$$S = \frac{\pi \left(\frac{l}{a_1}\right)^{1/2}}{10 \times 5^{1/2} \left(\frac{a_2}{a_1} - 1\right) \lambda^{1/2}} \ln \frac{\frac{a_2}{a_1} + \left(\frac{l^2}{a_1^2} + \frac{a_2^2}{a_1^2}\right)^{1/2}}{1 + \left(\frac{l^2}{a_1^2} + 1\right)^{1/2}}. \quad \dots\dots(6)$$

This is the required shape factor since it is a function of l/a_1 and a_2/a_1 only. Curves of S are plotted in Figure 4. As would be expected, the value of S tends to unity for long, thin coils.

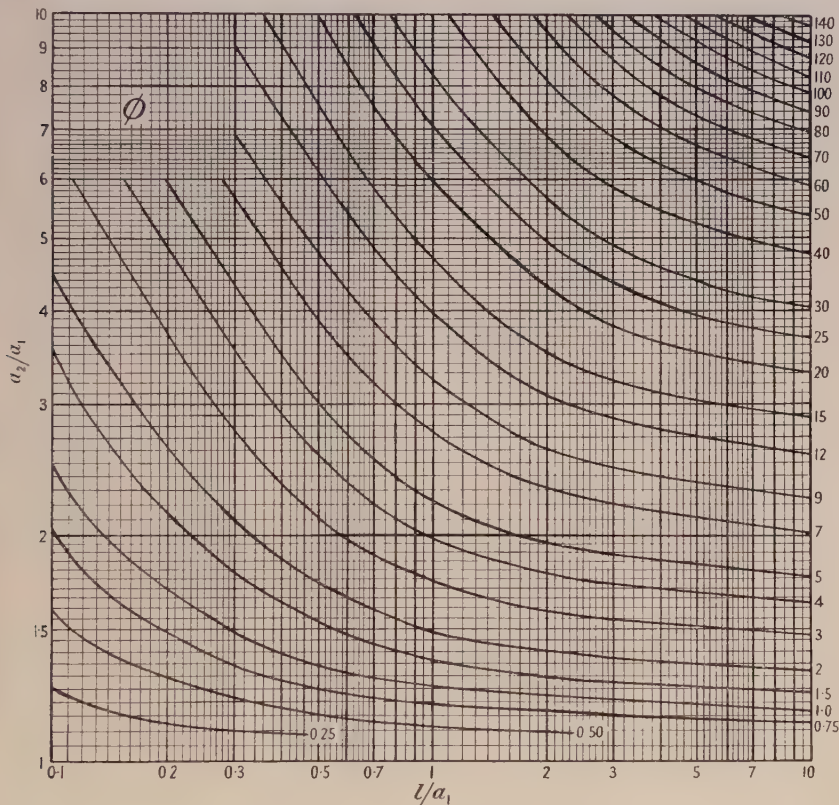


Figure 5.

$\frac{R}{L} = \frac{\rho 10^9}{a_1^2 \lambda_s \phi}$ R resistance of coil in ohms., ρ specific resistance (ohm. cm.),
 L inductance of coil in henries, a_1 internal coil radius (cm.), λ_s space factor.

Now $R/L = 10^9 \rho / a_1^2 \lambda_s \phi$ where ρ is the specific resistance of the material of the coil (in ohm.cm.), λ_s the space factor* and ϕ a quantity which is a function only of the shape of the coil.

$$\phi = \frac{2}{\pi} \times 10^3 \frac{l}{a_1} \lambda \left(\frac{a_2/a_1 - 1}{a_2/a_1 + 1} \right).$$

* The proportion of the coil winding volume occupied by conducting material is called the space factor.

Values of ϕ (†) are plotted in Figure 5 and values of J as a function of RT/L are set out in the Table. For values of RT/L up to 1.8, J may be represented by $(1 - RT/8L)$ with an accuracy closer than 0.2%.

Calculation of K for a Coil

Thus, to calculate the magnetic field produced at the centre of a coil, operated in the manner previously described, it is necessary to calculate K . This can be done by making use of the curves in Figures 4 and 5 and the values in the Table. The value of K is completely determined by l , a_1 , a_2 , λ_s , ρ and T .

As an example, consider a coil with $l = 5$ cm., $a_1 = 2.5$ cm., $a_2 = 4$ cm., $\lambda_s = 0.7$, $\rho = 1.724 \times 10^{-6}$ ohm.cm. and $T = 1$ millisec. In this case $l/a_1 = 2$ and $a_2/a_1 = 1.6$ and thus $\phi = 3.15$ and $R/L = 125.1$. Now $RT/L = 0.1251$ and hence $J = 0.984$; since $S = 0.803$ the value of K is 0.790.

Table

RT/L	J	Difference per 0.1 of RT/L	RT/L	J	Difference per 0.1 of RT/L
0	1	0.0125	2.5	0.693	0.0113
0.01	0.999		3	0.638	0.011
0.05	0.994		3.5	0.586	0.0104
0.1	0.987		4	0.537	0.0098
0.2	0.975				Per 1 of RT/L
0.3	0.962		5	0.451	0.086
0.4	0.950		6	0.379	0.072
0.5	0.937		7	0.319	0.060
0.6	0.925		8	0.270	0.049
0.8	0.900		10	0.195	0.038
1.0	0.875		12	0.143	0.026
1.2	0.850		15	0.0923	0.0169
1.4	0.825	0.012	20	0.0463	0.0092
1.6	0.800		25	0.0239	0.0045
1.8	0.775	0.012	30	0.0125	0.0023
2.0	0.751		40	0.0035	0.0009
2.2	0.727	0.012	50	0.00099	
			∞	0	

If the coil is used with a condenser bank containing 1,000 joules a field of 19,980 (approximately 20,000) gauss will be produced at its centre. Note that, with the above specifications, the ratio R/L is determined. Also, since

$$T = 2\pi \left(\frac{1}{LC} - \frac{R^2}{4L^2} \right)^{-1/2}$$

the product LC is determined. Hence, when any one of R , L , C is specified the values of the other two are fixed.

Limitations of the Data

Before considering the design of coils it is desirable to point out the limitations of the application of the data contained in this paper. In the curves for inductance (Figure 3) it has been assumed that the inductance is independent of the space factor, which is true when the latter is near unity. According to Grover (1922, p. 462), "only when the wires are relatively far apart will the correction (to be

† The quantity ϕ is identical with Cockcroft's ϕ_1 (1928). However, additional values have been calculated for the curves in Figure 5.

added to the inductance) exceed a few tenths of 1%". As these inductance curves have been used in the calculation of the ϕ and S curves any deviation from the former will be reflected in the latter. Secondly, the data only apply accurately to relatively low frequencies, as at radio frequencies the calculated inductance is reduced slightly and the resistance increased by the skin effect. Also, at these frequencies the coil capacity becomes appreciable and radiation losses may no longer be negligible.

§3. EXAMPLE OF THE DESIGN OF A COIL

As a source of energy a condenser of capacity $7\mu\text{F.}$ and maximum working potential 25 kv. is available. Consider the design of a coil to produce a maximum magnetic field with this source, given that its length is to be 20 cm. and internal radius 2.9 cm. The pulse length is to be 10 milliseconds and, from considerations of the insulation requirements, a space factor* of 0.7 seems possible. Assume that the mean temperature of the coil is 20°C. , then the value of ρ is the specific resistance of copper at this temperature. Values of K calculated from these data are plotted as a function of a_2/a_1 in Figure 7. K has a maximum value of 0.759 when $a_2/a_1 = 1.5$.

Heating of Coil

At this point it is necessary to consider the energy dissipated in the coil and the resultant temperature rise per pulse. The temperature rise per pulse

$$\delta t = \int_0^T \frac{Ri^2 dT}{v\sigma d}$$

where i is the current at any instant, v the volume of the coil windings and d and σ respectively the density and specific heat of the material of the coil. Assume that R is constant during a pulse and take $\frac{1}{2}I_1^2$ as the mean value of i^2 where I_1 is the amplitude of the current vector at $\frac{1}{2}T$. Thus, with sufficient accuracy

$$\delta t = \frac{RI_1^2 T}{2v\sigma d}$$

where $I_1 = VJ_1(C/L)^{1/2}$ with $J_1 = 1 - RT/4L$ for small values of RT/L . Values of δt calculated from this expression are plotted in Figure 7.

Now it is desired to operate this coil with one pulse per second for considerable periods. With $a_2/a_1 = 1.5$ and neglecting thermal conduction the rise in temperature per minute of operation would be 32.7°C. Even with mica insulation and a Tufnol former it is not advisable to have an increase in temperature greater than 150°C. and for this reason, a larger coil is required. For example, with $a_2/a_1 = 2.4$ the temperature rise is only 4.1°C. per minute. Such a coil, even with no loss of heat, could be operated for at least 30 minutes and, with efficient cooling of the outer surface, this time could be extended indefinitely.

Choosing a coil of this size the appropriate wire gauge is now to be determined. The resistance per unit length

$$\frac{Ra_1^{1/2}\lambda^{1/2}}{\pi L^{1/2}(a_1 + a_2)} = 1.074 \times 10^{-4} \text{ ohm/cm.}$$

* A higher space factor could be achieved if wire of rectangular section were used.

Hence 17 s.w.g. is the nearest gauge as it has a resistance of 1.068×10^{-4} ohm/cm. If wire of the calculated resistance were used 3,520 turns would be required.

A coil based on this design has been constructed and is illustrated in Figure 6. There are only 3,410 turns on the coil as its length is slightly less than

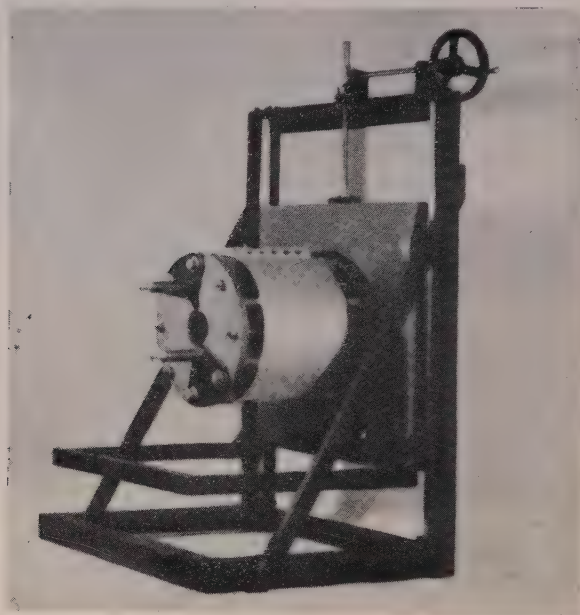


Figure 6. Coil in its mounting. The coil can be supported with its axis either vertical or horizontal by screwing the base plate to the appropriate part of the frame.

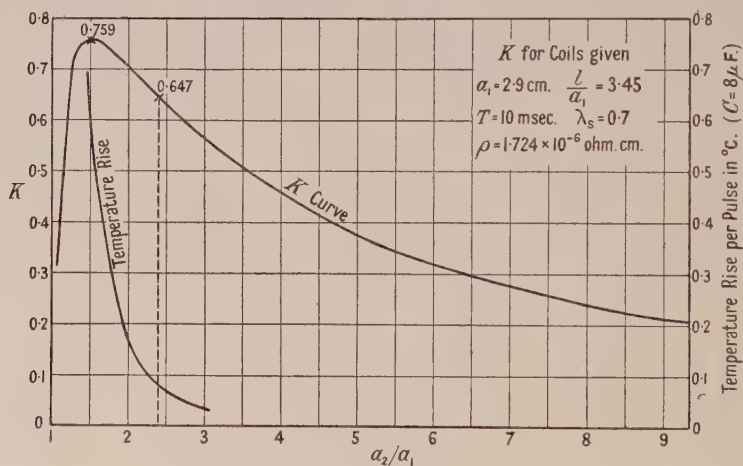


Figure 7.

Note. In this Figure $T = 10$ msec. should read $T = 10.7$ msec.

20 cm. and 17 s.w.g. is very slightly thicker than required. With this coil $H = 21,200$ gauss with $C = 7 \mu\text{F}$. and $V = 25,000$ volts.*

* Since the coil was constructed the condenser bank has been increased to $8 \mu\text{F}$., giving $H = 22,700$ gauss and $T = 10.7$ msec.

Mechanical Stresses in Coil

With intense magnetic fields the stresses in a coil may become very large. Cockcroft (1928) has given formulae and data which enable these stresses to be calculated. The main resultant force is perpendicular to the axis and outwards (compensated by binding the coil) but with very intense fields (say, of the order of 500 kilogauss) the forces on the inner parts of the coil may be so great as to cause the copper to flow towards the outer surface.

The maximum values of the stresses occur at the mid-point of the external surface and, with the coil designed above, are 6.9 kg/cm² in a direction perpendicular to the axis and 4.3 kg/cm² parallel to it. The total bursting force would be approximately 4,800 kg. The copper windings should stand this force, but, nevertheless, the coil is reinforced with eight $\frac{1}{2}$ -inch thick radial Tufnol strips, securely held by the end cheeks, pressed against the outer surface of the coil and with a brass band round their outer edges. The bolts securing the brass band are insulated from one end to minimize eddy currents. The Tufnol strips are set radially to facilitate efficient cooling of the surface of the coil.

§ 4. K AS A FUNCTION OF ITS PARAMETERS

K may be regarded as an efficiency constant for the operation of a coil in the way specified at the beginning of this article. However, it must be pointed out that the field produced also depends on the energy stored and the volume enclosed by the inner diameter of the coil.

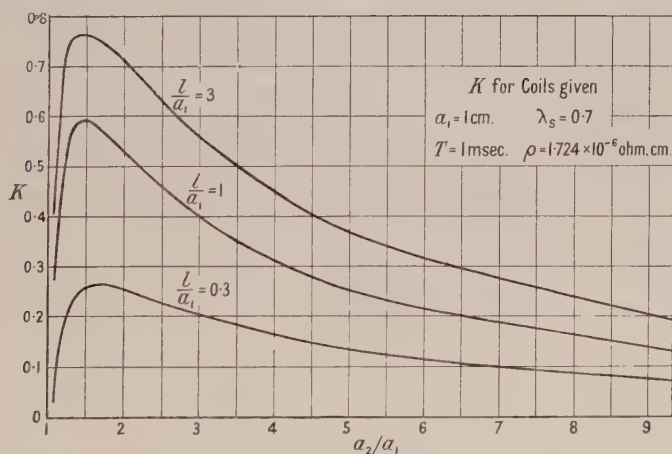


Figure 8.

Figure 8 gives examples of the way in which K (as a function of a_2/a_1) depends on l/a_1 . The value of a_2/a_1 for maximum K does not change much but, as would be expected, K is much smaller for shorter coils. In Figure 9 can be seen the very great change in K produced by changes in a_1 . This arises from the fact that, with smaller a_1 , the resistance of the coil becomes much more appreciable and, not only is K much smaller, but the value of a_2/a_1 at which the maximum of K occurs is larger. Figure 10 illustrates the way in which K depends on T .

Now, the only way in which K depends on parameters other than those of shape (i.e. l/a_1 and a_2/a_1) is in the expression for RT/L (of which J is a function) :

$$\frac{RT}{L} = \frac{\rho 10^9 T}{a_1^2 \lambda_s \phi}.$$

The effect due to a_1 varies inversely as its square, whereas that due to T is proportional to its first power. From the expression for RT/L we see that

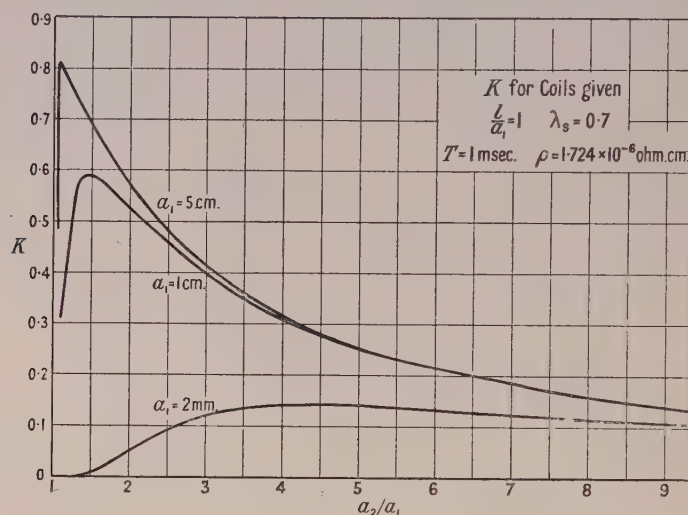


Figure 9.

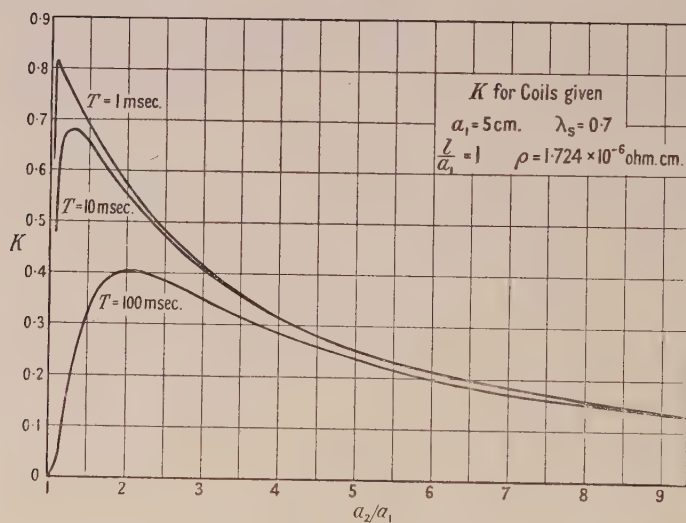


Figure 10.

any proportional change in ρ or $1/\lambda_s$ has the same effect on the value of K as the same proportional change in T .

The curves in Figures 8, 9, 10 and the above considerations should be of use when a coil is to be designed, making it possible to assess rapidly the influence of the various parameters on the magnetic field produced.

§ 5. SPATIAL VARIATIONS OF THE MAGNETIC FIELD

In many investigations one other property is important, viz. the degree of uniformity of the magnetic field. As the requirements of uniformity depend very much on the particular investigation, no general criterion will be presented, but merely data which make it possible to calculate the degree of uniformity of the field produced by a particular coil. As would be expected, the relative values of the field at various points near a coil depend only on the shape of the coil.

The value of the field at the centre of a coil is given by equation (4) and the value at a point on the axis distant x from the centre by

$$H_{0x} = \frac{2\pi nI}{20l(a_2 - a_1)} \times \left[(l+x) \ln \frac{a_2 + \{(l+x)^2 + a_2^2\}^{1/2}}{a_1 + \{(l+x)^2 + a_1^2\}^{1/2}} + (l-x) \ln \frac{a_2 + \{(l-x)^2 + a_2^2\}^{1/2}}{a_1 + \{(l-x)^2 + a_1^2\}^{1/2}} \right]. \quad \dots\dots(7)$$

If (7) is divided by (4) and then both numerator and denominator of the right-hand side of the resulting expression are divided by a_1 , H_{0x}/H_{00} is obtained as a function of a_2/a_1 , l/a_1 and x/a_1 . Thus, if in a design problem, instead of l/a_1 being specified, H_{0x}/H_{00} is specified for a given value of x/a_1 then, from equations (4) and (7), the value of l/a_1 for each a_2/a_1 can be calculated. However, the value of H_{0x}/H_{00} is almost independent of a_2/a_1 and thus it will often be possible to obtain the appropriate value of l/a_1 for one value of a_2/a_1 , and then use it with all required values of a_2/a_1 .

In general the magnetic field at points off the axis is not in the direction of the axis, but, with the rotationally symmetrical coils being considered, it will only have components parallel to the axis and in a radial direction. The general expressions for these components in terms of the value of the field at the axis are (Cosslett 1946) :

$$\text{In the direction of } x : H_{rx} = H_{0x} - \frac{r^2}{4} H_{0x}'' + \frac{r^4}{64} H_{0x}^{(4)} \dots \frac{(-1)^n}{(n!)^2} \left(\frac{r}{2}\right)^{2n} H_{0x}^{(2n)} \quad \dots\dots(8)$$

$$\text{and in the direction of } r : H_{rx} = -\frac{r}{2} H_{0x}' + \frac{r^3}{16} H_{0x}''' \dots \frac{(-1)^n}{n!(n-1)!} \left(\frac{r}{2}\right)^{2n-1} H_{0x}^{(2n-1)} \quad \dots\dots(9)$$

The differentiation is with regard to x . The coefficients can be obtained from equation (7) by differentiation but, in general, the full expressions for these and, consequently, the components of the field involve a very large number of terms. However, the case of the central plane of the coil ($x=0$) is much simpler. As the coils are symmetrical with regard to their central plane the value of the radial component of H_{r0} is zero for all values of r . For small values of r the axial component may be represented by

$$H_{r0} = H_{00} - \frac{r^2}{4} H_{00}''$$

where H_{00} is given by equation (4), and, by repeated differentiation of equation (7) and putting $x=0$,

$$H_{00}'' = \frac{2\pi nI}{10(a_2 - a_1)} \left[\frac{3}{(a_2^2 + l^2)^{1/2} \{a_2 + (a_2^2 + l^2)^{1/2}\}} - \frac{3}{(a_1^2 + l^2)^{1/2} \{a_1 + (a_1^2 + l^2)^{1/2}\}} \right. \\ \left. - \frac{l^2}{(a_2^2 + l^2)^{3/2} \{a_2 + (a_2^2 + l^2)^{1/2}\}} + \frac{l^2}{(a_1^2 + l^2)^{3/2} \{a_1 + (a_1^2 + l^2)^{1/2}\}} \right. \\ \left. - \frac{l^2}{(a_2^2 + l^2) \{a_2 + (a_2^2 + l^2)^{1/2}\}^2} + \frac{l^2}{(a_1^2 + l^2) \{a_1 + (a_1^2 + l^2)^{1/2}\}^2} \right]. \quad \dots\dots(10)$$

ACKNOWLEDGMENTS

The author wishes to acknowledge help and suggestions given in this work by Professor J. Sayers and assistance given by Mr. N. L. Allen. He is indebted to the English Electric Co. for the gift of an experimental glass ignitron which formed a vital part of the electronic switch. This work was made possible through the award to the author of a British Council Scholarship.

Note added in proof. Since the completion of this paper, a paper by G. Raoult, (1949) has come to the author's attention. It is entitled "Réalisation de champs magnétiques intense par impulsions. Applications aux phénomènes de polarisation rotatoire et de biréfringence magnétique". In this, besides other work, Raoult describes coils, with the requisite theory, for producing half-wave intense magnetic field pulses. His theory for the design of coils is somewhat similar to that above but, in his final expressions, he has neglected the effect of the resistance of the coil on the peak current obtained. In other words, he has assumed that $J=1$. In Raoult's work $k_1 = (20a_1/l)^{1/2} 10^3 S$ and $D = 1/10\lambda^{1/2}$.

REFERENCES

- COCKCROFT, J. D., 1928, *Phil. Trans. Roy. Soc. A*, **227**, 317.
 COSSLETT, V. E., 1946, *Introduction to Electron Optics* (Oxford: Clarendon Press), p. 106.
 GROVER, F. W., 1922, *Scientific Papers of the Bureau of Standards*, **18**, 415.
 RAOULT, G., 1949, *Ann. Phys., Paris*, 12^e serie, **4**, 369.

A Theory of Contact Noise in Semiconductors

By G. G. MACFARLANE

Telecommunications Research Establishment, Ministry of Supply

MS. received 8th May 1950

ABSTRACT. A theory of contact noise is described in which the low-frequency noise is attributed to the random movement of adsorbed ions on the surface of a semiconductor from which an electron current is being drawn. Emission of electrons is assumed to take place only at localized patches on the surface and the adsorbed ions are assumed to give rise to a Schottky barrier layer, in which the potential maximum is linearly related to the concentration of ions. Diffusion of the ions over the surface gives rise to random fluctuations in the concentration of ions in a patch which results in random fluctuations in the height of the potential barrier and the emission current. It is shown that for a circular patch the spectral power density of the noise current varies with mean current j_0 and frequency f as $j_0^{2/x} f^x$ over a small range of frequency and that x varies monotonically from -0.75 at the lowest frequencies to -1.125 at the highest frequencies. It is also shown that for a long thin rectangular patch the index x varies monotonically from -0.5 to -1.5 as the frequency is increased from zero. The dependence of the noise power density on temperature is also discussed.

§ 1. INTRODUCTION

IN a previous paper (Macfarlane 1947) the author has described a theory of contact noise which depends on a diffusion conduction process in the atomic layers next to the emitting surface of a crystal. The noise was attributed to the diffusion of clusters of mobile atoms on to the contact surface, their ionization on the surface and subsequent conduction away from the surface in the applied field. On the basis of a simple model it was shown that the spectral power density of the current noise should depend on mean current j_0 and frequency f as $j_0^{x+1} f^{-x}$. The index x , which lies between 1 and 2, depends on the concentration N of atoms in a mobile cluster. As x tends to 1, N tends to ∞ . However, experiments on silicon crystal rectifiers (Miller 1947), carbon granule microphones (Christensen and Pearson 1936, Miller 1949), germanium crystal rectifiers and lead sulphide photosensitive layers (Harris, Abson and Roberts 1947) show that in some cases x is very nearly equal to unity and in other cases it must be taken less than unity. In addition some recently published measurements (Campbell and Chipman 1949) on resistors have shown that the index of f varies from about -1 at low frequencies to -1.6 at high frequencies. In order to explain these results on the above theory it would be necessary to assume enormous concentrations of atoms in mobile clusters. It is therefore apparent that this theory, in spite of its success in giving the observed dependence on current and frequency with micro-crystalline layers of PbS (Harris, Abson and Roberts 1947), is inadequate.

In order to overcome these difficulties the author has developed a new theory, in which the noise is attributed to the random modulation of the Schottky barrier potential at emitting patches by random fluctuations in the concentration of mobile adsorbed ions. In its simplest form the theory refers to thermionic emission from a semiconductor, but it can be applied equally well to emission from one crystallite to another at contacts.

The idea is that the surface of a semiconducting crystal is covered by a partial film of adsorbed atoms, which have become negative ions by the capture of electrons from the crystal. As a result a Schottky space charge layer is set up at the surface, as in Bardeen's (1947) theory of surface states. The height of the potential barrier is proportional to the concentration of ions. The adsorbed ions are assumed to move at random over the surface of the crystal. When an electric field is applied to the crystal, emission of electrons is assumed to take place only at localized patches on the surface. Fluctuations in the concentration of ions in a patch occur due to the diffusion of ions out of and into the patch. These fluctuations in number of ions in a patch give rise to fluctuations in the height of the potential barrier at the patch and therefore to fluctuations in emission of electrons.

Since the electron emission is controlled by the concentration of ions in a patch the problem is to study the correlation in the number of ions in a patch and its dependence on time.

The problem is essentially the same as a classical one in the study of the Brownian movement in colloidal solutions. It is to find the correlation function for the fluctuation in the number of particles in a cylindrical volume within a much larger volume of colloidal solution. An account of the relevant theory of colloidal statistics is given by Chandrasekhar (1943).

In applying the formulae for contact noise to a multicrystalline layer or mass of semiconducting crystals it must be clearly realized that there are also other sources of noise, such as the Johnson noise of the bulk resistance, fluctuations in the number of current carriers, and noise due to the 'spreading' resistance. The power density of these other sources is, however, independent of frequency at least at low frequencies, whereas contact noise per unit bandwidth increases as the frequency is decreased. If a frequency power spectrum of the total noise is known it is only necessary to subtract out the constant noise power, observed at high frequencies, in order to obtain the spectrum of the contact noise.

In a very recent article, which came to the notice of the author after the theory to be described below had been worked out, Richardson (1950) has described in a most interesting manner a theory of contact noise in which the noise is also attributed to a diffusing adsorbed layer. He considers the region of multiple contact between two rough surfaces and assumes that the conductance per unit area is a function of the separation of the surfaces and the total concentration of adsorbate, near the point in question. By an analysis quite different from the one given below he derives an expression for the spectral power density which varies with frequency as f^{-1} . Since the total noise power would diverge to infinity with this law Richardson suggests a modification to remove the divergence. With our model we arrive at a different expression which does not suffer from this defect. As we shall show it gives a law of the form $j_0^2 f^x$ over a small frequency range, where the index x varies from -0.75 at very low frequencies to -1.125 at very high frequencies for a circular patch and from -0.5 to -1.5 for a long thin rectangular patch.

§2. ANALYSIS OF THE PATCH MODEL

We consider emission of electrons from a localized surface patch A of an emitter. Emission from the surface immediately surrounding A is assumed to be negligible. We assume that the current j through the patch A depends on the

number n of adsorbed ions within the patch as $\exp(an)$ and that the adsorbed ions can move at random over the entire surface of A and the surrounding surface.

With these assumptions we can calculate the auto-correlation function and from it, by Khintchine's theorem, the spectral power density of the noise current emitted by the patch in the following manner.

The first step is to calculate the mean number of ions \bar{m} in a patch A after time τ from the instant when n ions occur in A . In doing this we assume that the motions of the ions are independent of each other and that all positions in A have equal *a priori* probability. Then if the probability that an ion somewhere in A will have emerged from it during the time τ is P , the number of ions which on the average will leave the patch in τ is nP and therefore the number remaining is $n(1 - P)$. In addition the number entering A on the average in τ is NP regardless of the initial value of n . The average number of ions in the patch after time τ is therefore

$$\bar{m} = n(1 - P) + NP. \quad \dots\dots(1)$$

Now in accordance with our assumptions the current j through the patch A depends on n as $j = j_0 e^{a(n-N)}$, where j_0 is the mean current. The noise current is therefore

$$\Delta j = j - j_0 = j_0 [e^{a(n-N)} - 1] \simeq j_0 a(n - N). \quad \dots\dots(2)$$

The approximation used in (2) is justified provided the noise current is small compared with the mean current.

The auto-correlation function of the noise current is therefore

$$\begin{aligned} f(\tau) &= \overline{\Delta j(n) \Delta j(m)} \\ &= \overline{(j_0 a)^2 (n - N)(m - N)} \\ &= \overline{(j_0 a)^2 (n - N)^2 (1 - P)} \\ &= (j_0 a)^2 N(1 - P). \end{aligned} \quad \dots\dots(3)$$

In the third line of (3) we have averaged with respect to m keeping n constant and using (1), and in the fourth line we have used the well-known result that the mean square deviation for random events is equal to the mean.

The next step is to consider the probability P . Suppose firstly that the patch A is a circular disc of radius r and that the diffusion constant for the movement of ions on the surface is D , then it can be shown (Chandrasekhar 1943) that the probability P that an ion somewhere within A will have emerged from it during the time τ is

$$P = e^{-x} [I_0(x) + I_1(x)], \quad \dots\dots(4)$$

$$\text{where} \quad x = (\tau_0 / \tau)^{1/4} \quad \dots\dots(5)$$

$$\text{and} \quad \tau_0 = (2r)^2 / D. \quad \dots\dots(6)$$

Using Khintchine's theorem (Wang and Uhlenbeck 1945) we can now write down an expression for the spectral power density of the noise current.

$$R(\omega) = 4 \int_0^\infty f(\tau) \cos(\omega\tau) d\tau = 4(j_0 a)^2 N \tau_0 F(p), \quad \dots\dots(7)$$

$$\text{where} \quad F(p) = \int_0^\infty \{1 - \exp(-x^{-1/4}) [I_0(x^{-1/4}) + I_1(x^{-1/4})]\} \cos(px) dx \quad \dots\dots(8)$$

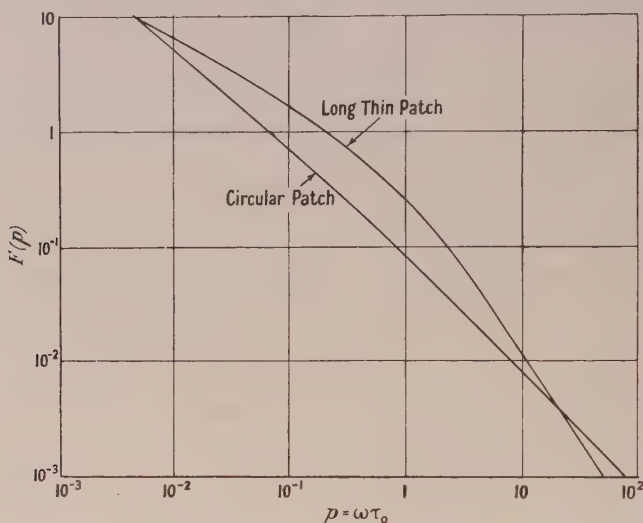
$$\text{and} \quad p = \omega \tau_0. \quad \dots\dots(9)$$

The function $F(p)$ has been evaluated from the series given in the Appendix and is shown in the Figure. Two limiting formulae are useful.

$$\text{When } p \ll 1 \quad F(p) \simeq 0.2345p^{-3/4} \quad \dots\dots(10)$$

$$\text{and when } p \gg 1 \quad F(p) \simeq 0.1466p^{-9/8} \quad \dots\dots(11)$$

In the preceding analysis $R(\omega)$ is the mean square noise current at a single localized patch or contact. It was derived on the assumption of a constant voltage across the contact. When there are many such contacts, as in a multi-crystalline resistor or at contacts between rough surfaces, the noise fluctuation of the total input current is a weighted sum of the separate fluctuations at the contacts. The weighting factor will depend on the current at the contact and on the current



which a series E.M.F. at the contact would produce at the input to the resistor. It will therefore depend on the position of the contact in the resistor.

As an example consider a resistor which can be represented by m sets of contacts in parallel, each set consisting of n contacts in series. Between adjacent series contacts assume a 'bulk' resistance. Let the resistance of the pq th contact be r_{pq} and the 'bulk' resistance in series be R_{pq} . Then a simple circuit analysis shows that the mean square noise current at input is

$$\overline{\Delta j^2} = j_0^2 R^2 \sum_{p=1}^m \sum_{q=1}^n c_{pq} r_{pq}^2 / R_p^4, \quad \dots\dots(12)$$

where j_0 is the mean current at input, R the total resistance of the resistor, $R_p = \sum_{q=1}^n (R_{pq} + r_{pq})$ and

$$c_{pq} = 4a^2 N_{pq} \tau_{pq} F(\omega \tau_{pq}). \quad \dots\dots(13)$$

As a further simplification suppose that all the contacts have the same resistance r_0 and all the resistances R_{pq} are equal to R_0 . Then

$$\overline{\Delta j^2} = j_0^2 \{r_0 / (R_0 + r_0)\}^2 \bar{c} / mn. \quad \dots\dots(14)$$

Although this last expression applies only to a very simple resistor it does indicate that the power density of the noise current decreases as the number of contacts is increased.

On account of the summation in (12) the variation of noise power density with frequency will not be quite given by (8). However, at high enough frequencies where (11) is valid, $c_{pq} \sim 0.5864a^2N_{pq}\tau_{pq}^{-1/8}\omega^{-9/8}$ and $\overline{\Delta j^2}$ is then directly proportional to $\omega^{-9/8}$. Similarly at low enough frequencies $\overline{\Delta j^2}$ varies with frequency as $\omega^{-3/4}$.

§ 3. THE EFFECT OF PATCH SHAPE ON THE SPECTRUM

In § 2 we assumed a circular patch. However the shape of a patch does have an interesting effect on the spectrum, as we can see by evaluating $R(\omega)$ for a long thin strip. Then diffusion takes place primarily across the strip. If the width of the strip is h the probability P is given by (Chandrasekhar 1943)

$$1 - P = \text{erf}(x^{-1/2}) - (x/\pi)^{1/2}[1 - e^{-1/x}], \quad \dots\dots(15)$$

where $x = \tau_0/\tau$ and $\tau_0 = h^2/4D$.

The spectral power density of the noise current is then

$$R(\omega) = 4(j_0a)^2N\tau_0F(p), \quad \dots\dots(16)$$

where $p = \omega\tau_0$ and

$$F(p) = \int_0^\infty \{\text{erf}(x^{-1/2}) - (x/\pi)^{1/2}[1 - e^{-1/x}]\} \cos(px) dx. \quad \dots\dots(17)$$

The function $F(p)$ has been evaluated from the formulae

$$F(p) = \sum_{n=1}^{\infty} \frac{(-)^n \sqrt{\pi} p^{n-3/2}}{4\Gamma(n+1)\Gamma(n+\frac{1}{2}) \sin \pi(\frac{1}{2}n - \frac{3}{4})} + \sum_{n=0}^{\infty} \frac{(-)^{n+1} \sqrt{\pi} p^{2n}}{2\Gamma(2n+2)\Gamma(2n+5/2)} \quad \dots\dots(18)$$

$$\simeq (2p)^{-1/2} \text{ for } p \ll 1 \quad \dots\dots(19)$$

$$\text{and} \quad \simeq (2p)^{-3/2} \text{ for } p \gg 1. \quad \dots\dots(20)$$

These formulae were derived by the method given for (8) in the Appendix. $F(p)$ for a long thin strip is shown plotted in the Figure for comparison with $F(p)$ for a circular patch.

§ 4. DISCUSSION OF THE NOISE SPECTRUM

Consider firstly the spectrum for a circular patch. If $F(p)$ is replaced by a power law cp^x over a small range of p then it can be seen from formulae (10) and (11) and from the Figure that x varies from -0.75 when $p \ll 1$ to -1.125 when $p \gg 1$. From this it follows that the integral of $F(p)$ taken over the entire frequency range from $p=0$ to $p=\infty$ is finite, notwithstanding the fact that $F(p)$ tends to infinity as p tends to zero.

It will be observed that the spectral power density of the noise current increases with the square of the mean current and directly with the average number of adsorbed ions in a patch.

Only an approximate expression for the dependence of $R(\omega)$ on temperature can be given unless the variation with temperature of the mean number, N , of ions in a patch is known. If we assume N independent of temperature T we have

$$a = E_0/kT, \quad D = D_0 e^{-E/kT}, \quad \tau_0 = (2r)^2 D_0^{-1} e^{E/kT}, \quad \dots (21)$$

where E is the activation energy for diffusion of ions over the surface and E_0 is the change in height of the barrier potential at a patch produced by one ion. Then, if $\omega\tau_0 \gg 1$, we get from (7) and (11) that

$$R(\omega) \sim 0.1868 \pi j_0^2 N D_0^{1/8} (2r)^{-1/4} (E_0/kT)^2 e^{-E/8kT} \omega^{-9/8} \\ \propto T^{-2} e^{-E/8kT}. \quad \dots (22)$$

From (22) it follows that $R(\omega)$ increases with T for temperatures below $T_c = E/16k$ and decreases with increase of T for temperatures above T_c . If $E \simeq 0.1$ ev., which is probably rather a high value for surface diffusion, $T_c \simeq 60^\circ \text{K}$. Then for temperatures above 60°K . and for high frequencies $R(\omega)$ should decrease as the temperature is increased. Evidence that $R(\omega)$ does decrease with increase of temperature is provided by measurements on silicon rectifiers (Miller 1949).

Although little is known of the values of the diffusion constants D_0 and E , for diffusion of adsorbed ions over a crystal face both D_0 and E are likely to be much smaller than for diffusion of impurities through a crystal (Mott and Gurney 1948). In order to appreciate the magnitude of τ_0 take $D_0 = 10^{-4} \text{ cm}^2/\text{sec}$, $E = 0.1$ ev., and take the radius of a patch as 10^{-4} cm . Then $\tau \simeq 0.016 \text{ sec}$. at room temperature.

Consider now the effect of patch shape on the spectrum. We have found that, when $\omega\tau_0 \gg 1$, $R(\omega) \propto \omega^{-9/8}$ for a circular patch and $R(\omega) \propto \omega^{-3/2}$ for a long thin rectangular patch and that, when $\omega\tau_0 \ll 1$, $R(\omega) \propto \omega^{-3/4}$ for a circular patch and $R(\omega) \propto \omega^{-1/2}$ for a long thin rectangular patch. Deviations in the index x in the expression $R(\omega) \propto \omega^x$ can therefore be explained in terms of patch shape so long as x lies in the range $-1.125 > x > -1.5$ at high frequencies and in the range $-0.75 < x < -0.5$ at the lowest frequencies. It has been found experimentally (Miller 1949) that for a photoelectric cell illuminated with a constant intensity of light $x \simeq -1$, for a carbon granule microphone $-1 > x > -1.1$, and for a carbon resistor $-1.1 > x > -1.2$. These results can therefore be explained by assuming nearly circular patches. For various types of resistor Campbell and Chipman (1949) have found that the index x varies from about -1 at a frequency of 20 kc/s. to about -1.6 at 500 kc/s. and that $R(\omega)$ increases as the square of the mean current. It would therefore be necessary to assume long thin patches in order to explain these results. For micro-crystalline layers of PbS it is found (Harris, Abson and Roberts 1947) that x may lie between -1 and -1.4 .

It appears therefore that the theory of contact noise described above, in which the noise is attributed to fluctuations in emission from localized patches on the surface of an emitter due to fluctuations in the number of ions in a patch, can provide a reasonable explanation of the observed results.

APPENDIX

EVALUATION OF THE INTEGRAL FOR $F(p)$

The Mellin transform of $1 - P(x) = 1 - \exp(-x^{-1/4})[I_0(x^{-1/4}) + I_1(x^{-1/4})]$ is (Macfarlane 1949)

$$F_1(s) = \frac{-2^{4s+2}\Gamma(\frac{1}{2} + 4s)\Gamma(-4s)}{\sqrt{\pi}\Gamma(2+4s)} \quad 0 < \sigma < \frac{1}{4}.$$

By using the inversion formula of the Mellin transform to express $1 - P$ as an integral in the s -plane and reversing the order of integration we get

$$\begin{aligned} \int_0^\infty [1 - P(x)] \cos(px) dx &= \frac{1}{2\pi i} \int_{\sigma-i\infty}^{\sigma+i\infty} F_1(s) ds \int_0^\infty x^{-s} \cos(px) dx \quad 0 < \sigma < \frac{1}{4} \\ &= \frac{-1}{2\pi i} \int_{\sigma-i\infty}^{\sigma+i\infty} \frac{4\Gamma(-4s)\Gamma(\frac{1}{2} + 4s)\Gamma(\frac{1}{2} - \frac{1}{2}s)2^{3s}}{\Gamma(2+4s)\Gamma(\frac{1}{2}s)} p^{s-1} ds \quad 0 < \sigma < \frac{1}{4}. \end{aligned}$$

The integrand has poles at

$$s = -\frac{1}{4}(n + \frac{1}{2}) = -\frac{1}{8}, -\frac{3}{8}, -\frac{5}{8}, \dots \text{ due to } \Gamma(\frac{1}{2} + 4s)$$

and at $s = n/4 \ (n > 0) = \frac{1}{4}, \frac{1}{2}, \frac{3}{4}, \dots \text{ due to } \Gamma(-4s)$

and double poles at

$$s = 2n + 1 = 1, 3, 5, \dots \text{ due to } \Gamma(-4s) \text{ and } \Gamma(\frac{1}{2} - \frac{1}{2}s).$$

Moving the contour steadily to the right we can take out the residues at the poles to the right of σ and get the following convergent series for $F(p)$.

$$\begin{aligned} F(p) &= \sum_{\substack{n=1 \\ n \neq 8r-4}}^\infty \frac{\sqrt{\pi}(-)^{n+1}\Gamma(n+\frac{1}{2})2^{n-1}p^{n/4-1}}{\Gamma(n+1)\Gamma(n+2)\Gamma(\frac{1}{4}n)\cos(n\pi/8)} \\ &+ \sum_{n=0}^\infty \frac{(-)^n\Gamma(8n+\frac{9}{2})2^{8n+4}p^{2n}}{\sqrt{\pi}\Gamma(8n+6)\Gamma(8n+5)\Gamma(2n+1)} \left[4\psi(8n+\frac{9}{2}) - 4\psi(8n+6) - 4\psi(8n+5) \right] \\ &\quad \left[-\psi(2n+1) + \ln(16p) \right] \end{aligned}$$

The first few terms are

$$\begin{aligned} &0.23447p^{-3/4} - 0.31333p^{-1/2} + 0.34892p^{-1/4} - 0.14378 + 0.03646 \ln p \\ &- 0.04953p^{1/4} + 0.00718p^{1/2} - 0.00123p^{3/4} + \dots \end{aligned}$$

Moving the contour to the left we obtain an asymptotic series for $F(p)$ from the residues at the poles of $\Gamma(\frac{1}{2} + 4s)$.

$$\begin{aligned} F(p) &\sim \sum_{n=0}^\infty \frac{(-)^n\Gamma(n+\frac{1}{2})\Gamma(n-\frac{1}{2})\Gamma(\frac{1}{4}n+\frac{8}{9})}{\pi^{3/2}\Gamma(n+1)} \sin \pi \left(\frac{1}{8}n + \frac{1}{16} \right) 2^{-n-1/2} p^{-n/4-9/8} \\ &\sim 0.14659p^{-9/8} - 0.04925p^{-11/8} - 0.01394p^{-13/8} - 0.01093p^{-15/8} \\ &- 0.01328p^{-17/8} \dots \end{aligned}$$

ACKNOWLEDGMENT

The author desires to thank the Ministry of Supply for permission to publish this paper, which is reproduced with the permission of the Controller, H.M. Stationery Office.

REFERENCES

- BARDEEN, J., 1947, *Phys. Rev.*, **71**, 717.
 CAMPBELL, R. H., and CHIPMAN, R. A., 1949, *Proc. Inst. Radio Engrs.*, **37**, 938.
 CHANDRASEKHAR, S., 1943, *Rev. Mod. Phys.*, **15**, 1, Chap. III.
 CHRISTENSEN, C. J., and PEARSON, G. L., 1936, *Bell Syst. Tech. J.*, **15**, 197.
 HARRIS, E. J., ABSON, W., and ROBERTS, W. L., 1947, T.R.E. Report T2051 (unclassified).
 MACFARLANE, G. G., 1947, *Proc. Phys. Soc.*, **59**, 366; 1949, *Phil. Mag.*, Ser., **7**, 188.
 MILLER, P. H., 1947, *Proc. Inst. Radio Engrs.*, **35**, 252; 1949, See review article prepared by S. J. ANGELLO, *Electrical Engineering*, **68**, 870.
 MOTT, N. F., and GURNEY, R. W., 1948, *Electronic Processes in Ionic Crystals*, 2nd Edition. (Oxford: Clarendon Press).
 RICHARDSON, J. M., 1950, *Bell Syst. Tech. J.*, **29**, 117.
 WANG, M. C., and UHLENBECK, 1945, *Rev. Mod. Phys.*, **17**, 323.

Dielectric Loss and Dielectric Constant Measurements in Supercooled Liquids

BY C. DODD AND G. N. ROBERTS
 University College and Queen Mary College, London

Communicated by E. N. da C. Andrade; MS. received 26th June 1950

ABSTRACT. In order to provide further evidence in support of the structural change which takes place in a liquid when it is supercooled, measurements of dielectric loss at high frequencies and of dielectric constant have been made on various polar liquids. The evidence from the dielectric loss measurements is inconclusive but for the four liquids tested a significant discontinuity in the dielectric constant-temperature curve has been established at the melting point in each case.

§ 1. INTRODUCTION

THE work of Dodd and Hu Pak Mi (1949) has shown for certain polar liquids that, although there is no discontinuity of the viscosity η at the melting point, there is a sharp change in the course of the line of $\log \eta$ plotted against $1/T$ at this point. Such a phenomenon can only result from some sort of structural change in the liquid as it supercools and any such change should also show itself in the temperature variation of other properties of the liquid.

The present paper describes measurements made on the dielectric loss and dielectric constant of several liquids over a range of temperature on both sides of the melting point.

§ 2. DIELECTRIC LOSS

The apparatus for the determination of the dielectric loss was one in use in the research department of Electrical Engineering at Queen Mary College, London. Oscillations of wavelength 3 cm. from a klystron were fed into an H_{01} cavity resonator containing the liquid, and were passed through coaxial cable to a crystal detector, variable attenuator and galvanometer. The resonator was in a constant temperature bath and a thermocouple in contact with the movable piston attached

to a micrometer shaft registered the temperature of the liquid. The width of the resonance curve was obtained from the positions of the micrometer shaft when the galvanometer deflections were half the maximum value. From this width the dielectric loss was calculated. In Figure 1 the variation of loss with temperature is shown by plotting ϵ''/ϵ_0 against temperature for both normal and supercooled liquid phenyl ether (M.Pt. $26.9^\circ\text{C}.$) where ϵ'' is the imaginary part of the complex dielectric constant and ϵ_0 the dielectric constant of free space. It is seen that over this range the scatter of the points is too great for any indication of a discontinuity at the melting point to be apparent.

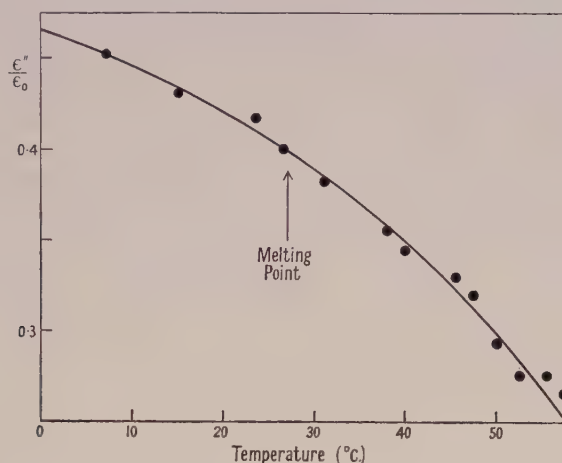


Figure 1.

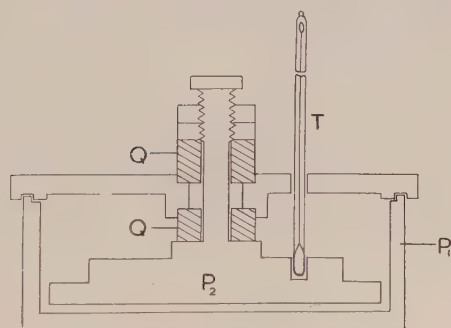


Figure 2.

§ 5. DIELECTRIC CONSTANT

In order to measure small changes in the dielectric constant of a liquid to a high degree of accuracy, a test condenser was joined in parallel with a standard and a variable condenser in a circuit tuned to a frequency of 244 kc/s.

The test condenser (Figure 2) was of the parallel plate type, the plates P_1 , P_2 of diameter about 6 cm. being separated by a distance of the order of 1 mm. by the quartz washers QQ. The empty capacity was determined at various temperatures by a modified Hartshorn circuit. This value was about 28 pF. and changed by only 0.18 pF. for a temperature change of $40^\circ\text{C}.$ The capacity varied regularly with temperature and showed no hysteresis when taken over a heating cycle. The

whole cell was then filled with liquid, the thermometer T registering the temperature to an accuracy within 0.02°C ., and was immersed in a bath whose temperature could be maintained constant to better than 0.01°C .

The variable condenser was of the cylindrical type, the capacity being varied by movement of the inner cylinder. The total movement available was 1,500 divisions on the micrometer, one division (10^{-3} cm.) corresponding to a capacity change of 0.01074 pF . A change of half a division caused a measurable change in the resonant position.

The setting of the micrometer condenser to give resonance was found with the test condenser at various temperatures both above and below the melting point of the liquid. The liquids chosen, which were all polar, readily supercooled and remained in the liquid state throughout. The micrometer condenser setting C is plotted against temperature for phenyl ether, M.Pt. 26.9°C ., $\mu = 1.17$ (Figure 3); salol, M.Pt. 42°C ., $\mu = 3.15$ (Figure 4); menthol, M.Pt. 42°C ., $\mu = 1.56$ (Figure 5), and azoxybenzene, M.Pt. 36°C ., $\mu = 1.70$ (Figure 6); μ is the dipole moment, in all cases $\times 10^{18}$. Because of the large ionic loss for azoxybenzene at the lower frequency (244 kc/s.), the circuit was tuned to a frequency of 1.65 Mc/s. for this liquid. Values for the dielectric constant K deduced from the corresponding micrometer condenser settings, are given as ordinates on the right-hand side of the graphs.

§ 4. DISCUSSION

Examination of Figures 3, 4, 5 and 6 shows in each case that for the liquid above its melting point the points lie fairly well on a straight line. Those for the super-

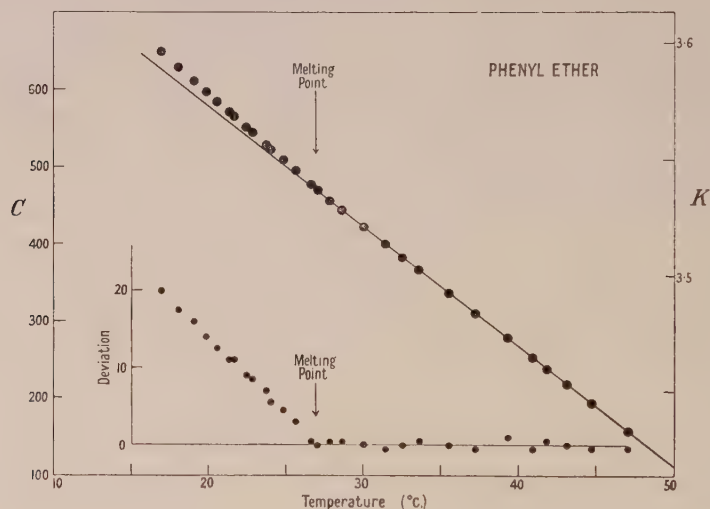


Figure 3.

cooled liquid also lie on a line which is, however, inclined to the line for the normal liquid. In each case these lines intersect in the neighbourhood of the melting point. This discontinuity at the melting point is brought out more strikingly by the insets to the graphs, where the deviations of *all* points from the straight line, fitted by least squares, for the liquid above the melting point, are plotted against

temperature. It should be mentioned that in order to avoid any systematic error arising in the apparatus, the dielectric constant was measured first in the region above the melting point, then in the slightly supercooled region, back into the normal region, further into the supercooled region, and so on.

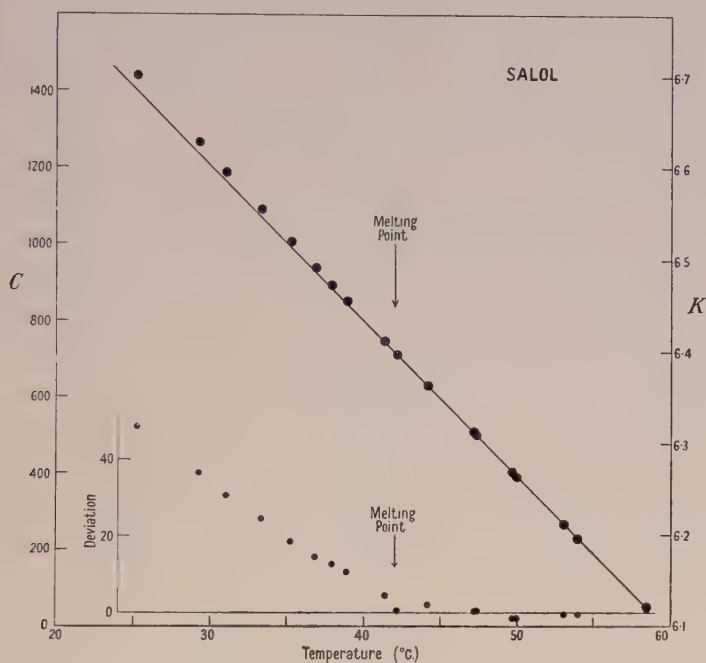


Figure 4.

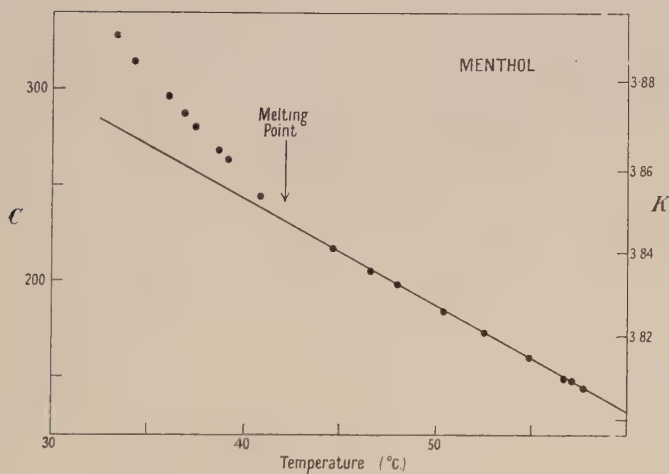


Figure 5.

For phenyl ether, salol and menthol similar discontinuities at their melting points have been found by Dodd and Hu (1949) for the variation of viscosity with temperature. The experimental technique used for these viscosity measurements

is not, however, easily adaptable to azoxybenzene, which is a dark, almost opaque liquid.

It would therefore appear that the change occurring in the nature of the liquid as it enters the supercooled region is responsible for both the discontinuity in

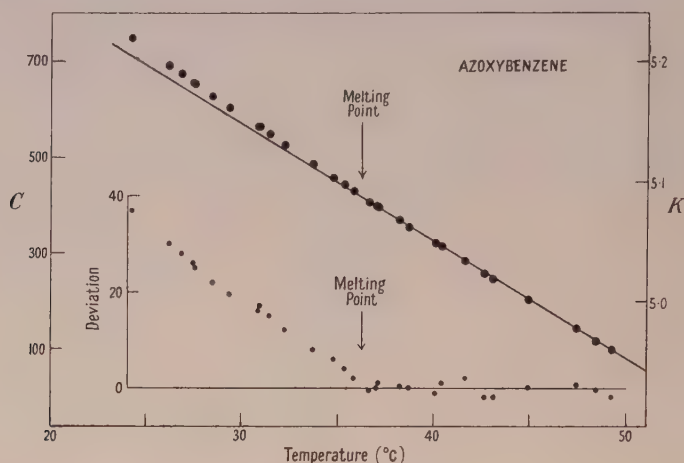


Figure 6.

dielectric constant and the discontinuity in viscosity. The search for similar discontinuities in other physical properties of these supercooled liquids is continuing.

ACKNOWLEDGMENTS

We should like to express our gratitude to Professor W. J. John of the Electrical Engineering Department, Queen Mary College, for permission to use apparatus in his department, and to the Department of Scientific and Industrial Research for a grant to one of us (G.N.R.).

REFERENCE

DODD, C., and HU PAK MI, 1949, *Proc. Phys. Soc. B*, **62**, 454.

LETTERS TO THE EDITOR

The Dielectric Strength of Aluminium Oxide Films

Fröhlich (1937) has shown that, under the influence of an applied electric field F , electrons in a crystal will gain energy A from the field and lose energy B to the lattice vibrations, and that the resultant energy change $B-A$ is given by $B-A=B-(e^2/m)\tau F^2$, where e and m are the electronic charge and mass respectively, and τ is the average time between collisions. Electrical breakdown occurs when electrons possessing energy greater than the ionization energy J gain energy from the field. Accordingly, the breakdown field strength is inversely proportional to the square root of the relaxation time. Hence $F \propto l^{-1/2}$, where l is the mean free path of the electrons. If the latter is decreased by introducing foreign ions into the crystal, or by raising the temperature, the dielectric strength increases. In a thin film the value of B increases as the film thickness approaches the mean free path, since the number of collisions with the film boundary increases, and thus the dielectric strength of thin films of dielectric should rise with decreasing film thickness. Fröhlich has

calculated the order of such an increase for mica. Austen and Whitehead (1940) using mica of thickness varying from 10^{-4} to 10^{-5} cm. have verified his predictions, and more recently Plessner (1948) working with CaF, NaF and KBr films has also confirmed Fröhlich's theory.

This theory may be extended to films of amorphous materials, such as aluminium oxide, for which there should be a similar increase of strength although, since the electronic mean free path in amorphous substances is considerably less than in crystalline material, the effect should only occur to any marked extent in very thin films, for example films of thickness probably less than 100 Å.

The aluminium oxide films used in the present investigation were made by partially anodizing a thick aluminium film, formed by evaporation of the metal on an optical flat in a vacuum of 10^{-6} mm. Hg. The metal film was partially immersed in an aqueous solution of ammonium phosphate, and to prevent 'peeling' of the film the flat was subjected to ionic bombardment before evaporation.

The thickness of the oxide film was measured by employing equal chromatic order interference fringes. A cross section of the film is shown in Figure 1. It projects beyond the adjacent aluminium film, so that the oxide film may be defined by the two distances

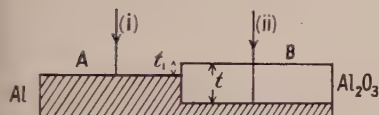


Figure 1.

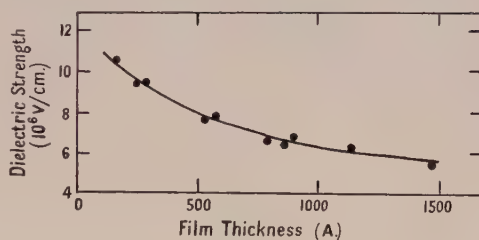


Figure 2.

t its thickness and t_1 the step between surfaces A and B. Hass (1949) has shown recently that the ratio t_1/t is constant, independent of t and equal to 0.27. Thus the optical path difference between rays (i) and (ii) reflected from the air-aluminium and the oxide-aluminium surfaces, respectively, is given by $2(\mu - 0.27)t$. Taking $\mu = 1.65$ —as given by Hass—the optical path difference between the rays is $2.76t$. When placed in contact with a semi-silvered optical flat, the step may be detected by means of fringes of equal chromatic order, formed by reflection at the film-optical flat surfaces, white light and a constant deviation spectrometer being used to produce these fringes. Since a thin surface oxide layer exists at the air-aluminium interface, phase changes at the oxide-aluminium and air-aluminium interfaces are equal. The fringes on both sides of the step were parallel and, accordingly, the oxide films were of uniform thickness.

Attempts were made to measure the film thickness directly by completely anodizing aluminium deposited on a film base of gold, nickel or platinum. With this arrangement the film thickness could be measured independently of the refractive index and the constant t_1/t but such metals 'peeled off' the flat during electrolysis.

The potential difference across the oxide film was applied by means of two spherical electrodes—steel ball bearings $\frac{1}{16}$ in. in diameter—one in contact with the surface A and the other lightly sprung so as to rest on B. The pre-breakdown currents, measured with gradually increasing potentials, were similar to those obtained by von Hippel (1938) with mica and alkali halide crystals. They are probably produced by strong field emission from the cathode although it has been suggested that they may be formed by ejection of electrons from impurity centres at high field strengths.

At a certain voltage this pre-breakdown current suddenly increased to a very high value and this voltage represents the breakdown value. Many measurements were made with the same film at different places on the film and averaged. In all experiments the film was in a vacuum and at 15° C. Figure 2 shows the variation of dielectric strength with film thickness. As the latter increased from 100 Å. to 1,000 Å. the strength decreased from 11×10^6 v/cm. to 6×10^6 v/cm. The value at 1,000 Å. agrees with that found by Güntherschulze and Betz (1936) for aluminium oxide in bulk.

The dielectric strength of one film was measured at 15° c. and at 100° k. It increased from 8×10^6 v/cm. to 9.5×10^6 v/cm. Similar results were found by von Hippel and Maurer (1941) using soda lime glass. This indicates that aluminium oxide has an amorphous structure and supports Hass' statement that no pores exist in the oxide film formed by anodization.

The relationship between formation voltage and film thickness in the present experiments is similar to that found by Hass (1949) and by Güntherschulze and Betz (1936). It is linear, but whereas the latter obtained a slope of 11 A/volt and Hass 13 A/volt, the present work gives 14 A/volt.

The Physical Laboratories,
The Washington Singer Laboratories,
University College, Exeter.
7th July 1950.

P. D. LOMER.

AUSTEN, A. E. W., and WHITEHEAD, S., 1940, *Proc. Roy. Soc. A*, **176**, 33.
FRÖHLICH, H., 1937, *Proc. Roy. Soc. A*, **160**, 230.
GÜNTHERSCHULZE, A., and BETZ, H., 1936, *Z. Phys.*, **100**, 539.
HASS, G., 1949, *J. Opt. Soc. Amer.*, **39**, 532.
VON HIPPEL, A., 1938, *Phys. Rev.*, **54**, 1096.
VON HIPPEL, A., and MAURER, R. J., 1941, *Phys. Rev.*, **59**, 820.
PLESSNER, K. W., 1948, *Proc. Phys. Soc.*, **60**, 243.

Ferromagnetic Resonance in Manganese Arsenide

Manganese arsenide is known to have a ferromagnetic critical point in the region of 40° c. and to exhibit pronounced temperature hysteresis (Bates 1928, 1929, 1931, 1933). Below the critical point ferromagnetic properties are clearly marked, and at room temperature the material has a saturation intensity of magnetization comparable with that in nickel at the same temperature. An investigation has been made into the ferromagnetic resonance absorption in this material at a wavelength of 1.25 cm. and at temperatures from 18 to 50° c.

The intensity of magnetization in small rod samples was measured by a simple ballistic method throughout the required temperature range and in applied magnetic fields up to 5,000 oersteds. It will be seen that at room temperature a value of about 400 E.M.U. is found for I , whereas Bates (1933) obtained a value of about 600; in each case satisfactory checks against a pure nickel sample were made. The reason for this discrepancy is being investigated.

From each rod, very thin discs were cut and mounted to form part of the lower end of a cylindrical cavity resonating in an H_{111} mode. The power absorbed in the specimen, at constant microwave frequency, was measured as a function of the strength of an applied steady magnetic field. The applied field, H_{\max} , for maximum power absorption was thus determined at each temperature. Using the relations first developed by Kittel (1947, 1948), it follows for a specimen of the form used that

$$g = \frac{2 \times 10.7}{\lambda_a (BH)_{\max}^{1/2}},$$

where g is the Landé splitting factor, λ_a is the free space wavelength in centimetres, and B and H are expressed in kilo-oersteds.

Specimen results obtained with one sample are shown in the Table. Near the critical point the intensity of magnetization is changing very rapidly with temperature, the total absorption is small, and the experimental accuracy is therefore decreased.

$$\lambda_a = 1.25_2 \text{ cm.}$$

t (° c.)	20.0	29.8	33.1	35.0	36.0	37.0	37.8	39.0	39.75	41.7	45 and 50
H_{\max} (oe.)	2700	2725	2800	2800	2925	3050	3280	3650	4150	~4550	4500 to 5000
I (E.M.U.)	408	390	383	378	365	331	267	120	50	—	—
g	3.7 ₂	3.7 ₅	3.7 ₁	3.7 ₂	3.6 ₆	3.6 ₆	3.6 ₈	3.9 ₃	3.8 ₄	3.7 ₆	3.4 ₄ to 3.8 ₀

Three different specimens were examined and, within the limits of experimental error, the g -value determined by the above equation does not vary up to the critical point. At room temperature, the three g -values found were 3.7_2 , 3.7_5 , and 3.8_2 .

It is of interest that resonance absorption could be detected above 45°C . where the manganese arsenide has paramagnetic properties. The absorption is small and broad, so that the position of the peak can only be found approximately, but it appears to be such as to suggest little, if any, change from the ferromagnetic g -value. There is no discontinuity observable at the critical point, the width of the absorption curve slowly increasing with the temperature. At 50°C ., the width is about 20% greater than at room temperature. These latter observations are in accordance with those of Bloembergen (1950) whose results for nickel and supermalloy were published during the course of this investigation.

Of particular interest, however, is the very large g -value which is obtained. Previously published results by various authors (see Kittel 1949) have given values mainly of the order of 2.20 and the excess of this above the value 2.00 for an electron spin has been qualitatively interpreted in terms of the contribution of the orbital moment (Kittel 1949, Polder 1949, Van Vleck 1950). Kittel has shown that if g is the g -value deduced from microwave absorption measurements and g' that from direct gyromagnetic measurements, g should be greater than 2.00 by the amount that g' is less than 2.00 for small variations about the electron spin value.

If this type of explanation is to hold in the case of manganese arsenide, one would expect g' to be very much less than 2.00. It is thought that there has been no such measurement on manganese arsenide itself, but Galavics (1939) has reported measurements on an Mn-Sb alloy stated to be Mn_3Sb , for which he obtained a value for g' between 1.9 and 2.0.

It is hoped to continue this investigation with other materials of the types Mn-P, Mn-Sb, Mn-Bi, and results will be reported later.

The authors wish to record their thanks to Professor L. F. Bates, who kindly supplied the manganese arsenide samples, for his continued interest and advice.

The University,
Nottingham.
25th July 1950.

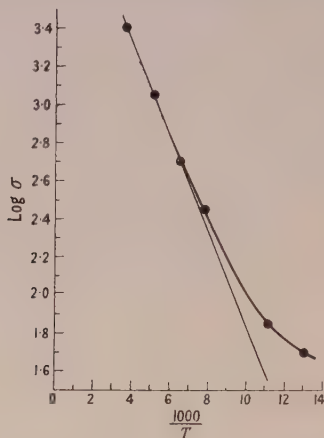
G. D. ADAM.
K. J. STANDLEY.

- BATES, L. F., 1928, *Proc. Roy. Soc. A*, **117**, 680; 1929, *Phil. Mag.*, **8**, 714; 1931, *Proc. Phys. Soc.*, **43**, 87; 1933, *Phil. Mag.*, **16**, 657.
BLOEMBERGEN, N., 1950, *Phys. Rev.*, **78**, 572.
GALAVICS, F., 1939, *Helv. Phys. Acta*, **12**, 581.
KITTEL, C., 1947, *Phys. Rev.*, **71**, 270; 1948, *Ibid.*, **73**, 155; 1949, *Ibid.*, **76**, 743.
POLDER, D., 1949, *Phil. Mag.*, **40**, 99.
VAN VLECK, J. H., 1950, *Phys. Rev.*, **78**, 266.

Electrical Conductivity of Gray Tin

Gray tin has a non-metallic crystal structure similar to diamond (Bijl 1919, Brownlee 1950), i.e. it is the end-member of the series carbon-silicon-germanium-gray tin. One would therefore expect its electrical properties to be appropriate to its position in the series; but there seem to be no reliable experimental results available in the literature. It was originally reported that gray tin was a superconductor, but de Haas (1928) and Sharvin (1945) showed that this was incorrect, at least above 1.2°K . Busch (private communication) has obtained some values for electrical conductivity of gray tin powder which show it to be a semiconductor. On the other hand Moesveld (1937) reported that it was a normal metallic conductor. It seemed unlikely that results of real value could be obtained until a way was found of preparing gray tin in massive crystalline form free from white tin. Normally it is prepared by keeping tin at a temperature well below its transition point (13.2°C .) when the metal crumbles into a friable powder. The large change in specific gravity from 7.31 to 5.75 is no doubt the cause of this disintegration. Unfortunately, subsequent compression of the powder tends to transform it back to white tin, even when the compression is carried out at low temperature.

In transforming a kilogram of spectroscopically pure tin it was found that amongst the large quantity of fine powder produced were a few lumps of gray tin several millimetres in linear dimensions. Suitable electrodes were pressed against these lumps and their electrical conductivity measured for small D.C. currents, using a milliammeter and potentiometer. No contact non-linearity was observed, but precautions were necessary to eliminate the rather large thermo-electric E.M.F. generated under non-uniform temperature conditions.



α -tin: variation of conductivity with temperature.

The variation of conductivity with temperature is shown in the Figure; the values given for specific conductivity must be regarded as only approximate as there was some difficulty in measuring the cross section and electrode areas of the specimens. Almost identical results were obtained for three different specimens.

It is seen that gray tin is an intrinsic semiconductor, in which the conductivity is given by

$$\sigma = A \exp(-\epsilon/2kT).$$

From the upper portion of the curve we obtain $A \simeq 6 \times 10^4 \text{ ohm}^{-1} \text{ cm}^{-1}$, and $\epsilon = 0.098 \text{ eV}$. At the lower temperatures the presence of impurities in the tin is presumably causing enhanced conductivity and a lower activation energy. Gray tin thus fits consistently into the series of intrinsic homopolar semiconductors as shown in the Table below. The very small energy difference between the filled and unfilled bands is noteworthy, and leads to the high conductivity at 0° C ., remarkable for a semiconductor, of approximately $2.5 \times 10^3 \text{ ohm}^{-1} \text{ cm}^{-1}$.

	ϵ	A
Silicon	1.12	0.9×10^4
Germanium	0.75	3.3×10^4
Gray tin	0.1	6×10^4

The author wishes to acknowledge the award of a Leverhulme Research Fellowship.

Department of Electrical Engineering,
Imperial College of Science and Technology,
London, S.W.7.
6th July 1950.

J. T. KENDALL.

- BIJL, A. J., 1919, *Proc. Acad. Sci. Amst.*, **21**, 405.
BROWNLEE, L. D., 1950, *Nature, Lond.*, (in the press).
DE HAAS, W. J., 1928, *Proc. Acad. Sci. Amst.*, **31**, 350.
MOESVELD, A. L., 1937, *Z. Phys. Chem. A*, **178**, 455.
SHARVIN, G., 1945, *J. Phys., USSR*, **9**, 350.

Development of the Low Pressure Electrodeless Discharge in a High-Frequency Electric Field

The starting of a high-frequency electrodeless discharge with the mean free paths of electrons much larger than the dimensions of the glass vessel has recently been investigated (Gill and von Engel 1947, 1948). In these experiments a cylindrical glass tube containing gas at this low pressure was placed in a uniform high-frequency electric field (wavelength order 10 m.) directed parallel to the axis. It was shown that, if an electron starting at one end wall with a small energy and in a suitable phase of the field crossed the tube in one half-cycle, and hit the opposite end wall fast enough to release more than one secondary electron, then an electron avalanche would develop. The starting field strength should therefore depend on the material of the end walls, and not on the gas. This was confirmed by experiment. As the discharge develops a current passes through the gas and the field decreases. This working field strength, and the spectrum emitted, are characteristic of the gas, and do not depend on the material of the vessel.

It was derived that in the initial stages of the discharge electrons have maximum energy (about 100 ev.) when they hit an end wall. This is enough to release between one and two secondary electrons per incident electron, most of which contribute to the development of the avalanche, whilst a few are lost to the side walls. This maximum energy is also much greater than the ionization energy of any gas.

But in the fully developed discharge both photographic measurements at wavelengths of about 3,000 Å. and visual observation show that most of the light is emitted from the centre of the cylindrical vessel and very little from the ends. Assuming that this light comes directly from atoms excited by collisions with electrons, it appears that the electrons are fastest in the central region. A cloud of electrons seems here to oscillate with small amplitude about a space charge of positive ions in the centre of the tube. Very few of these electrons hit the end wall; if they did they would be lost. But it is known that when losses to the walls are large (e.g. beyond cut-off wavelength (Gill and von Engel 1948) no field, however large, can start the discharge.

As far as we know no attempt has been made to describe the transition from the initial to the final stage of such a discharge. At first sight it would appear that, of the few ions formed in the gas in the earlier stages, most would be produced near the walls where the electrons are fastest. Two clouds of positive space charges would then be formed near the end walls, and this would continue to make the electrons fastest near the ends of the tube. (The effect of the positive wall charge caused by secondary electron emission has been considered, but found irrelevant here.)

This, however, is not true. A calculation of the energy of an electron as a function of position along the tube shows that any electron capable of starting the discharge acquires energy equal to the ionization energy of any gas well before it reaches the centre of the tube. The ionization produced is obtained by combining this result with known ionization probabilities.

Now electrons crossing the tube in one direction produce a distribution of ions in space which increases rapidly towards the centre, and then slowly from the centre to the far wall. Electrons crossing in the opposite direction produce a symmetrically opposite distribution. The sum gives the maximum number of ions at the centre. As the multiplication process continues the number of ions increases, but the maximum ionization is always at the centre.

When the number of ions becomes considerable the field in which electrons move is the applied field plus the field due to this positive space charge. As the latter increases the electrons reach their maximum speed progressively nearer the centre of the tube. New electrons are now produced (by ionization of gas atoms) near the centre, and start oscillating in a phase different from that of the main cloud. Some are lost to the walls; most oscillate in the gas with a maximum speed near the centre, their amplitudes becoming smaller the larger the positive ion space charge. These are the electrons which are found in the final stage of the discharge. The electrons originally produced by secondary emission from the walls are progressively lost to the end walls as their speed at the ends

of the tube is reduced by the influence of the positive ion space charge. These electrons neutralize the positive wall charge.

Positive ions in the gas drift to the walls owing to self-repulsion in the ion cloud. However, electrons produced in the gas in unfavourable phases of the applied field are also lost to the wall, neutralizing these positive ions and charging the walls slightly negatively.

Thus it appears that the transition from multiplication by secondary emission to an equilibrium state sustained only by ionization in the gas can only occur when the electrons produced by the first process are all replaced by electrons produced in the gas which then oscillate with an amplitude smaller than the length of the vessel.

The Clarendon Laboratory,
Oxford.
10th August 1950.

G. FRANCIS.
A. VON ENGEL.

GILL, E. W. B., and VON ENGEL, A., 1947, *Nature, Lond.*, **159**, 404; 1948, *Proc. Roy. Soc. A*, **192**, 446.

REVIEWS OF BOOKS

An Introduction to Heat Transfer, by M. FISHENDEN and O. A. SAUNDERS.
Pp. x+205. 1st Edition. (Oxford: The University Press, 1950.) 15s.

There seems to be a general trend towards putting the engineering treatment of heat-transfer problems on to a more systematic basis than has been the practice in the past, and the authors of this book have been among those who were instrumental in bringing it about.

They have now published a book, distinct from their earlier joint writings, in which the whole subject is surveyed on a reasoned basis.

The first chapter deals with radiation, whether the theoretical simple radiation from a black body or the complicated phenomena encountered, for example, when considering the radiation from the flames in a furnace. The questions which arise when geometrical considerations intervene, or when the emitting and receiving surfaces are of different emissivities, are considered.

The next chapter is on conduction, and does not deal in detail with the calculation of heat flow in complex systems, though it does treat the theory of sufficient cases for most practical applications. The theory is a matter for mathematicians, and is treated in separate books, of which that by Carslaw and Jaeger is probably the best known, though a recent one by Ingersoll, Zobel and Ingersoll should not be overlooked, especially as it and the book under review are in a sense complementary, and share the same outlook—that of keeping basic physics in view while applying the theory in practice. In this chapter, Fishenden and Saunders describe in detail the graphical method due to Schmid for calculating heat flow, and they also refer to the use of relaxation methods, and to electrical analogies.

About 60% of the book is devoted to convection, first the general theory, then the relation between convection and friction, then forced and natural convection in the commonest shapes of system, concluding with convection to and from fluids which evaporate or condense in the course of the action.

The material is admirably presented, and is illustrated by worked examples, which add considerably to the value of the exposition. Many useful charts and tables are given, which will ease the work of calculation in specific applications to real systems.

J. H. A.

Die Übermikroskopie, by B. VON BORRIES. Pp. 416, with 70 plates and 225 line diagrams. 1st Edition. (Aulendorf, Württemberg: Editio Cantor, 1949). 48 D. Marks.

For some ten years now there have been available commercial models of the electron microscope which can far surpass the optical microscope in resolving power and which, although several times as expensive as the latter, are not exorbitantly priced as modern physical apparatus goes. Nevertheless the amount of research work of fundamental importance with which it can be credited remains relatively small. After considerable

enthusiasm, in principle, over the introduction of the new instrument, there has followed in many quarters a certain caution in regard to its practical application. This degree of disillusionment has been due in some part to a lack of understanding of the natural limitations attaching to its technique, so that an immediate extrapolation was often expected to be possible from optical practice into the smaller orders of dimensions. In fact the preparative methods, and the way in which image contrast arises, are so different in electron microscopy that quite new interpretative methods are required. This is not to say that a great deal of important progress has not already been made in metallurgy, biology and most of the applied sciences with the aid of the electron microscope. But much more might have been possible if a clearer realization had existed of the natural limitations to its use.

It is with the exploration of these limitations that Dr. von Borries, who was responsible with Dr. E. Ruska for the original development of the magnetic electron microscope, has principally concerned himself in recent years. An account of these researches forms the core of his present book. He has investigated the instrumental factors of illumination brightness, which determines the maximum magnification which can be used and hence the resolution limit, the recording sensitivity, which sets a lower limit to the total amount of energy passing through the specimen during the exposure necessary to form an image, and the fluorescent efficiency of viewing screens, which determines the lowest permissible illumination for focusing and hence the temperature rise in the specimen. In the light of these findings he examines the possibility of electron microscopy of living material, as limited by the thermal and ionizing effects of the electron beam. The lethal dosage is so quickly reached that observation would only be practicable at low magnification, and hence at low resolving power; only in the case of a few organisms could the optical limit be exceeded, even if a sufficiently high voltage were available to penetrate them.

Aside from the biological aspect of the enquiry, with its pessimistic conclusion, the author presents a great deal of valuable information as to the efficiency of electron guns, the scattering and energy loss which accompany the passage of electrons through matter, and the characteristics of photographic emulsions towards electron illumination. The present limit set to resolving power by the aberrations of electrons is also fully discussed, although possible means of correction are hardly mentioned.

As the book is primarily intended for scientists who may wish to assess the positive value of the electron microscope in their particular field of research, the detailed exposition of its limitations is preceded by a review of its principles and constructional features, and is followed by a survey of its applications in pure and applied science, the three sections being of approximately equal length. An appendix has been added to bring the treatment up to date to the beginning of 1949, the main text having been completed a year earlier. The result admirably fulfils the author's intention of giving a well-balanced account of the present state of development of electron microscopy. Omissions of reference to non-German work, which in the difficult war and post-war conditions of communication might have been expected to be serious, are relatively minor, although it is admitted that in many cases the author has not had access to the full text of a paper cited. The illustrations are naturally almost entirely from German sources, and thus permit a much better assessment of the progress made in electron microscopy there since 1939 than was possible from the compressed and unillustrated FIAT reports.

The quality of the reproduction is high, but the same cannot be said of the rest of the technical production of the book. It is probably inevitable that the quality of the paper for the text should be poor, in present-day circumstances, but the binding could surely have been better executed. The pages have been inserted individually, not in stitched and folded sections, so that they come loose with very slight use. It is regrettable to have to make such a complaint as to the production of what is in all other respects an excellent monograph.

V. E. COSSLETT.

Colours and How We See Them, by H. HARTRIDGE. (Royal Institution Christmas Lectures 1946-47). Pp. xi + 158. 1st Edition. (London: G. Bell & Sons Ltd., 1949). 15s.

This book is based on the Royal Institution Christmas Lectures which Professor Hartridge gave to boys and girls in 1946, and the spirit of entertainment and instruction always associated with these lectures is well reflected in its pages. It is essentially an

experimental book in which a great many phenomena are mentioned. These include the spectrum, spectral absorption, colour mixture, interference, diffraction, applications of colour in science and medicine, dichroism, the effect of intermittent illumination and so on. Anyone invited to give a lecture on colour will find a wealth of demonstrations from which to draw, many of the experiments being illustrated in colour. The theoretical explanations of the phenomena do not go very deeply into the subject, but that is hardly to be expected in a book of this type. Quite reasonably, Professor Hartridge has not considered this the appropriate opportunity to enlarge on his theoretical ideas about colour vision.

W. D. WRIGHT.

Cathode-Ray Tube Traces, by HILARY MOSS. Pp. 66. 1st Edition. (London: Electronic Engineering, 1949.) 10s.

This monograph, based on articles published by the author in the journal *Electronic Engineering*, should be of interest to all users of the cathode-ray tube.

The subject matter in general is well presented and the mathematical arguments are not unduly complicated.

The first chapter merits separate mention, in that it deals in detail with the various forms of Lissajous Figure and, in addition to the basic theoretical considerations, points out various practical pitfalls.

Chapter II is disappointing, both in title ('Straight Line Time-Bases') and in content. It is surprising that the linear sawtooth waveform should be dismissed in a mere section of this chapter when various other time-bases of comparatively rare occurrence, such as the circular and spiral forms, should merit the whole of Chapter III.

On reading these chapters one gathers, perhaps wrongly, that Dr. Moss has over-concentrated his attention on time-bases of sinusoidal origin rather than on those of discontinuous form.

The remainder of the book is mainly devoted to the interpretation of various waveforms more usually encountered as the phenomenon under investigation.

A résumé is given of Fourier series and application is made to several of the common pulse waveforms. Beats and the amplitude modulated envelope are also treated.

The author deserves congratulations for his illustrations, but the bibliography is sketchy and would only serve as a first guide to further reading.

A. V. LORD.

Photoelasticity: Principles and Methods, by H. T. JESSOP and F. C. HARRIS. Pp. viii + 184. 1st Edition. (London: Cleaver-Hume Press Ltd., 1949). 28s.

A book on photoelasticity emanating from the Laboratory whence came the classic treatise on the subject by Coker and Filon commands immediate interest and attention. Work on photoelasticity continues at University College, London, and the senior author was the first Chairman of the recently formed Stress Analysis Group of the Institute of Physics.

Authors are not responsible for their publisher's advertisements, but the assertion on the dust jacket that it is a reference work is supported by the authors' statement in the preface that they have given in the text the sources of any original work quoted. Unfortunately, and this is the most serious criticism of the book, it is not true. Statements are often made without the name of the worker responsible being given, seldom if ever is a reference accompanied by chapter and verse, and there is not even a bibliography from which one might hope to guess at the origin. The tabulated data in the appendix would inspire more confidence if reference were made to the sources.

A laboratory such as that of the authors which is the centre of so much work on the subject provides an *embarras de richesses* and the authors seem to have had difficulty in selecting and arranging their material. The book gives the impression of having been hurriedly put together, and not enough care has been spent in critically examining it before printing. For example on page 39 the authors state that a convenient convention of signs is the Cartesian; yet on page 43, they give the distances from a principal point of a lens system to the corresponding principal focus, H_1F_1 or H_2F_2 as both equal to f_0 ; whereas in

a Cartesian system one must be the negative of the other. Again on page 63, the definitions of the stress-optical coefficients leave the reader guessing as to which refers to the ordinary and which to the extraordinary ray, and what is the sign of the difference between them. Again on page 60 a compensator is said to be between 'crossed' polarizer and analyser, yet it is not until page 65 that a definition of this term is given. When much is left vague, the exact analysis of the mode of working of quarter-wave plates given in the appendix, seems a little out of place, especially in a book which sets out to be a guide to "those who wish to undertake practical work on stress-exploration".

The book is well printed and the diagrams are clear, but the half tone illustrations are poorly reproduced; it is a pity these were not grouped together and printed separately on glazed paper; justice would then have been done to the skill of Mr. Storrer the photographer. It would seem that the worked examples are invaluable, and the descriptions of the practical requirements of the optical bench are admirable, although emphasis should have been placed on the need for examination in parallel light, more particularly when the specimens are thick and highly stressed.

It is to be hoped that when the authors prepare a second edition they will expand Chapters IV and V on polarization and photoelasticity, and will give references throughout, so as to enable those who may wish to go more deeply into the subject to do so with less difficulty.

A. M. TAYLOR.

Symposium on Electronics, edited by A. G. PEACOCK. Pp. xiii + 199. 1st Edition. (London: Chapman and Hall in collaboration with S.I.M.A., 1949.) 16s.

The first of a series of annual Symposia on Electronics in Research and Industry, organized by the Scientific Instruments Manufacturers Association, was held in London in 1948. The papers presented at this Symposium are published here in book form, and cover a variety of applications of electronic methods to the solution of instrument problems. Recent advances in the measurement of frequency, small displacements, ionizing radiations, low gas pressures and sound are described, and accounts are also given of the use of electronic techniques in computing, the radiosonde, ultrasonics, spectroscopy, picture telegraphy and metal detection. Because of the large number of subjects covered the treatment of each is brief and descriptive. For this reason the book is primarily of interest only to those non-specialists who wish to have a general summary of a few of the many ways in which electronic equipment is being applied, both in research and in industrial production. Accounts are given of the discussions which followed the presentation of each paper, but the space so occupied could, in the reviewer's opinion, have been more usefully allocated to the expansion of some of the papers.

J. M. MEEK.

Ultra-Violet and Daylight Rays, by J. R. ASHWORTH. Pp. x + 73. 1st Edition. (Liverpool: University Press, 1949.) 6s.

This monograph presents the results of Dr. Ashworth's measurements of ultra-violet and visible light received at ground level over the 16 years from 1932 to 1947. He has used a simple type of photographic measuring technique, which is described and compared with other techniques. The results are given in the form of tables and graphs, showing the variation of the average intensities of visible and of ultra-violet light, with wavelength near 3600 Å. measured in arbitrary units. Evidence is given that these very simple measurements have some real significance, and are not unduly affected by the characteristics of the particular place where they were made (Rochdale).

The results are interpreted as showing that the visible light emitted from the sun is roughly constant throughout the sunspot cycle, but that the ultra-violet is more intense at times of sunspot maximum. These conclusions are, however, not directly deducible from the observations because, according to the author's theory, the variable ionization produced by the ultra-violet in the upper atmosphere in turn produces variable absorption in both the ultra-violet and the visible light reaching the earth.

It is unfortunate that the theory is left in a very speculative and indefinite form. It is suggested that the absorption occurs in Region E of the ionosphere, and is due somehow to the ionization of this region; it would be interesting to know in more detail what Dr. Ashworth believes this mechanism of absorption to be. Reference to his published papers fails to provide any more detail.

J. A. RATCLIFFE.

Les ondes électromagnétiques centimétriques, par LOUIS DE BROGLIE. Pp. 274. (Paris: Éditions de la 'Revue d'Optique Théorique et Instrumentale', 1948.) 800 fr.

Each year since 1944 M. Louis de Broglie has organized a conference to summarize the state of knowledge in some important branch of physics. In 1947 one of these conferences, occupying five days, was held to discuss what was known of centimetric electromagnetic waves, and the proceedings are recorded in the volume here reviewed.

The object was not to repeat the numerous accounts which have already appeared of the workings of radar, and of the magnetron, which led to the possibility of centimetre radar, but to choose nine separate and less well-known aspects of the subject and to ask nine separate authors to report on these. These reports are collected in this volume. They deal with the subjects of: the exchange of energy in electron tubes; the effects of space charge in velocity-modulated tubes; the effects of curvature in waveguides; excitation of and coupling to cavity resonators; measurements at centimetre wavelengths; aerials; propagation; radiation from the sun and the galaxy; the use of centimetre waves in nuclear physics.

In a conference of this kind it was inevitable that the treatment should differ from subject to subject. Some of the papers describe some special point rather fully; those on space charge and on curved wave guides are of this type. Others, for example those on aerials and propagation, attempt to provide a broad survey without much detail.

All the subjects dealt with are advancing so rapidly that a report of a conference held three years ago must inevitably seem somewhat out of date. Since the study of extra-terrestrial radiation was only started seriously after the end of the war, it is perhaps only natural that the corresponding section of the report now seems most out of date. It is also a little surprising to see this subject, whose advance has depended so largely on measurements of metre waves, so fully discussed in a volume dealing with centimetre waves.

J. A. RATCLIFFE.

Recent Advances in the Physiology of Vision, by H. HARTRIDGE. Pp. xii + 401. (London: J. and A. Churchill Ltd., 1950.) 25s.

Much of Professor Hartridge's book is concerned with topics belonging to physiological optics and colour physics, in which physiologists and physicists have been equally active. Eye motions and the dioptric properties of the eye, visual resolving power, spectral luminosity functions, the directional sensitivity of the retina, quantum notions in vision, colour discrimination, the trichromatic and other colour theories, etc., are treated, along with the topography of the nerve fibres in optic nerve, optic tract and visual cortex, the electrical response of the retina, the effect of light stimuli on the Berger rhythms, the visual pigments, electric and magnetic phosphenes, and so on. The author's object has been to survey a very wide field, giving enough of the older work to make clear where advances have been made.

It is probable that no worker in the subject of vision will read this book without wanting to take issue with Professor Hartridge on some of his contentions. But a work of this kind, particularly one dealing with vision, can scarcely be criticized for not presenting a coherent and generally accepted picture. It can be judged successful if it draws the reader's attention to new results and gives some idea of how people are interpreting or speculating about them. Professor Hartridge's book does all these things, and is, perhaps, particularly strong on the 'speculating'. The style is easy, but the arrangement of material leaves something to be desired. In a number of cases the same subject is dealt with in widely separated sections. For example, eye-motions and their measurement are discussed in Section 8 (p. 64) and in Section 54 (p. 329), but there seems no justification for dividing the material in this way. Among several topics omitted which might have been expected to earn a place may be

mentioned particularly W. J. Schmidt's polarized-light analysis of the structure of the outer segments of the retinal rods, an analysis largely confirmed by the electron microscope photographs of rods recently obtained by Sjöstrand.

Of the author's handling of visual theories it is sufficient to say that most physicists would demand more precise and quantitative reasoning to support some of the statements made. A few comments on other aspects of the presentation may be added. Although the crux of Hecht, Schlaer and Pirenne's work on quanta and visual thresholds is the relation between the 'sharpness' of the threshold and the minimum number of quanta involved, no mention is made of this relation in the two pages devoted to the work in question. The results of Mandelbaum and Mintz on the dark adaptation of the colour receptors, briefly described on p. 50, are stated to refer to rod vision. This is clearly a mistake, which is aggravated by a suggested connection of the results with dark-adaptation measurements by Miles which certainly do refer to rod vision. In deploring the lack of information on the variation of visual acuity with pupil size the author seems to have overlooked the extensive measurements of Fabry and Arnulf published in 1937 (*La vision dans les instruments*, Editions de la Revue d'Optique). An explanation is given of how the binocular threshold may be lower than the monocular threshold purely on account of 'probability summation' (pp. 237-238). This is immediately followed by a statement implying that any such difference must arise from physiological summation. It is asserted (p. 203) that the coefficient curves for protanomalous subjects show no negative coefficients in any part of the spectrum when primaries 650, 530, and 460 $m\mu$ are used, and the curves shown in Figure 160 are cited in support. The figure is obviously wrong, as at wavelengths below 460 $m\mu$ the coefficients do not add up to unity, and the statement itself is incorrect.

A number of other criticisms of the same kind could be made, but taken as a whole the book provides a collection of facts and current speculations on vision which will prove of value to all students of the subject.

W. S. S.

Méthodes de calcul dans des problèmes de mécanique. Pp. 102. (Paris: Centre National de la Recherche Scientifique, 1949.) No price.

In the spring of 1948, two international conferences on methods of calculation in problems of mechanics were organized at Marseilles and Paris by the C.N.R.S.; the papers contributed to these conferences have been collated and published in this volume. The contributors and topics are as follows: J. Valensi (Marseilles), "The role of applied mathematics in engineering"; D. N. de G. Allen (London), "Relaxation methods and problems of frameworks"; "Relaxation methods and the solution of differential equations", together with "Supplementary notes on the application of relaxation methods"; Th. Vogel (Marseilles), "The escalator method for the calculation of eigenfrequencies"; M. Picone (Rome), "New points of view in harmonic analysis"; L. Couffignal (Paris), "Calculating machines for harmonic analysis according to the method of H. and Y. Labrouste"; J. M. Burgers (Delft), "Problems related to the theory of turbulence"; L. Malavard (Paris), "Some recent applications of the method of electrical analogies"; A. van Vijngaarden (Amsterdam), "Potential flow about a solid of revolution"; F. H. van den Dungen (Brussels), "The application of the calculus of variations in fluid mechanics"; L. Couffignal "The role of numerical calculation in scientific and technical research".

The papers naturally vary in style and standard but they are, without exception, lucidly written and the book can be thoroughly recommended to a physicist or engineer who wishes to acquire some idea of modern techniques used in the realm of classical mechanics. R. M. D.

Glass-to-Metal Seals, by J. H. PARTRIDGE. Pp. xii+238. 1st Edition. (Sheffield: Society of Glass Technology, 1949.) 25s.

This is a comprehensive and authoritative guide to the art of sealing metals to glasses. The production of graded glass-to-glass seals is therefore also dealt with in detail. The problems of stress distribution, so vital in determining success or failure, are ably and adequately discussed.

This book should be available to all workers, both scientific and technical, in every physics and chemistry laboratory; it is first-class.

G. I. F.

CONTENTS FOR SECTION A

	PAGE
Mr. B. D. HYAMS, Mr. M. G. MYLROI, Mr. B. G. OWEN and Dr. J. G. WILSON. A Magnetic Cosmic-Ray Spectrograph with Counter Recording	1053
Mr. B. G. OWEN. A Magnetic Cosmic-Ray Spectrograph with Counter Recording—II: The Electronic and Recording System	1074
Dr. E. P. GEORGE and Mr. A. C. JASON. Observations on Cosmic-Ray Penetrating Showers at High Altitude, Sea Level and Below Ground	1081
Dr. D. M. RITSON. Slow Mesons in the Backward Flux of the Cosmic Radiation	1098
Prof. L. JÁNOSSY and Mr. H. MESSEL. Fluctuations of the Electron-Photon Cascade—Moments of the Distribution	1101
Mr. L. R. B. ELTON. The Effect of Nuclear Structure on the Elastic Scattering of Fast Electrons	1115
Mr. J. IRVING. Non-physical Solutions in Classical Finite Electron Theory	1125
Dr. A. LAGERQVIST, Mr. E. LIND and Dr. R. F. BARROW. The Band-Spectrum of Barium Oxide	1132
Dr. M. AFAF. Band-Spectrum of ZrO	1156
Letters to the Editor :	
Mr. F. K. GOWARD and Mr. J. J. WILKINS. The Photo-Disintegration of Oxygen into Four Alpha-Particles	1171
Mr. J. J. WILKINS and Mr. F. K. GOWARD. Ground State ^8Be Nuclei in Photo-Disintegration Stars	1173
Mr. F. C. W. COLMER and Mr. D. J. LITTLER. Pile Neutron Absorption Cross Sections of some of the Elements	1175
Mr. D. J. RAVENHALL. The Effect of Screening of the Cross Section for Pair Production by Electrons	1177
Dr. J. H. FREMLIN and Miss MADELINE C. WALTERS. Background Tracks in Electron-Sensitive Nuclear Emulsions	1178
Mr. J. DARBY, Dr. J. HATTON and Dr. B. V. ROLLIN. The Attainment of very Low Temperatures by a Two-Stage Adiabatic Demagnetization Process	1179
Mr. J. DARBY, Dr. J. HATTON and Dr. B. V. ROLLIN. Superconductivity of Lead Sulphide, Selenide and Telluride	1181
Dr. K. MENDELSSOHN and Mr. J. L. OLSEN. Heat Flow in Superconductive Alloys	1182
Mr. J. K. HULM. The Dielectric Properties of some Alkaline Earth Titanates at Low Temperatures	1184
Reviews of Books	1185
Contents for Section B	1186
Abstracts for Section B	1186

ABSTRACTS FOR SECTION A

A Magnetic Cosmic-Ray Spectrograph with Counter Recording, by B. D. HYAMS, M. G. MYLROI, B. G. OWEN and J. G. WILSON.

ABSTRACT. An instrument is described in which the momentum of single cosmic-ray particles is measured, the particles leaving the instrument in a sufficiently collimated beam for use in subsequent experiments. The 'maximum detectable momentum' of the apparatus is about 3×10^{10} ev/c., almost all particles are collected within 10° of the zenith and in directions individually defined to $\pm 1^\circ$, the output is about 400 particles/day, and the proportion of spurious records is of the order of, or less than, 0.1%.

A Magnetic Cosmic-Ray Spectrograph with Counter Recording—II: The Electronic and Recording System, by B. G. OWEN.

ABSTRACT. The paper describes the electronic selection and recording systems of the spectrograph and the performance and overall serviceability of the equipment as shown in continuous operation over about one year.

Observations on Cosmic-Ray Penetrating Showers at High Altitude, Sea Level and Below Ground, by E. P. GEORGE and A. C. JASON.

ABSTRACT. Penetrating showers have been investigated, using Geiger counters, at a depth of 30 m. below ground, at sea level and at an altitude of 3,457 m. The influence of the geometry of the absorbers was studied. The transition curves for local showers, corrected for this geometric effect, give the following collision lengths of the generating particles: Pb, 180 ± 40 ; Al, 85 ± 15 ; Paraffin ~ 80 gm/cm². These values correspond to a collision cross section close to the geometric cross section of the nuclei. From the results obtained for extensive penetrating showers, it is concluded that most of the penetrating particles in these showers appear to be generated in the atmosphere. In 40 days, no penetrating showers were recorded below ground. Using photographic plates, the density distribution of shower tracks associated with nuclear disintegrations was found to be similar at sea level and 3,457 m.

Slow Mesons in the Backward Flux of the Cosmic Radiation, by D. M. RITSON.

ABSTRACT. Using the method of 'delayed coincidences' measurements have been made at sea level on the flux of slow mesons travelling backwards from the ground.

Fluctuations of the Electron-Photon Cascade—Moments of the Distribution, by L. JÁNOSSY and H. MESSEL.

ABSTRACT. The second moments of the electron-photon cascades are evaluated. It is found that the mean square fluctuation at the cascade maximum is that expected for a Poisson distribution or less; before and after the maximum the fluctuation exceeds greatly that expected for a Poisson distribution. The correlation coefficient between electrons and photons is zero for small thicknesses or near the cascade maximum. For other regions the correlation coefficient is positive. Both mean square fluctuation and correlation between electrons and photons can be understood qualitatively in terms of fluctuation of effective depth.

The Effect of Nuclear Structure on the Elastic Scattering of Fast Electrons, by L. R. B. ELTON.

ABSTRACT. The cross section for the scattering of electrons by atomic nuclei is investigated at energies for which the nuclei can no longer be treated as point charges. Two simple nuclear models are used. A general expression is obtained using Born's approximation, and an exact numerical calculation is carried through for 20 mev. electrons scattered by gold nuclei. It is concluded that at this energy considerable deviations from the formulae which treat the nucleus as a point charge should be expected, and that these should furnish some information about the charge distribution within the nucleus.

Non-physical Solutions in Classical Finite Electron Theory, by J. IRVING.

ABSTRACT. An approximate linear form of the Peierls-McManus equations of motion for an electron is shown to yield runaway solutions for a particular influence function, which otherwise satisfies all the conditions imposed by the theory. The general problem is to discuss the existence of complex roots of a transcendental equation for an arbitrary form of the influence function. It is shown that this equation always has roots. These, however, may be such that the corresponding motion of the free electron is of a damped nature. It has not been found possible to construct a function which avoids runaway solutions or to prove whether or not such a function exists when all conditions are satisfied.

The Band-Spectrum of Barium Oxide, by A. LAGERQVIST, E. LIND and R. F. BARROW.

ABSTRACT. The band-spectrum of BaO between 5000 and 7000 Å., which consists of a single $^1\Sigma-^1\Sigma$ system, has been the subject of a new rotational analysis in which the following bands have been examined: 5,0, 4,0, 3,0, 3,1, 2,0, 2,1, 1,1, 1,2, 0,2, 0,3 and 0,4. The constants derived are:

$$\begin{aligned} B_v'' &= 0.3124_9 - 0.0013_6(v'' + \tfrac{1}{2}) - 0.0000_2(v'' + \tfrac{1}{2})^2 & B_v' &= 0.2584 - 0.0011_1(v' + \tfrac{1}{2}) \\ D'' &= 26.5 \times 10^{-8} & D' &= 28 \times 10^{-8} \\ r_e'' &= 1.940 \times 10^{-8} \text{ cm.} & r_e' &= 2.133 \times 10^{-8} \text{ cm.} \\ \omega_e'' &= 669.8_1, & x_e'' \omega_e'' &= 2.05_4 & \omega_e' &\sim 500, & x' \omega' &= 1.6 \\ & & \nu_{0,0} &= 16,722.2_5 \text{ cm}^{-1}. \end{aligned}$$

In the upper state some 16 perturbations have been found. They appear to arise from interactions with at least four electronic states or substates. Fairly complete information about one of the perturbing levels has been obtained. The constants of this state are:

$$\begin{aligned} B_v &= 0.2254 - 0.0013_5(v + \tfrac{1}{2}), \\ G_v &= 450.4(v + \tfrac{1}{2}) - 2.9(v + \tfrac{1}{2})^2, \\ \nu_{0,0} &= 17476.7 \text{ cm}^{-1}. \end{aligned}$$

The band-constants of the other perturbing states are very similar to those given above.

Band-Spectrum of ZrO, by M. AFAF.

ABSTRACT. The spectrum of ZrO has been photographed in the ultra-violet, the visible and the infra-red, from arcs running under special conditions. This has made possible the identification of three new systems in the ultra-violet, as well as two less conspicuous ones in the infra-red. It has also made it possible to extend the blue system α of ZrO.

THE PHYSICAL SOCIETY

MEMBERSHIP

Membership of the Society is open to all who are interested in Physics:

FELLOWSHIP. A candidate for election to Fellowship must as a rule be recommended by three Fellows, to two of whom he is known personally. Fellows may attend all meetings of the Society, are entitled to receive Publications 1 (either Section A or Section B), 4 and 5 below, and may obtain the other publications at much reduced rates.

STUDENT MEMBERSHIP. A candidate for election to Student Membership must be between 18 and 26 years of age and must be recommended from personal knowledge by a Fellow. Student Members may attend all meetings of the Society, are entitled to receive Publications 1 (either Section A or Section B) and 4, and may obtain the other publications at much reduced rates.

Books and periodicals may be read in the Society's Library, and a limited number of books may be borrowed by Fellows and Student Members on application to the Honorary Librarian.

Fellows and Student Members may become members of the *Colour Group*, the *Optical Group*, the *Low Temperature Group* and the *Acoustics Group* (specialist Groups formed in the Society) without payment of additional annual subscription.

PUBLICATIONS

1. *The Proceedings of the Physical Society*, published monthly in two Sections, contains original papers, lectures by specialists, reports of discussions and of demonstrations, and book reviews. Section A contains papers mainly on atomic and sub-atomic subjects; Section B contains papers on macroscopic physics.

2. *Reports on Progress in Physics*, published annually, is a comprehensive review by qualified physicists.

3. *The Handbook of the Physical Society's Annual Exhibition of Scientific Instruments and Apparatus*. This Exhibition is recognized as the most important function of its kind, and the Handbook is a valuable book of reference.

4. *The Bulletin*, issued at frequent intervals during the session, informs members of programmes of future meetings and of the business of the Society generally.

5. *Physics Abstracts (Science Abstracts A)*, published monthly in association with the Institution of Electrical Engineers, covers the whole field of contemporary physical research.

6. *Electrical Engineering Abstracts (Science Abstracts B)*, published monthly in association with the Institution of Electrical Engineers, covers the whole field of contemporary research in electrical engineering.

7. *Special Publications*, critical monographs and reports on special subjects prepared by experts or committees, are issued from time to time.

MEETINGS

At approximately monthly intervals throughout each annual session, meetings are held for the reading and discussion of papers, for lectures, and for experimental demonstrations. Special lectures include: the *Guthrie Lecture*, in memory of the founder of the Society, given annually by a physicist of international reputation; the *Thomas Young Oration*, given biennially on an optical subject; the *Charles Chree Address*, given biennially on Geomagnetism, Atmospheric Electricity, or a cognate subject; and the biennial *Rutherford Memorial Lecture*. A Summer Meeting is generally held each year at a provincial centre, and from time to time meetings are arranged jointly with other Societies for the discussion of subjects of common interest.

Each of the four specialist Groups holds about five meetings in each session.

SUBSCRIPTIONS

Fellows pay an Entrance Fee of £1 1s. and an Annual Subscription of £3 3s. Student Members pay only an Annual Subscription of 15s. Second Section of *Proceedings* 20s. No entrance fee is payable by a Student Member on transfer to Fellowship.

*Further information may be obtained from the Secretary-Editor
at the Offices of the Society:*

1 LOWTHER GARDENS, PRINCE CONSORT ROAD, LONDON S.W. 7
Telephone: KENsington 0048, 0049

PHYSICAL SOCIETY PUBLICATIONS

Fellows and Student Members of the Society may obtain ONE copy of each publication at the price shown in brackets. In most cases the cost of postage and packing is extra.

- Noise and Sound Transmission.* Report of the 1948 Summer Symposium of the Acoustics Group of the Physical Society. Pp 200. In paper covers. 17s. 6d. (10s. 6d.) Postage 6d.
- Resonant Absorbers and Reverberation.* Report of the 1947 Summer Symposium of the Acoustics Group of the Physical Society. Pp. 57. In paper covers. 7s. 6d. (5s.) Postage 6d.
- The Emission Spectra of the Night Sky and Aurorae, 1948.* Papers read at an International Conference held under the auspices of the Gassiot Committee in London in July 1947. Pp. 140. In paper covers. 20s. (12s. 6d.) Postage 6d.
- The Strength of Solids, 1948.* Report of Conference held at Bristol in July 1947. Pp. 162. In paper covers. 25s. (15s. 6d.) Postage 8d.
- Report of International Conference on Fundamental Particles (Vol. I) and Low Temperatures (Vol. II), 1947.* Conference held at Cambridge in July 1946. Pp. 200 (Vol. I), pp. 184 (Vol. II). In paper covers. 15s. each vol. (7s. 6d.) Postage 8d.
- Meteorological Factors in Radio-Wave Propagation, 1947.* Report of Conference held jointly with the Royal Meteorological Society in April 1946. Pp. 325. In paper covers. 24s. (12s. + postage 1s.)
- Handbook of the 34th Exhibition of Scientific Instruments and Apparatus, 1950.* Pp. xii + 266. In paper covers. 5s. (2s. 6d.) Postage 1s.
- Handbook of the 33rd Exhibition of Scientific Instruments and Apparatus, 1949.* Pp. 272. In paper covers. 5s. (2s. 6d.) Postage 1s.
- Catalogue of the 32nd Exhibition of Scientific Instruments and Apparatus, 1948.* Pp. 288. In paper covers. 5s. (2s. 6d.) Postage 1s. (Half price from 5th April 1949).
- Catalogue of the 31st Exhibition of Scientific Instruments and Apparatus, 1947.* Pp. 298. In paper covers. 2s. 6d. (1s. 6d.) Postage 1s.
- Report on Colour Terminology, by a Committee of the Colour Group.* Pp. 56. In paper covers. 7s. (3s. 6d.)
- Report on Defective Colour Vision in Industry, by a Committee of the Colour Group.* 1946. Pp. 52. In paper covers. 3s. 6d. (1s. 9d. + postage 4d.)
- Science and Human Welfare.* Conference held by the Association of Scientific Workers, Physical Society and other bodies. 1946. Pp. 71. In paper covers. 1s. 6d. (9d.) Postage 4d.
- Report on the Teaching of Geometrical Optics, 1934.* Pp. 86. In paper covers. 6s. 3d. Postage 6d.
- Report on Band Spectra of Diatomic Molecules, 1932.* By W. JEVONS, D.Sc., Ph.D. Pp. 308. In paper covers, 25s.; bound in cloth, 30s. (15s.) Postage 1s.
- Discussion on Vision, 1932.* Pp. 327. In paper covers. 6s. 6d. (3s. 3d.) Postage 1s.
- Discussion on Audition, 1931.* Pp. 151. In paper covers. 4s. (2s.) Postage 1s.
- Discussion on Photo-electric Cells and their Application, 1930.* Pp. 236. In paper covers. 6s. 6d. (3s. 3d.) Postage 8d.
- The Decimal Bibliographic Classification (Optics, Light and Cognate Subjects), 1926.* By A. F. C. POLLARD, D.Sc. Pp. 109. Bound in cloth. 4s. (2s.) Postage 8d.
- Motor Headlights, 1922.* Pp. 39. In paper covers. 1s. 6d. (9d.) Postage 4d.
- Report on Series in Line Spectra, 1922.* By A. FOWLER, C.B.E., Sc.D., F.R.S. Pp. 182. In paper covers. 30s. (15s.) Postage 8d.
- A Discussion on the Making of Reflecting Surfaces, 1920.* Pp. 44. In paper covers. 2s. 6d. (1s. 3d.) Postage 4d.
- Reports on Progress in Physics.* Vol. XIII (1950). Pp. 424. Bound in cloth. 50s. (25s.) Postage 1s.
- Reports on Progress in Physics.* Vol. XII (1948-49). Pp. 382. Bound in cloth. 42s. (25s.) Postage 1s.
- Reports on Progress in Physics.* Vol. XI (1946-48). Pp. 461. Bound in cloth. 42s. (25s.) Postage 1s.
- Reports on Progress in Physics.* Vols. IV (1937, reprinted 1946) and X (1944-45). Bound in cloth. 30s. each. (15s.) Postage 1s.
- The Proceedings of the Physical Society.* From Vol. I (1874-75), excepting a few parts which are out of print. Prices on application to Messrs. Wm. Dawson Ltd., 102 Wigmore St., London W.1.
- The Transactions of the Optical Society.* Vols. 1 (1899-1900) - 33 (1931-32), excepting a few parts which are out of print. Prices on application to Messrs. Wm. Dawson Ltd., 102 Wigmore St., London W.1.

Orders, accompanied by remittances, should be sent to

THE PHYSICAL SOCIETY

1 Lowther Gardens, Prince Consort Road, London S.W.7